

Copyright Warning & Restrictions

The copyright law of the United States (Title 17, United States Code) governs the making of photocopies or other reproductions of copyrighted material.

Under certain conditions specified in the law, libraries and archives are authorized to furnish a photocopy or other reproduction. One of these specified conditions is that the photocopy or reproduction is not to be "used for any purpose other than private study, scholarship, or research." If a user makes a request for, or later uses, a photocopy or reproduction for purposes in excess of "fair use" that user may be liable for copyright infringement,

This institution reserves the right to refuse to accept a copying order if, in its judgment, fulfillment of the order would involve violation of copyright law.

Please Note: The author retains the copyright while the New Jersey Institute of Technology reserves the right to distribute this thesis or dissertation

Printing note: If you do not wish to print this page, then select "Pages from: first page # to: last page #" on the print dialog screen



The Van Houten library has removed some of the personal information and all signatures from the approval page and biographical sketches of theses and dissertations in order to protect the identity of NJIT graduates and faculty.

ABSTRACT

On Orthogonal Collocation Solutions of Partial Differential Equations

by
Herli Surjanhata

In contrast to the h -version most frequently used, a p -version of the Orthogonal Collocation Method as applied to differential equations in two-dimensional domains is examined. For superior accuracy and convergence, the collocation points are chosen to be the zeros of a Legendre polynomial plus the two endpoints. Hence the method is called the Legendre Collocation Method. The approximate solution in an element is written as a Lagrange interpolation polynomial. This form of the approximate solution makes it possible to fully automate the method on a personal computer using conventional memory.

The Legendre Collocation Method provides a formula for the derivatives in terms of the values of the function in matrix form. The governing differential equation and boundary conditions are satisfied by matrix equations at the collocation points. The resulting set of simultaneous equations is then solved for the values of the solution function using LU decomposition and back substitution.

The Legendre Collocation Method is applied further to the problems containing singularities. To obtain an accurate approximation in a neighborhood of the singularity, an eigenfunction solution is specifically formulated to the given problem, and its coefficients are determined by least-squares or minimax approximation techniques utilizing the results previously obtained by the Legendre Collocation Method. This combined method gives accurate results for the values of the solution function and its derivatives in a neighborhood of the singularity.

All results of a selected number of example problems are compared with the available solutions. Numerical experiments confirm the superior accuracy in the computed values of the solution function at the collocation points.

**ON ORTHOGONAL COLLOCATION SOLUTIONS
OF PARTIAL DIFFERENTIAL EQUATIONS**

by

Herli Surjanhata

**A Dissertation
Submitted to the Faculty of
New Jersey Institute of Technology
in Partial Fulfillment of the Requirements for the Degree of
Doctor of Philosophy**

**Department of Mechanical Engineering
January, 1993**

Copyright © 1993 by Herli Surjanhata

ALL RIGHTS RESERVED

APPROVAL PAGE

On Orthogonal Collocation Solutions of Partial Differential Equations

Herli Surjanhata

Dr. Harry Herman, Dissertation Adviser
Associate Chairperson and Professor of Mechanical Engineering, NJIT

Dr. Denis Blackmore, Committee Member
Professor of Mathematics, NJIT

Dr. Zhiming Ji, Committee Member
Assistant Professor of Mechanical Engineering, NJIT

Dr. Bernard Koplik, Committee Member
Chairperson and Professor of Mechanical and Industrial Engineering, NJIT

Dr. Nouri Levy, Committee Member
Associate Professor of Mechanical Engineering, NJIT

BIOGRAPHICAL SKETCH

Author: Herli Surjanhata

Degree: Doctor of Philosophy

Date: January, 1993

Undergraduate and Graduate Education:

- Doctor of Philosophy in Mechanical Engineering, New Jersey Institute of Technology, Newark, New Jersey, 1993
- Master of Science in Mechanical Engineering, New Jersey Institute of Technology, Newark, New Jersey, 1984
- Bachelor of Science in Mechanical Engineering, University of Trisakti, Jakarta, Indonesia, 1976

Major: Mechanical Engineering

Presentations and Publications:

Spencer, Herbert Harry, and H. Surjanhata. "Plate Buckling Under Partial Edge Loading." Presented in OSU, Columbus, Ohio, September 1985, at *19th Midwestern Mechanics Conference*, 1985.

Spencer, Herbert Harry, and H. Surjanhata. "On Plate Buckling Coefficients." *Journal of Engineering Mechanics*, ASCE, Vol. 112, No. 3, March 1986.

Spencer, Herbert Harry, and H. Surjanhata. "The Simplified Buckling Criterion Applied to Plates with Partial Edge Loading." *Journal Applied Scientific Research*, Netherlands, Vol. 43, No. 2, 1986.

Dedicated to my parents, and my wife
for their love and sacrifice.

ACKNOWLEDGMENT

The author would like to express his sincere gratitude to his supervisor, Dr. Harry Herman, for his valuable guidance and encouragement during the course of this research. The author also wishes to express his gratitude to the members of his Advisory Committee Professors: Dr. Bernard Koplik, Dr. Nouri Levy, Dr. Denis Blackmore and Dr. Zhiming Ji for their valuable comments and suggestions.

Special thanks to his friend Wen-hua Zhu for his technical suggestions and encouragements during the period of his research.

Finally, the author would like to express his deep appreciation and gratitude to his wife Liani and his son Brian for their sacrifices and understanding, and also to his parents Lin-Kee Chung and Nyuk-Chun Lian, especially to his mother who is undergoing a chemotherapy treatment at this time, for their love and encouragements during the course of this study.

TABLE OF CONTENTS

Chapter	Page
1 INTRODUCTION	1
2 LEGENDRE COLLOCATION METHOD	5
2.1 Introduction	5
2.2 One-dimensional Lagrangian Trial Solution	9
2.3 Differentiation of a Lagrange Interpolation Polynomial	12
2.4 Coefficient Matrices for First and Second Derivatives	15
2.5 Zeros of Legendre Polynomials	18
2.6 Legendre Collocation Method Applied to Differential Equation in Two-dimensional Domain	20
2.7 Linear Transformation of Two-dimensional Domains	22
2.8 The Legendre Collocation Element Formulation in Two-dimensional Domains	24
2.9 Treatment of Corners	33
3 TREATMENT OF BOUNDARY SINGULARITIES	37
3.1 Introduction	37
3.2 Eigenfunctions Solution for Torsion of an L-shaped Bar	41
3.3 Discrete Least-Squares Approximation for Torsion of L-shaped Bar	47
3.4 Minimax Fit at Chebyshev Zeros	56
3.5 Series Solution for the Problem of Motz	59

4 APPLICATIONS	67
4.1 Introduction	67
4.2 Torsion of A Square Bar	68
4.3 The Problem of Motz	81
4.4 Solution of Laplace's Equation in L-shaped Domain	107
5 CONCLUDING REMARKS	127
APPENDIX	
A Solution of Dirichlet Problem for Laplace's Equation by Separation of Variables	130
B Solution of Mixed-Boundary Conditions for Laplace's Equation by Separation of Variables	136
C Weights of Gauss-Legendre Quadrature	140
D The Position of the Collocation Points	145
REFERENCES	146

LIST OF TABLES

Table	Page
3.1 Interpolation points θ_k along the sector arc from $\theta = 0$ to $\theta = 1.5\pi$	59
4.1 Maximum Stress Function Ψ - Torsion of Square Bar	71
4.2 k - value for Maximum Shearing Stress - Torsion of Square Bar	72
4.3 k_1 - value for Torque - Torsion of Square Bar	73
4.4 Comparison of torsion function ψ at the collection points	79
4.5 Shearing stress τ_{zy} at the collocation points	80
4.6 Pointwise convergence of a solution u on a square grid points of 3.5×3.5 . The results shown are based on a mesh size on each element: $3 \times 3, 5 \times 5, 7 \times 7, 9 \times 9$	92
4.7 Comparison results of solution u of the problem of Motz on a unit mesh	93
4.8 The coefficients c_n computed from interpolated results obtained through the Legendre Collocation Method with 9×9 mesh size	94
4.9 Comparison the solution u or ϕ on the sector arc of the problem of Motz (see Figure 4.10)	95
4.10 Comparison results of the solution u of the problem of Motz on a 0.25 unit mesh in the neighborhood of the singular point O	96
4.11 The derivative $\frac{\partial u}{\partial x}$ of the problem of Motz on a 0.25 unit mesh in the neighborhood of the singular point O	97
4.12 The derivative $\frac{\partial u}{\partial y}$ of the problem of Motz on a 0.25 unit mesh in the neighborhood of the singular point O	98

4.13	Pointwise convergence of least-squares approximation on the eigensolution u in the neighborhood of the singular point O. The results are on a 0.25 unit mesh and based on 9×9 mesh size for each element in the Legendre Collocation Method solution	99
4.14	Pointwise convergence of minimax approximation on the eigensolution u in the neighborhood of the singular point O. The results are on a 0.25 unit mesh and based on 9×9 mesh size for each element in the Legendre Collocation Method solution	100
4.15	Pointwise convergence of $\frac{\partial u}{\partial x}$ of least-squares approximation on the eigensolution u in the neighborhood of the singular point O. The results are on a 0.25 unit mesh and based on 9×9 mesh size for each element in the Legendre Collocation Method solution	101
4.16	Pointwise convergence of $\frac{\partial u}{\partial y}$ of least-squares approximation on the eigensolution u in the neighborhood of the singular point O. The results are on a 0.25 unit mesh and based on 9×9 mesh size for each element in the Legendre Collocation Method solution	102
4.17	Pointwise convergence of $\frac{\partial u}{\partial x}$ of minimax approximation on the eigensolution u in the neighborhood of the singular point O. The results are on a 0.25 unit mesh and based on 9×9 mesh size for each element in the Legendre Collocation Method solution	103
4.18	Pointwise convergence of $\frac{\partial u}{\partial y}$ of minimax approximation on the eigensolution u in the neighborhood of the singular point O. The results are on a 0.25 unit mesh and based on 9×9 mesh size for each element in the Legendre Collocation Method solution	104
4.19	Numbering scheme for the domain shown in Figure 4.18	113
4.20	Comparison results of the solution ϕ between the Legendre Collocation Method and exact solution at the collocation points	114
4.21	Percentage relative error of the solution ϕ at the collocation points	115
4.22	Pointwise convergence of the solution ϕ at 0.5×0.5 grid points	116
4.23	Comparison the solution ϕ along the sector arc with a fixed radius $r = 0.5$ and at various angles θ (from 0 to 1.5π)	118

4.24 Pointwise convergence of the least-squares solution ϕ at 0.0025 \times 0.0025 grid points near singularity	120
4.25 Pointwise convergence of $\frac{\partial \phi}{\partial x}$ of the least-squares solution ϕ at 0.0025 \times 0.0025 grid points near singularity	121
4.26 Pointwise convergence of $\frac{\partial \phi}{\partial y}$ of the least-squares solution ϕ at 0.0025 \times 0.0025 grid points near singularity	122
4.27 Comparison of the solution ϕ at 0.0025 \times 0.0025 grid points near singularity	123
4.28 Comparison of $\frac{\partial \phi}{\partial x}$ at 0.0025 \times 0.0025 grid points near singularity	124
4.29 Comparison of $\frac{\partial \phi}{\partial y}$ at 0.0025 \times 0.0025 grid points near singularity	125

LIST OF FIGURES

Figure	Page
2.1 ($N-1$) th -degree approximate function	10
2.2 Domain and boundary conditions for Poisson equation	21
2.3 Linear mapping of real element onto parent element	23
2.4 A typical interior collocation point where the governing equation is evaluated	28
2.5 Inter-element boundary point IBC at which the continuity of the function and normal derivative is imposed	29
2.6 Boundary points located at left-side vertical and top-side horizontal boundaries	30
2.7 Boundary points located at right-side vertical and bottom-side horizontal boundaries	31
2.8 A corner with known values of the function and normal derivative	33
2.9 A corner with known values of normal derivative	34
2.10 Definition at a corner for a 5×5 mesh for each element	36
3.1 Legendre collocation points in the neighborhood of a singularity	38
3.2 Circular sector for Poisson equation in polar coordinates	43
3.3 Mixed boundary conditions on a line	61
4.1 9×9 mesh for a square bar under torsion. Global numbering scheme is shown with $NPX = NPY = 9$	70
4.2 Convergence study of maximum shearing stress of square bar under torsion	74
4.3 View of torsion or stress function Ψ plotted based on 9×9 mesh solution	75

4.4 Contour plot of torsion function Ψ	75
4.5 Three-dimensional plot of the shearing stress τ_{xy} obtained using 9×9 mesh size	76
4.6 Three-dimensional plot of the magnitude of resultant shearing stress	77
4.7 Contour plot of the magnitude of resultant of shearing stress	78
4.8 Geometric definitions for the problem of Motz	82
4.9 The domain is divided into two elements, and 7×7 - Legendre collocation grids for each element are shown	83
4.10 An half circle sector isolated for a special treatment in the neighborhood of a singular point O	87
4.11 Plot of the solution values along the arc from 0 to π as shown in Table 4.9	95
4.12 Three-dimensional plot of the solution u obtained through the Legendre Collocation Method	105
4.13 Contour plot of solution u in the neighborhood of singularity	105
4.14 Contour plot of $\frac{\partial u}{\partial x}$ in the neighborhood of singularity	106
4.15 Contour plot of $\frac{\partial u}{\partial y}$ in the neighborhood of singularity	106
4.16 L-shaped domain and boundary conditions for Laplace's equation	107
4.17 Polar coordinates (r, θ) related to cartesian coordinates (x, y)	109
4.18 L-shaped domain for Laplace's equation is shown with three element, and 9×9 mesh size for each element	111
4.19 Three-dimensional view of the solution ϕ of Laplace's equation with the boundary conditions defined in Figure 4.16	117
4.20 Plot of the solution ϕ along the sector arc as tabulated in Table 4.23	118

4.21 Grid points nearest to the singularity for each element with 9×9 mesh size	119
4.22 Contour plot of solution ϕ in the neighborhood of singularity	126

CHAPTER 1

INTRODUCTION

The problems of mathematical physics, such as electrostatics, quantum mechanics, elasticity theory, hydrodynamics etc. generally lead to partial differential equations or to ordinary differential equations. These equations have to be integrated subject to the initial and/or boundary conditions of each specific problem. The necessity of solving these problems as accurately as possible in cases in which an analytical solution is unobtainable has lead to the development of numerical solution techniques such as the Finite Difference Method, the Finite Element Method and the Boundary Element Method. Among the simplest methods to apply are the Orthogonal Collocation Methods.

The formulation and improvement of various Orthogonal Collocation Methods have attracted the interest of many investigators over the past quarter century. There have been many publications providing surveys or accounts of these studies, for example, the book by Villadsen and Michelsen [1]. A brief account of the methods appeared in the books by Finlayson [2], and Prenter [3]. Most of the earlier developments of the Orthogonal Collocation Method were applied to one-dimensional problems, and when applied to two-dimensional problems they were limited to the use of lower degree polynomials in constructing the approximate solution, e.g. cubic Lagrangian polynomial, cubic splines, cubic Hermite polynomials [1,4].

In the Orthogonal Collocation Method, the zeros of an orthogonal polynomial are chosen to be the collocation points. The method was apparently first applied to differential equations by Frazer, Jones and Skan [5] and independently by Lanczos [6,7], and was developed further for solving ordinary

differential equations using Chebyshev series by Clenshaw and Norton [8], Norton [9], and Wright [10]. These applications were primarily for initial-value problems. Horvay and Spiess [11] utilized polynomials which were orthogonal on the boundary. Major contributions to the method were made by Villadsen and Stewart [12] when they developed orthogonal collocation for boundary-value problems. They chose the trial functions to be sets of orthogonal polynomials which satisfied the boundary conditions, and called the method an *Interior Collocation* technique. They also treated problems with trial solutions consisting of sets of orthogonal polynomials which satisfied the differential equations with collocation on the boundary. This was called *Boundary Collocation*. The zeros of an orthogonal polynomial were used as the boundary collocation points. They also solved for the values of the solution function at the collocation points rather than using arbitrary function coefficients in the expansion of the approximate solution. This simplified the procedure for obtaining the solution. It is important to note here that most of the problems solved using the Orthogonal Collocation Method by previous investigators were chemical engineering problems.

Collocation methods have been used to solve integral equations for more than sixty years. More recently, the so-called *h*-, *p*- and *hp*-versions of the standard Finite Element Method have attracted the interests of many investigators in this fields [13,14,15]. The accuracy of the *h*-version is achieved by refining the mesh size; and the *p*-version improves its accuracy by increasing the polynomial degree. The *hp*-version balances a combination of mesh refinement and an increase of the polynomial degree of the shape functions. The *h*-, *p*- and *hp*-version techniques using the Finite Element Method have been applied to the Boundary Integral Element Method [16,17,18].

A major purpose of this study is to develop the *p*-version of the Orthogonal Collocation Method as applied to differential equations, so that it can be easily

automated for the computer. The Orthogonal Collocation Method formulated here differs from the procedures presented by previous investigators in that we confine ourselves to the use of the zeros of one orthogonal set, namely the Legendre polynomials as the interior collocation points as well as boundary collocation points. In a series of numerical experiments, we found that the use of the Legendre polynomials yielded the best accuracy. Furthermore, we require the approximate solution, which is constructed using Lagrange interpolation functions, to satisfy the governing differential equations and boundary conditions only at the collocation points. Thus, a ***mixed collocation*** technique is adopted; it generalizes and simplifies the procedure in solving the problem using a computer, and the convergence of the solution is achieved by simply increasing the degree of the polynomial used in the approximate solution. The method developed in this study provides the derivatives, in terms of the values of the function in matrix form by performing matrix multiplication. Here we follow Villadsen and Michelsen [1,19] who used a repeated differentiation of the approximate solution, and evaluated it at the collocation points. We extend further the use of the so-called Legendre Collocation Method to problems containing boundary singularities. The goal is to develop a solution method, capable of finding the approximate solutions as well as the approximate partial derivatives of a given problem, especially in a neighborhood of the singularity without using a fine mesh. The resulting combined method is described in Chapters 2 and 3.

Chapter 2 discusses the development and formulation of the p -version finite element technique of the Legendre Collocation Method. The automated p -version technique is made possible by the use of the Lagrange interpolation functions to construct an approximate solution, with the zeros of a Legendre polynomial as the interior and boundary collocation points. The recurrence formulas for obtaining the first derivative at the collocation points are presented in detail, and as a result,

this derivative can be expressed in terms of the values of the solution at the collocation points in matrix form. Matrix operations of the discretization matrix for the first derivative will generate the matrices for higher order derivatives which will be substituted into the differential equation. In the same manner, the boundary conditions are satisfied, and the whole problem is then reduced to a set of matrix equations which are easily generated and solved on a computer.

Like all polynomial approximations, the Legendre Collocation Method is unsatisfactory in a small neighborhood of a singularity. Thus, a special treatment is required. Chapter 3 gives a systematic treatment in the form of eigenfunction solutions in a neighborhood of the singularity which are specifically formulated for these problems. The coefficients are determined by least-squares or minimax approximation techniques utilizing the results given by the Legendre Collocation Method. This combined method gives the solution and its derivatives which are important in the sample problems treated, because they represent the stresses in a neighborhood of a singularity.

In Chapter 4, we report and discuss the numerical results on several examples. The techniques of Chapters 2 and 3 are applied to the problems, and the results are compared with the available solutions obtained by previous investigators. The numerical solution at the collocation points or at intermediate interpolation points might be interesting in itself, but the intention of this chapter is to give numerical evidence of the effectiveness of the method developed in this study; also, to show how well all the techniques of the previous chapters work together. In Chapter 5, we present our concluding remarks on this study.

Finally, the two general solutions of an angular region as representative of boundary singularity are shown in the appendix. The formulation for obtaining the weights of a Gauss-Legendre quadrature is presented as well as a table of the Legendre collocation points.

CHAPTER 2

LEGENDRE COLLOCATION METHOD

2.1 Introduction

This chapter deals with the Legendre Collocation Method for two-dimensional problems. The term *Legendre Collocation Method* is used here to signify that the solution of a P.D.E. for a two-dimensional region is obtained by using the zeros of a Legendre polynomial as the interior and boundary collocation points, which are also the Gauss-points in numerical integration. Since the results obtained by this method are the function values at the zeros of a Legendre polynomial, the numerical integration formula can be immediately applied to a problem that requires integration over the domain, such as torsion problems. This is one of the advantages of collocating at the roots of a Legendre polynomial.

For simplicity, the formulation in this chapter will be confined to elliptic equations applied to rectangular domains or regions that can be divided into several rectangles such as torsion of a bar of L-shaped cross section. In addition, the *p*-version rather than the *h*-version or *hp*-version technique [13,14,15,17,18] is emphasized. Thus, the domain is broken up into a fixed number of (relatively) large subdomains or elements, and high-order basis functions are used to construct a trial solution within each element. In this approach, convergence is achieved by increasing N , the number of collocation points within the elements, while keeping the number of elements fixed. Clearly, the logical choice for polynomials passing through the collocation points in this case will be Lagrange interpolation functions that can be easily constructed and increased to any desired degree N of the polynomial as will be shown later in this chapter.

As mentioned above, the emphasis in this study is on a higher-degree approximation or p -version technique. Finlayson [2] stated that in higher approximations the choice of collocation points is not crucial, but a choice in a certain way is possible and will make the calculations both convenient and accurate. Furthermore, Stewart and Villadsen [12,20] have pointed out, that a positioning of the collocation abscissas at the zeros of orthogonal polynomials leads to a rapidly convergent interpolation scheme, even for the functions that are poorly represented by polynomials. Therefore it appears to be a natural choice to use the zeros of a Legendre polynomial as the collocation points [4,20].

The application of the Legendre Collocation Method can be outlined as follows:

1. By giving as the only input N , the degree of the Legendre polynomial in computer program, the zeros of the Legendre polynomial are calculated and chosen as the interior collocation points. In addition, the two end points of the interval $[-1,1]$ are added as additional collocation points. This inclusion will enable us to ensure the continuity of both the function and the normal first derivative values across element boundaries, also to provide us with collocation points on the regional boundaries where the boundary conditions for the problem should be imposed. Thus, the total number of collocation points on the interval will be $(N + 2)$ points.
2. A one-dimensional trial solution in the form of a Lagrange interpolation polynomial is taken, and matrices **A** and **B** representing the first and second derivatives, respectively, are established. These derivatives are expressed in terms of the values of the function at the collocation points. The coefficients of matrix **A** are obtained by differentiation of the Lagrange interpolation polynomial and then evaluated at the collocation

points. The coefficients for the matrix \mathbf{B} are computed by simply squaring \mathbf{A} . Thus, the discretization matrices \mathbf{A} and \mathbf{B} are both $(N+2) \times (N+2)$. When the i^{th} row of \mathbf{A} is multiplied by the values of the function at the collocation points on the interval under consideration, one obtains the first derivative at a point which corresponds to row number i .

3. The Legendre Collocation Method proceeds by breaking up the computational domain into rectangular macro-elements forming the region. The trial solution in a two-dimensional domain is just the product of Lagrange polynomials in each of the dimensions. Therefore the derivatives at the chosen collocation points can be replaced by summations of particular rows obtained by operating with products of the matrix \mathbf{A} applied in the x and y directions multiplied by the known or unknown function values at the collocation points in the appropriate row. When the method is applied to the chosen domain, each macro-element is mapped from the physical (x,y) space into a local (ξ,η) coordinate system, and a set of simultaneous equations is generated as a result of satisfying the following conditions:

- The discrete approximation of the governing differential equation is satisfied at each **interior collocation point** of each element.
- The values of the function and normal derivative are required to be continuous at **collocation points located at inter-element boundaries**. Since a global numbering scheme is adopted for the entire domain, continuity of the function values is automatically ensured.

- Boundary conditions are satisfied at the **collocation points on the boundaries.**
 - At all **corners of the domain**, the boundary conditions are satisfied. In such cases where both the normal derivative and function values are prescribed at a corner, only the function value is chosen to be satisfied. If, the normal derivatives in both the x and y directions are prescribed at a corner, both derivatives are normalized so that satisfaction in both directions is possible.
4. The sets of linear equations occurring in the illustrative problems have been solved using LU decomposition together with forward and backward substitution to give the solution at the collocation points. The solutions at any other points can be easily computed by employing the two-dimensional Lagrange interpolation polynomials previously constructed. For problems with no singularities, the first derivatives at collocation points representing stresses or fluxes can be calculated by simply multiplying the solution function vectors by \mathbf{A} . For problems with singularities, a special treatment is necessary and has been developed for an accurate approximation in a neighborhood of a singularity.

In this study, the trial solutions chosen satisfy the governing differential equation and boundary conditions at the collocation points. Thus, the Legendre Collocation Method employed here is considered as a mixed collocation technique as defined in References [12,21].

2.2 One-dimensional Lagrangian Trial Solution

In many practical problems, it is impossible to determine the exact solution to the governing differential equations. The *exact solution* defined in this context is an explicit expression for the solution, in terms of known functions, which exactly satisfies the governing differential equations and boundary conditions.

As an alternative, the Legendre Collocation Method formulated in this study, seeks approximate solutions. These are explicit expressions in terms of known functions, but they only satisfy the governing equations and boundary conditions at the collocation points.

The construction of an approximate or a trial solution consists of constructing expressions for each trial function in terms of specific, known functions. The Legendre Collocation Method makes use of the classical method of Lagrange in approximating a function with given values at a discrete number of points by a finite sum of polynomials. The Lagrange interpolation polynomials are algebraically simple, and easy to work with. They provide a systematic procedure for constructing trial functions and for evaluating their derivatives at collocation points. Most important, the procedure can be easily implemented and automated for computers. For the same reason, the Lagrange formulation is widely used in the Finite Element Method [22,23].

An approximate solution will be denoted by a letter with a hat over it. Thus, \hat{u} will denote an approximate solution for u .

In the one-dimensional case, the $(N - 1)^{\text{th}}$ -degree Lagrange interpolation polynomial formula for a trial solution in the arbitrary interval $[x_1, x_N]$ can be defined as

$$\hat{u}(\xi) = \sum_{i=1}^N \ell_i(\xi) u_i \quad (2.1)$$

where N is the total number of interpolation points, u_i is the value of solution at the i^{th} point, and $\ell_i(\xi)$ are Lagrange interpolating functions which have the property

$$\ell_i(\xi_j) = \delta_{ij} = \begin{cases} 1 & \text{for } i = j \\ 0 & \text{for } i \neq j \end{cases} \quad (2.2)$$

and δ_{ij} is the Kronecker delta as defined above. It is important to note here that the interpolation points or nodes, are also collocation points. Thus, N is also the number of collocation points. Here the interior points within interval are chosen to be the zeros of a $(N-2)^{\text{th}}$ -degree Legendre polynomial, and the two end-points are purposely included as collocation points, for reasons previously discussed.

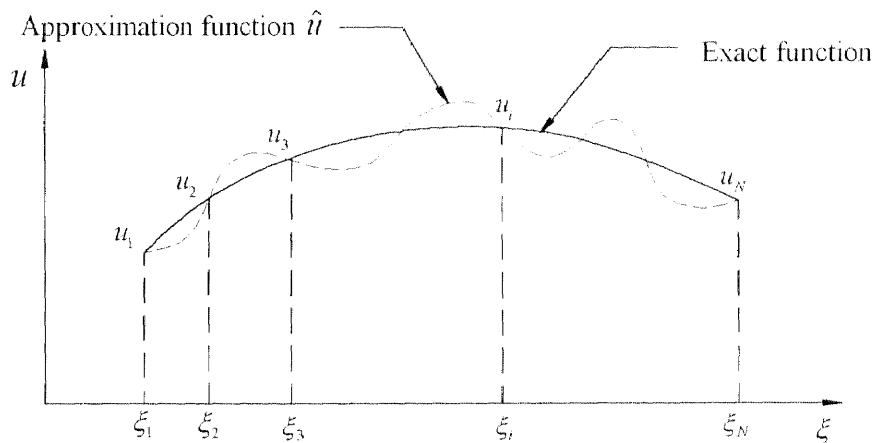


Figure 2.1 $(N-1)^{\text{th}}$ -degree approximate function.

The Lagrange interpolation function is defined by [24]

$$\begin{aligned}\ell_i(\xi) &= \frac{(\xi - \xi_1)(\xi - \xi_{i-1})(\xi - \xi_{i+1}) \dots (\xi - \xi_N)}{(\xi_i - \xi_1)(\xi_i - \xi_{i-1})(\xi_i - \xi_{i+1}) \dots (\xi_i - \xi_N)} \\ &= \prod_{\substack{j=1 \\ j \neq i}}^N \frac{(\xi - \xi_j)}{(\xi_i - \xi_j)}\end{aligned}\quad (2.3)$$

Another formulation of ℓ_i can be written as [1,19]

$$\ell_i(\xi) = \frac{P_N(\xi)}{(\xi - \xi_i)P'_N(\xi_i)} \quad (2.4)$$

where

$$\begin{aligned}P_N(\xi) &= (\xi - \xi_1)(\xi - \xi_2) \dots (\xi - \xi_N) \\ &= \prod_{j=1}^N (\xi - \xi_j)\end{aligned}\quad (2.5)$$

is a node polynomial of N^{th} -degree with the leading coefficient equal to one, and $P'_N(\xi_i)$ is the first derivative of $P_N(\xi)$ defined as

$$P'_N(\xi_i) = \frac{d}{dx}[P_N(\xi)] \Big|_{\xi=\xi_i} = \prod_{\substack{j=1 \\ j \neq i}}^N (\xi_i - \xi_j) \quad \text{for } \xi = \xi_i \quad (2.6)$$

and evaluated at point ξ_i , which is the i^{th} collocation point. In this study, the interior collocation points are the zeros of a $(N-2)^{\text{th}}$ -degree Legendre polynomial.

An approximate solution expressed as a Lagrange interpolation polynomial, as in Equation (2.1), is a variable-order polynomial, and it can be easily automated to be constructed to any degree desired on a computer. As in the computer program written for this study, one needs only to input any desired integer ($N-2$) as the order of the Legendre polynomial, two end-points are automatically added,

geometric coordinates of the domain are supplied, and then the problem is solved. These are the only inputs needed to solve the problem using the Legendre Collocation Method. From the standpoint of a p -version Legendre Collocation Method, this automation is highly desirable since increased accuracy is achieved by increasing N . Another important attraction of these polynomials is that the undetermined coefficients u_i in Equation (2.1) are also the solutions at the collocation points once the problem is solved. Solution values at any other locations in the domain can be computed by interpolation from the polynomials previously constructed.

2.3 Differentiation of a Lagrange Interpolation Polynomial

To apply the Legendre Collocation Method directly to differential equations, the derivatives at the collocation points are expressed in terms of the values of the solution function at collocation points. These derivatives at the collocation points are obtained by matrix operations on the column vector of the solution function. The solution function vector must include the boundary conditions. The column vector for the derivatives must include the boundary conditions on the derivatives. The resultant matrices are substituted into the differential equation(s). In order to obtain the coefficient matrices for first and second derivatives, Equation (2.1) has to be differentiated. Thus,

$$\left. \frac{d \hat{u}}{d \xi} \right|_{\xi = \xi_j} = \sum_{i=1}^N \left[\frac{d \ell_i(\xi)}{d \xi} \right]_{\xi = \xi_j} u_i \quad (2.7)$$

As shown in the right-hand side of the above equation, it becomes important to find the expression for the derivatives of the Lagrange interpolation function $\ell_i(\xi)$.

If Equation (2.4) is re-written as

$$\frac{P_N(\xi)}{P'_N(\xi_i)} = (\xi - \xi_i) \ell_i(\xi) \quad (2.8)$$

and then is differentiated, we obtain

$$\frac{P'_N(\xi)}{P'_N(\xi_i)} = (\xi - \xi_i) \ell'_i(\xi) + \ell_i(\xi) \quad (2.9)$$

$$\frac{P''_N(\xi)}{P'_N(\xi_i)} = (\xi - \xi_i) \ell''_i(\xi) + 2\ell'_i(\xi) \quad (2.10)$$

.

.

$$\frac{P^{(k)}_N(\xi)}{P'_N(\xi_i)} = (\xi - \xi_i) \ell^{(k)}_i(\xi) + k \ell^{(k-1)}_i(\xi) \quad (2.11)$$

where k in Equation (2.11) denotes the k^{th} -derivative.

Normally only $\ell'_i(\xi)$ is of interest as we shall see. For $\xi = \xi_i$, Equation (2.10) becomes

$$\ell'_i(\xi_i) = \frac{1}{2} \frac{P''_N(\xi_i)}{P'_N(\xi_i)} \quad \text{for } \xi = \xi_i \quad (2.12)$$

Using Equation (2.9), for $\xi = \xi_j \neq \xi_i$ and noting that $\ell_i(\xi_j) = 0$, one obtains

$$\ell'_i(\xi_j) = \frac{1}{(\xi_j - \xi_i)} \frac{P'_N(\xi_j)}{P'_N(\xi_i)} \quad \text{for } \xi = \xi_j \neq \xi_i \quad (2.13)$$

As shown in Equation (2.12) and (2.13), it is necessary to compute the first and second derivatives of $P_N(\xi)$ at collocation points. The recurrence relation for

$P_N(\xi)$, which is very suitable for computer programming will be used as a basis for finding recurrence expressions for the derivatives. The node polynomial in Equation (2.5) can be generated by the recurrence formulas [1,19]:

$$\begin{aligned} P_0(\xi) &= 1 \\ P_j(\xi) &= (\xi - \xi_j) P_{j-1}(\xi) \quad \text{for } j = 1, 2, \dots, N \end{aligned} \tag{2.14}$$

We differentiate Equation (2.14) twice to yield

$$P'_j(\xi) = (\xi - \xi_j) P'_{j-1}(\xi) + P_{j-1}(\xi) \tag{2.15}$$

$$P''_j(\xi) = (\xi - \xi_j) P''_{j-1}(\xi) + 2P'_{j-1}(\xi) \tag{2.16}$$

In general, for k^{th} differentiation, one has

$$P_j^{(k)}(\xi) = (\xi - \xi_j) P_{j-1}^{(k)}(\xi) + k P_{j-1}^{(k-1)}(\xi) \tag{2.17}$$

and the values of $P'_N(\xi_i)$ and $P''_N(\xi_i)$ are obtained by inserting ξ_i for ξ in Equations (2.15) and (2.16).

Equation (2.14) is started with $P_0(\xi) = 1$, as a result $P'_0(\xi) = 0$, and Equation (2.15) with $j = 1$ will be

$$P'_1(\xi) = (\xi - \xi_1) P'_0(\xi) + P'_0(\xi) = 1$$

Whence,

$$\begin{aligned} P'_2(\xi) &= (\xi - \xi_2) P'_1(\xi) + P'_1(\xi), \quad \text{where } P'_1(\xi) = (\xi - \xi_1) \\ &= (\xi - \xi_2) + (\xi - \xi_1) \end{aligned}$$

$$\begin{aligned} P'_3(\xi) &= (\xi - \xi_3) P'_2(\xi) + P'_2(\xi), \quad \text{where } P'_2(\xi) = (\xi - \xi_1)(\xi - \xi_2) \\ &= (\xi - \xi_3)(\xi - \xi_2) + (\xi - \xi_3)(\xi - \xi_1) + (\xi - \xi_1)(\xi - \xi_2) \end{aligned}$$

.

.

$$P'_N(\xi) = (\xi - \xi_N) P'_{N-1}(\xi) + P'_{N-1}(\xi)$$

Similarly, for Equation (2.16), the first iteration gives

$$P''_1(\xi) = (\xi - \xi_1) P''_0(\xi) + 2P'_0(\xi)$$

where $P_0'(\xi) = P_0''(\xi) = 0$; therefore

$$P_1''(\xi) = 0$$

$$P_2''(\xi) = (\xi - \xi_2)P_1''(\xi) + 2P_1'(\xi) = 2$$

$$P_3''(\xi) = (\xi - \xi_3)P_2''(\xi) + 2P_2'(\xi)$$

$$\vdots$$

$$P_N''(\xi) = (\xi - \xi_N)P_{N-1}''(\xi) + 2P_{N-1}'(\xi)$$

Clearly, the values of previously calculated $P_{j-1}''(\xi)$ and $P_{j-1}'(\xi)$ are used to obtain $P_j''(\xi)$ and $P_j'(\xi)$. Hence, the recurrence formulas presented above should be easy to implement on a computer.

2.4 Coefficient Matrices for First and Second Derivatives

It follows from Equation (2.7), that the values of the derivatives at collocation points can be expressed in terms of the values of the function, also at those points.

Equation (2.7) as the first derivative of an approximate solution \hat{u} at the i^{th} point is repeated here in another form

$$\hat{u}'_i = \sum_{j=1}^N \ell'_j(\xi_i) u_j \quad (2.18)$$

and for $i = 1, 2, \dots, N$, the vector of the first derivative of an approximate solution can then be expressed in matrix form as

$$\begin{Bmatrix} \hat{u}'_1 \\ \hat{u}'_2 \\ \vdots \\ \hat{u}'_N \end{Bmatrix} = \begin{bmatrix} \ell'_1(\xi_1) & \ell'_2(\xi_1) & \cdots & \ell'_N(\xi_1) \\ \ell'_1(\xi_2) & \ell'_2(\xi_2) & \cdots & \ell'_N(\xi_2) \\ \vdots & \vdots & \ddots & \vdots \\ \ell'_1(\xi_N) & \ell'_2(\xi_N) & \cdots & \ell'_N(\xi_N) \end{bmatrix} \begin{Bmatrix} u_1 \\ u_2 \\ \vdots \\ u_N \end{Bmatrix} \quad (2.19)$$

Note that the diagonal elements of the coefficient matrix are computed by Equation (2.12), and the off-diagonal coefficients are calculated by Equation (2.13). Equation (2.19) can also be written in compact form as

$$\hat{\mathbf{u}}' = \frac{d}{d\xi} \hat{\mathbf{u}} = \mathbf{A}\mathbf{u} \quad (2.20)$$

where $A_{ij} = \ell'_j(\xi_i)$ are the coefficients of the $N \times N$ matrix \mathbf{A} . Examination of Equations (2.19) and (2.20) reveals that the first derivative operator $\frac{d}{d\xi}$ is represented by the coefficient matrix \mathbf{A} . This matrix \mathbf{A} now becomes a basis for obtaining the higher derivatives expressed in terms of the values of the function at the collocation points.

Similarly to the expression in Equation (2.20), the second derivative can be written as

$$\frac{d^2}{d\xi^2} \hat{\mathbf{u}} = \frac{d}{d\xi} \left[\frac{d}{d\xi} \hat{\mathbf{u}} \right]$$

Noting that $\frac{d}{d\xi}$ can be replaced by \mathbf{A} , we have

$$\begin{Bmatrix} \hat{u}_1'' \\ \hat{u}_2'' \\ \vdots \\ \hat{u}_N'' \end{Bmatrix} = \begin{bmatrix} \ell'_1(\xi_1) & \ell'_2(\xi_1) & \cdots & \ell'_N(\xi_1) \\ \ell'_1(\xi_2) & \ell'_2(\xi_2) & \cdots & \ell'_N(\xi_2) \\ \vdots & \vdots & \ddots & \vdots \\ \ell'_1(\xi_N) & \ell'_2(\xi_N) & \cdots & \ell'_N(\xi_N) \end{bmatrix} \begin{Bmatrix} u_1' \\ u_2' \\ \vdots \\ u_N' \end{Bmatrix} \quad (2.21)$$

Replacing $\langle \hat{u}_1', \hat{u}_2', \dots, \hat{u}_N' \rangle$ with Equation (2.19), one has

$$\begin{Bmatrix} \hat{u}_1'' \\ \hat{u}_2'' \\ \vdots \\ \hat{u}_N'' \end{Bmatrix} = \begin{bmatrix} \ell'_1(\xi_1) & \ell'_2(\xi_1) & \cdots & \ell'_N(\xi_1) \\ \ell'_1(\xi_2) & \ell'_2(\xi_2) & \cdots & \ell'_N(\xi_2) \\ \vdots & \vdots & \ddots & \vdots \\ \ell'_1(\xi_N) & \ell'_2(\xi_N) & \cdots & \ell'_N(\xi_N) \end{bmatrix} \begin{bmatrix} \ell'_1(\xi_1) & \ell'_2(\xi_1) & \cdots & \ell'_N(\xi_1) \\ \ell'_1(\xi_2) & \ell'_2(\xi_2) & \cdots & \ell'_N(\xi_2) \\ \vdots & \vdots & \ddots & \vdots \\ \ell'_1(\xi_N) & \ell'_2(\xi_N) & \cdots & \ell'_N(\xi_N) \end{bmatrix} \begin{Bmatrix} u_1 \\ u_2 \\ \vdots \\ u_N \end{Bmatrix}$$

or

$$\frac{d^2}{d\xi^2} \hat{\mathbf{u}} = \mathbf{A}^2 \mathbf{u} \quad (2.22)$$

If we let $\mathbf{B} = \mathbf{A}^2$ then

$$\frac{d^2}{d\xi^2} \hat{\mathbf{u}} = \mathbf{B} \mathbf{u} \quad (2.23)$$

$$\text{where } B_{ij} = \sum_{j=1}^N \ell'_j(\xi_i) \ell'_i(\xi_j).$$

Alternatively, as in Reference [1,19], the coefficient matrix \mathbf{B} can also be obtained by differentiating of Equation (2.8) three times, so that

$$\frac{P''_N(\xi)}{P'_N(\xi)} = (\xi - \xi_i) \ell'''_i(\xi) + k \ell''_i(\xi)$$

and for $\xi = \xi_i$, the above equation yields

$$\ell''_i(\xi_i) = \frac{1}{3} \frac{P''_N(\xi_i)}{P'_N(\xi_i)}$$

as the coefficients located in the diagonal of the matrix \mathbf{B} . The off-diagonal elements can be computed by inserting $\xi = \xi_j \neq \xi_i$ into Equation (2.10) so that

$$\ell''_i(\xi_j) = \frac{1}{(\xi_j - \xi_i)} \left[\frac{P''_N(\xi_j)}{P'_N(\xi_i)} - 2\ell'_i(\xi_j) \right]$$

It is clear that, Equation (2.22) as the proposed computation for matrix \mathbf{B} is the simplest procedure. Furthermore, the coefficient matrix for any higher order derivative can be easily obtained.

In general, the k^{th} derivative of $\hat{\mathbf{u}}$ can be determined by

$$\frac{d^{(k)}}{d\xi^{(k)}} \hat{\mathbf{u}} = \mathbf{A}^k \mathbf{u} \quad (2.24)$$

where \mathbf{A}^k is the k^{th} power of matrix \mathbf{A} . Thus, any desired order of derivative expressed in terms of the values of the function at collocation points can be

obtained by simply raising \mathbf{A} to the k^{th} power. This can be performed easily on a computer, and it makes the Legendre Collocation Method very attractive.

It is important to note here that the order of the approximate solution \hat{u} should be higher than or at least equal to k . Otherwise, a square matrix \mathbf{A}^k will be zero and the higher order derivatives in the differential equation will not be taken into account.

2.5 Zeros of Legendre Polynomials

We present an automated method of calculating the zeros of Legendre polynomials. As previously stated, these points are used as interior collocation points. They are also the Gauss points in numerical integration. We start with the recurrence relation from the theory of Legendre polynomials in the interval $-1 \leq \xi \leq 1$ [25]:

$$\begin{aligned} P_0(\xi) &= 1 \\ (i+1)P_{i+1}(\xi) &= (2i+1)\xi P_i(\xi) - i P_{i-1}(\xi) \end{aligned} \quad (2.25)$$

for $i = 0, 1, 2, \dots, n$. Then by letting

$$j = i + 1, \quad \text{for } i = 0, 1, 2, \dots, n \text{ or } j = 1, 2, \dots, N$$

Equation (2.25) can be written as

$$P_j(\xi) = \frac{(2j-1)\xi P_{j-1}(\xi) - (j-1)P_{j-2}(\xi)}{j} \quad (2.26)$$

Expressed as in Equation (2.26), the recurrence relation becomes easy to program.

The derivative of a polynomial is calculated using the following recursion formula [25]

$$(\xi^2 - 1)P'_j(\xi) = j\xi P_j(\xi) - jP_{j-1}(\xi) \quad (2.27a)$$

or

$$P'_j(\xi) = \frac{j[\xi P_j(\xi) - P_{j-1}(\xi)]}{(\xi^2 - 1)} \quad (2.27b)$$

Using the available values calculated by Equations (2.26) and (2.27b), the roots of a polynomial are found by the iteration formula

$$\xi_{k+1} = \xi_k - \frac{P_N(\xi_k)}{P'_N(\xi_k)} \quad (2.28)$$

which is the well-known Newton's method.

Knowing that the zeros are symmetric in the interval from $x = -1$ to $x = +1$, one needs only to find half of the zeros, and the other half are obtained by reflecting about the origin by changing sign. To jump directly to the neighborhood of the desired root, where it converges by Newton's method, we will use the following initial 'guess' to approximate the k^{th} root [26]:

$$\xi_k = \cos\left(\frac{4k-1}{4N+2}\pi\right) \quad (2.29)$$

The above approximation is based on an asymptotic formula used to define the Legendre polynomial $P_N(\xi)$ in terms of θ where $\xi = \cos\theta$, and θ is computed using

$$\theta_k = \frac{4k-1}{4N+2}\pi + \frac{1}{8N^2}\cot\frac{4k-1}{4N+2}\pi + O(N^{-3}) \quad \text{for } k = 1, 2, \dots, N \quad (2.30)$$

Notice that Equation (2.29) uses only the first term of Equation (2.30). The refinement for the location of the zero is done by Newton's method as mentioned above.

As mentioned earlier, the Legendre Collocation Method provides the solution at the collocation points. The interior points within the interval are the zeros of a Legendre polynomial. Thus, for a problem that requires numerical integration, as in the St. Venant torsion problem, it is necessary to calculate the weights associated with the zeros of the Legendre polynomial that were previously

obtained by Newton's iteration formula in Equation (2.28). These weights, used in Gauss-Legendre quadrature can be computed from

$$w_i = \frac{2}{(1 - \xi_i^2)[P'_N(\xi_i)]^2} \quad (\text{C.16})$$

as derived in Appendix C. Notice that the formula for computing w_i also consists of terms needed for finding the zeros of the Legendre polynomial in (2.28). Thus, this computation is a simple matter once the zeros of the Legendre polynomial are calculated.

2.6 Legendre Collocation Method Applied to Differential Equations in Two-Dimensional Domain

The Legendre Collocation Method is based on the Orthogonal Collocation Method introduced by Villadsen and his co-workers [1,12,19,20,27], which consists of satisfying the differential equation(s) and/or boundary conditions at the zeros of a selected Jacobi Polynomial of a selected degree. Increasing the degree of the polynomial and, correspondingly the number of zeros, increases accuracy, but also the number of unknowns. In the Legendre Collocation Method, we use Legendre Polynomials exclusively, because it simplifies the treatment, and we found by numerical experimentation that this yields the best accuracy.

To illustrate the method, consider the Poisson equation

$$\nabla^2 u = \frac{\partial^2 u}{\partial x^2} + \frac{\partial^2 u}{\partial y^2} = f(x, y) \quad (2.31)$$

in the domain Ω as depicted in Figure 2.2, and subjected to essential, or Dirichlet, boundary conditions

$$u = \bar{u} \text{ on } \Gamma_1 \quad (2.32)$$

and natural or Neumann boundary conditions

$$\frac{\partial u}{\partial n} = \bar{q} \text{ on } \Gamma_2 \quad (2.33)$$

where the total boundary $\Gamma = \Gamma_1 + \Gamma_2$. Note that \bar{u} and \bar{q} are prescribed values of the function and the normal derivative on the boundaries Γ_1 and Γ_2 , respectively.

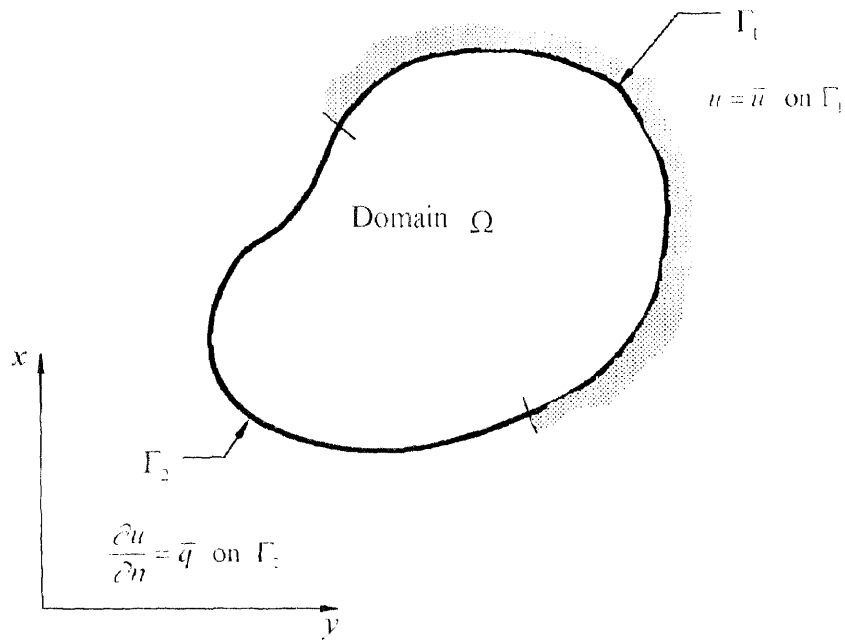


Figure 2.2 Domain and boundary conditions for Poisson equation.

Let \hat{u} be the approximate solution in terms of a series of known functions with arbitrary coefficients. This trial solution satisfies none of the given Equations (2.31), (2.32) and (2.33) everywhere so that the so-called *mixed collocation* technique is employed [12,21]. The mixed collocation method is a general technique that can be applied to any differential equations and boundary conditions. In contrast, the *interior collocation* technique uses a trial solution \hat{u} that satisfies the boundary conditions in Equations (2.32) and (2.34) identically,

and the undetermined coefficients in the trial solution are found by satisfying the governing differential equation (2.31) at n points in the domain Ω . **Boundary collocation** requires an approximate solution \hat{u} that satisfies the differential equation (2.31) identically, and the coefficients are adjusted to satisfy the boundary conditions in Equations (2.32) and (2.34) at n points on $\Gamma = \Gamma_1 + \Gamma_2$.

2.7 Linear Transformation of Two-dimensional Domains

As mentioned in the preceding sections, the interior collocation points are chosen at the zeros of a Legendre polynomial defined in the interval from $\xi = -1$ to $\xi = +1$. In addition to the n zeros of the Legendre polynomial, for each dimension, two end points are added as extra interpolation points in the trial solution. Therefore the total number of points in one dimension will be $(n+2)$ points, and the trial solutions will be $(n+1)$ -degree polynomials in the x - and y -directions.

In a procedure used by several investigators in this field [4,12,19, 28,29,30,31], the zeros of orthogonal polynomials are taken as the collocation points, and the domain is broken up into several pieces as in the Finite Element Method. This method is sometimes called Orthogonal Collocation on Finite Element [4]. By adding the two endpoints of each interval to the zeros of the Legendre polynomial in each direction, and using a global numbering scheme for the entire domain, the mapping of the boundary nodes of the so-called parent element ($\xi = \pm 1, \eta = \pm 1$) onto the boundary nodes of the real element in the rectangular domain $x \in (x_i, x_{i+1}), y \in (y_i, y_{i+1})$ (see Figure 2.3), will automatically ensure the continuity of the function values at the collocation points on inter-element boundaries. Furthermore, there are enough undetermined parameters to

enforce continuity of normal derivatives at the inter-element boundary collocation points.

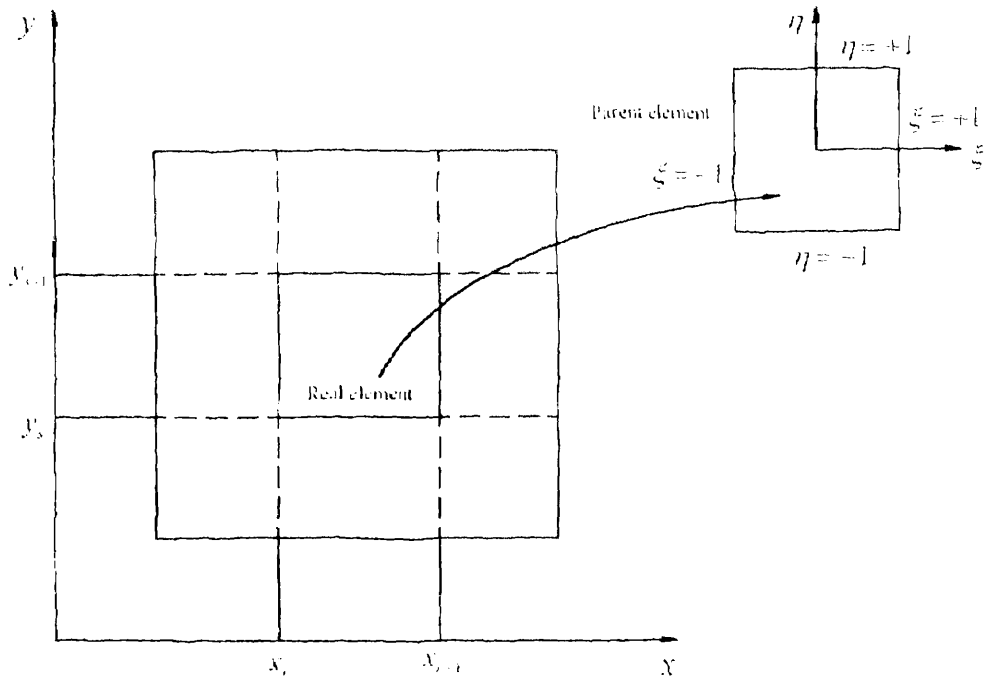


Figure 2.3 Linear mapping of real element onto parent element

Since the final solution is obtained as the function values at the zeros of a Legendre polynomial, we have "ready to use" function values for numerical integration. For example, in the problem of a rectangular bar under torsion, the torque is calculated by

$$\begin{aligned}
 M_t &= 2 \iint u dx dy \\
 &= 2c_1 c_2 \sum_{i=1}^{NLY} \sum_{j=1}^{NLY} w_i w_j u(x(\xi_i), y(\eta_j))
 \end{aligned} \tag{2.34}$$

where u is the Prandtl stress function, NLX and NLY are the number of collocation points, w_i and w_j are the weights corresponding to the zeros of the Legendre polynomial, and c_1 and c_2 are constants due to linear transformations in the x and y directions, respectively.

The transformation of rectangular shapes is straightforward so that

$$x = \frac{x_{r+1} + x_r}{2} + \frac{x_{r+1} - x_r}{2} \xi \quad (2.35)$$

and

$$y = \frac{y_{s+1} + y_s}{2} + \frac{y_{s+1} - y_s}{2} \eta \quad (2.36)$$

Hence, c_1 and c_2 are given by

$$c_1 = \frac{x_{r+1} - x_r}{2} = \frac{\Delta x^{(e)}}{2} \quad (2.37)$$

and

$$c_2 = \frac{y_{s+1} - y_s}{2} = \frac{\Delta y^{(e)}}{2}, \quad (2.38)$$

where $\Delta x^{(e)}$ and $\Delta y^{(e)}$ are element sizes in the x and y directions.

2.8 The Legendre Collocation Element Formulation in Two-dimensional Domains

As in the Finite Element Method, a trial solution is constructed in the parent element $\xi - \eta$ coordinate system. Thus, in each element, using a one-dimensional trial solution Equation (2.1) as a basis, the trial solution for a two-dimensional problem is defined by the tensor-product of the ξ and η spaces, so that

$$\hat{u}(\xi, \eta) = \sum_{i=1}^{NPX} \sum_{j=1}^{NPY} \ell_i(\xi) \ell_j(\eta) u_i \quad (2.39)$$

where NPX and NPY are the number of points in the ξ and η directions, respectively. This interpolation Equation (2.39) is not actually used in the solution process since the problem is solved in terms of the value of u_y at the collocation points. The collocation points are chosen at (ξ_i, η_j) where ξ_i and η_j are the same collocation points defined in one dimension.

In order to replace the Laplacian operator in Equation (2.31) and the normal derivative in the Neumann boundary conditions in Equation (2.33) with the derivatives expressed in terms of function values at the collocation points, Equation (2.39) has to be differentiated. The first partial derivative of Equation (2.39) with respect to ξ will be

$$\hat{u}_{,\xi} = \frac{\partial \hat{u}}{\partial \xi} = \sum_{i=1}^{NPX} \sum_{j=1}^{NPY} \ell'_i(\xi) \ell_j(\eta) u_y \quad (2.40)$$

At a collocation point $\hat{u}(\xi_k, \eta_m)$, all terms of $\ell_j(\eta_m)$ except that for $j = m$ will drop-out

$$\ell_j(\eta_m) = 1$$

Therefore, for each element, the first derivative with respect to ξ at the collocation points can be written as

$$\hat{u}_{,\xi}(\xi_k, \eta_m) = \frac{\partial}{\partial \xi} [\hat{u}(\xi_k, \eta_m)] = \sum_{i=1}^{NPX} \ell'_i(\xi_k) u_{im} \quad (2.41)$$

for $k = 1, 2, \dots, NPX$ and $m = 1, 2, \dots, NPY$

or in matrix form

$$\begin{Bmatrix} \hat{u}_{,\xi}(\xi_1, \eta_m) \\ \hat{u}_{,\xi}(\xi_2, \eta_m) \\ \vdots \\ \hat{u}_{,\xi}(\xi_{NPX}, \eta_m) \end{Bmatrix} = \begin{bmatrix} \ell'_1(\xi_1) & \ell'_2(\xi_1) & \cdots & \ell'_{NPX}(\xi_1) \\ \ell'_1(\xi_2) & \ell'_2(\xi_2) & \cdots & \ell'_{NPX}(\xi_2) \\ \vdots & \vdots & \ddots & \vdots \\ \ell'_1(\xi_{NPX}) & \ell'_2(\xi_{NPX}) & \cdots & \ell'_{NPX}(\xi_{NPX}) \end{bmatrix} \begin{Bmatrix} u_{1m} \\ u_{2m} \\ \vdots \\ u_{NPX,m} \end{Bmatrix} \quad (2.42)$$

for $m = 1, 2, \dots, NPY$. Examining the coefficient matrix in Equation (2.42), it is clear that this is the matrix \mathbf{A} in Equation (2.20). Thus, \mathbf{A} which used for calculating the first derivative at the collocation points is not only applicable for the one-dimensional problem, but is also valid for the two-dimensional case. Matrix \mathbf{A} now serves as a basis for computing the higher derivatives at the collocation points. Consequently, \mathbf{B} in Equation (2.23) can also be used to obtain the expression for the second partial derivative at the collocation points along the ξ and η directions. In concise form, Equation (2.42) will be

$$\hat{\mathbf{u}}_{,\xi} = \mathbf{AXu} \quad (2.43)$$

Similarly, the first derivatives with respect to η can be written as

$$\hat{u}_{,\eta}(\xi_k, \eta_m) = \frac{\partial}{\partial \eta} [\hat{u}(\xi_k, \eta_m)] = \sum_{j=1}^{NPY} \ell'_j(\eta_m) u_{kj} \quad (2.44)$$

where k and m have the same meaning as above. In matrix form, Equation (2.44) can be written as

$$\begin{Bmatrix} \hat{u}_{,\eta}(\xi_k, \eta_1) \\ \hat{u}_{,\eta}(\xi_k, \eta_2) \\ \vdots \\ \hat{u}_{,\eta}(\xi_k, \eta_{NPY}) \end{Bmatrix} = \begin{bmatrix} \ell'_1(\eta_1) & \ell'_2(\eta_1) & \cdots & \ell'_{NPY}(\eta_1) \\ \ell'_1(\eta_2) & \ell'_2(\eta_2) & \cdots & \ell'_{NPY}(\eta_2) \\ \vdots & \vdots & \ddots & \vdots \\ \ell'_1(\eta_{NPY}) & \ell'_2(\eta_{NPY}) & \cdots & \ell'_{NPY}(\eta_{NPY}) \end{bmatrix} \begin{Bmatrix} u_{k1} \\ u_{k2} \\ \vdots \\ u_{k,NPY} \end{Bmatrix} \quad (2.45)$$

Again, in a concise form, Equations (2.44) and (2.45) will be

$$\hat{\mathbf{u}}_{,\eta} = \mathbf{AYu}$$

Note that for $NPX = NPY$, \mathbf{AX} is the same as \mathbf{AY} . Similar conditions apply for \mathbf{B} in x and y directions.

Denoting the approximate solution at the k^{th} collocation point in ξ and the m^{th} collocation point in η as

$$\hat{u}_{km} = \hat{u}(\xi_k, \eta_m)$$

and replacing \mathbf{B} by \mathbf{BX} or \mathbf{BY} as required, the second derivative with respect to ξ at the collocation point (ξ_k, η_m) can be written as

$$\left. \frac{\partial^2 \hat{u}}{\partial \xi^2} \right|_{km} = \sum_{i=1}^{NPX} BX_{ki} u_{im} \quad (2.46)$$

where BX_{ki} are the coefficients of \mathbf{BX} in the k^{th} row. The second derivative with respect to η will be

$$\left. \frac{\partial^2 \hat{u}}{\partial \eta^2} \right|_{km} = \sum_{j=1}^{NPF} BY_{mj} u_{kj} \quad (2.47)$$

In the collocation method, the governing differential equation (2.31), and the boundary conditions in Equations (2.32) and (2.33) can be written as

$$\nabla^2 \hat{u}(\bar{r}_i) - f(\bar{r}_i) = 0 \quad \text{in the domain } \Omega \quad (2.48)$$

$$\hat{u}(\bar{r}_i) - \bar{u} = 0 \quad \text{on boundary } \Gamma_1 \quad (2.49)$$

$$\frac{\partial \hat{u}(\bar{r}_i)}{\partial n} - \bar{q} = 0 \quad \text{on boundary } \Gamma_2 \quad (2.50)$$

where \bar{r}_i are the collocation points in the domain and on the boundaries. In the Legendre Collocation Method, Equation (2.48) will be evaluated at the interior collocation points, which are the zeros of a Legendre polynomial. Equations (2.49) and (2.50) are satisfied at the collocation points on the boundaries.

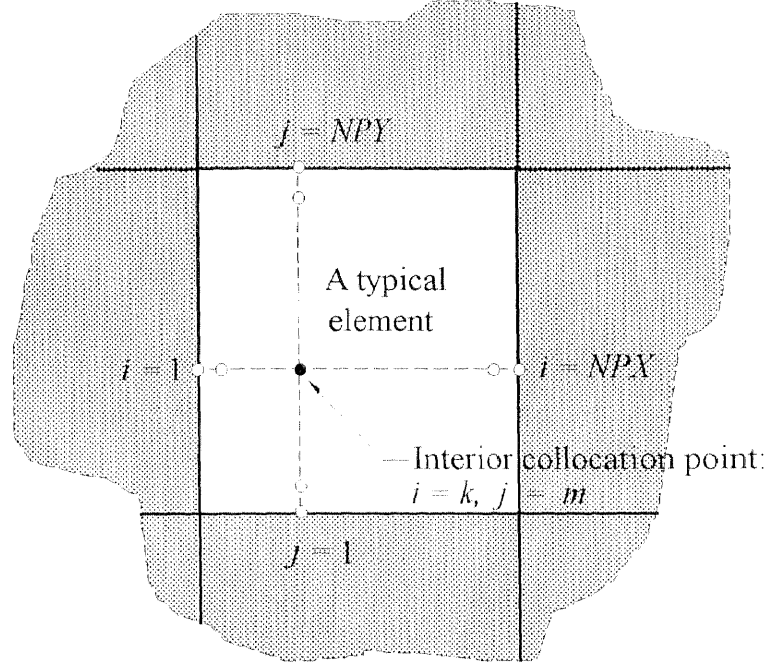


Figure 2.4 A typical interior collocation point where the governing equation is evaluated.

Equation (2.48) is applied at the km^{th} interior collocation point (see Figure 2.4), and mapping from the physical (x,y) coordinate into a local (ξ,η) coordinate as shown in Figure 2.3, the resulting equation will be

$$\left(\frac{2}{x_{r+1} - x_r}\right)^2 \sum_{i=1}^{NPX} BX_{ki} u_{im} + \left(\frac{2}{y_{s+1} - y_s}\right)^2 \sum_{j=1}^{NPY} BY_{mj} u_{kj} = f(x_k, y_m) \quad (2.51)$$

where in the above equation, the constants due to the transformation have been taken into account. Equation (2.51) has to be repeated for each interior collocation point inside the domain, such that $k = 2, 3, \dots, NPX - 1$ and $m = 2, 3, \dots, NPY - 1$. Furthermore, the problem is solved based on a global numbering scheme, where the local double indices km should be converted to a single index in the global

scheme. Thus, continuity of the solution at the inter-element boundary points is automatically satisfied (see Figure 2.5).

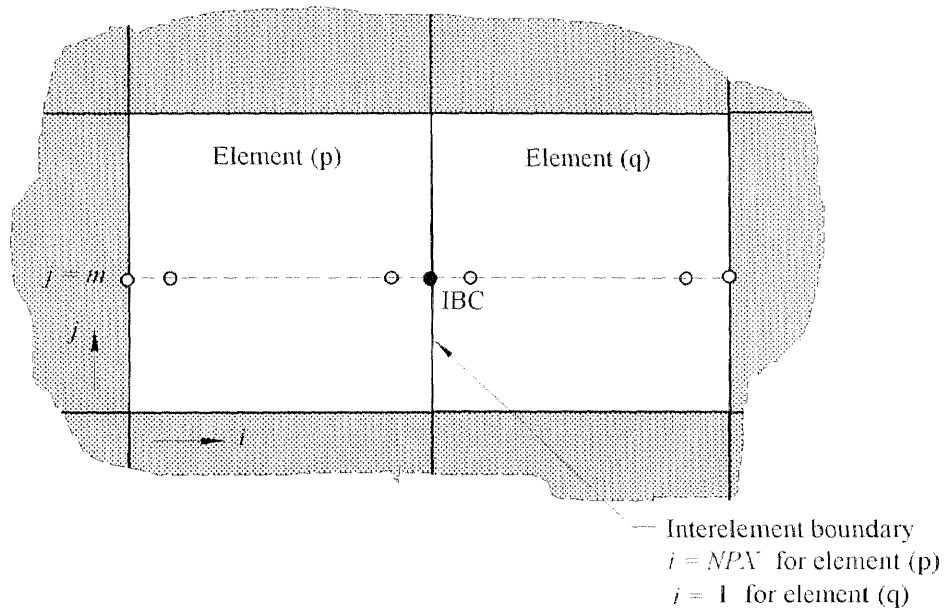


Figure 2.5 Inter-element boundary point IBC at which the continuity of the function and normal derivative is imposed.

As mentioned earlier, for a particular point IBC at an inter-element boundary point as shown in Figure 2.5, the continuity of the normal derivative can be imposed by requiring that

$$\frac{2}{\Delta x^{(p)}} \sum_{i=1}^{NPY} AX_{NPY,i} u_{im} = \frac{2}{\Delta x^{(q)}} \sum_{i=1}^{NPY} AX_{1i} u_{im} \quad (2.52)$$

where $\Delta x^{(p)}$ and $\Delta x^{(q)}$ are the element sizes of element (p) and element (q), respectively in the x direction. Equation (2.52) will be applied at all collocation points on the boundaries between elements. Similar equations can be obtained for satisfying the continuity of the normal derivative in the y direction.

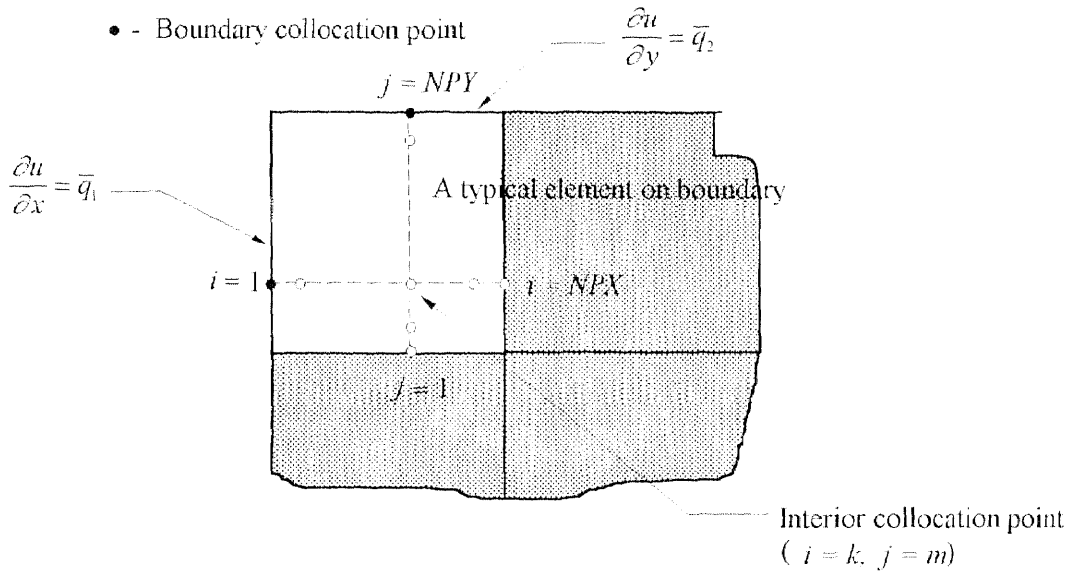


Figure 2.6 Boundary points located at left-side vertical and top-side horizontal boundaries

If the Neumann boundary condition in Equation (2.50) is prescribed on the left-side vertical boundary as shown in Figure 2.6, then for each boundary collocation point, the resulting equation is

$$\frac{2}{\Delta x^{(e)}} \sum_{i=1}^{NPX} AX_{1i} u_{im} = \bar{q}_1 \quad (2.53)$$

where $\Delta x^{(e)}$ is the size of element in x direction, and \bar{q}_1 is the prescribed normal derivative. As depicted in Figure 2.6, Equation (2.53) is applied at the m^{th} collocation point in the η direction.

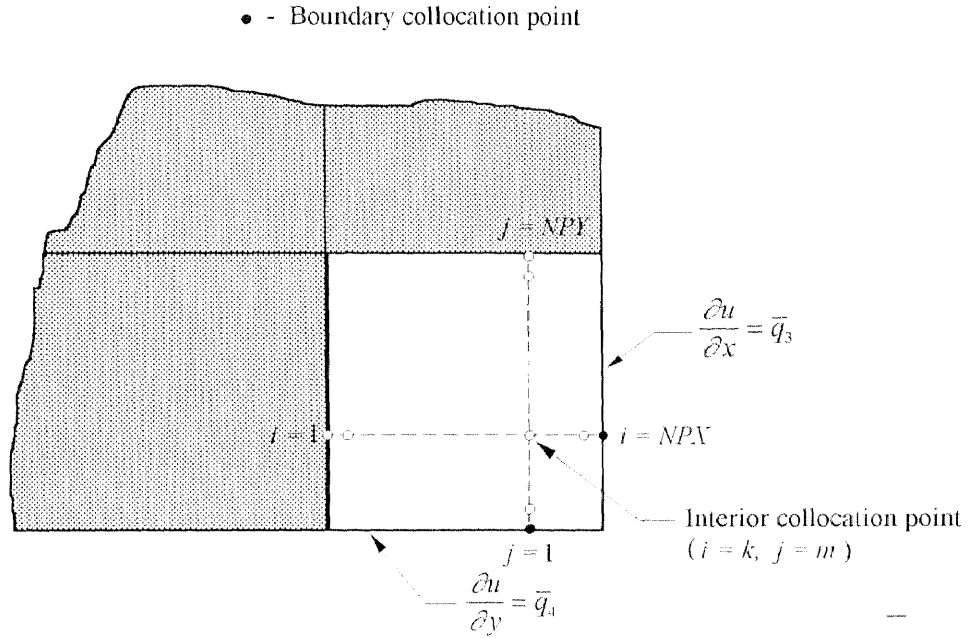


Figure 2.7 Boundary points located at right-side vertical and bottom-side horizontal boundaries

In case Equation (2.50) is prescribed on the top-side horizontal boundary (Figure 2.6), we will have

$$\frac{2}{\Delta y^{(e)}} \sum_{j=1}^{NPY} A Y_{NPY,j} u_{kj} = \bar{q}_2 \quad (2.54)$$

for the k^{th} boundary collocation point in ξ (see Figure 2.6).

Applying Equation (2.50) at the boundary collocation point on the right-side vertical boundary (Figure 2.7), where \bar{q}_3 is prescribed, we have

$$\frac{2}{\Delta x^{(e)}} \sum_{i=1}^{NPX} A X_{NPX,i} u_{im} = \bar{q}_3 \quad (2.55)$$

Similarly, for the boundary point located on the bottom-side of the horizontal boundary (Figure 2.7), the equation will be

$$\frac{2}{\Delta y^{(e)}} \sum_{j=1}^{NPY} A Y_{1j} u_{kj} = \bar{q}_4 \quad (2.56)$$

Equations (2.53), (2.54), (2.55) and (2.56) are repeated at all collocation points on the boundary where Neumann conditions such as specified in Equation (2.50) are prescribed. The corners of the domain require special treatment, as will be described in the next section.

It is a simple task to satisfy the Dirichlet boundary conditions expressed in Equation (2.49). The resulting set of simultaneous equations, globally assembled to satisfy the governing equations at the interior collocation points, Dirichlet and Neumann boundary conditions at boundary collocation points, and also conditions at all corner points can be written in matrix form as

$$\mathbf{K} \mathbf{u} = \mathbf{F} \quad (2.57)$$

where \mathbf{K} , the global coefficient matrix, may be called the *stiffness matrix* as in the conventional Finite Element Method, \mathbf{u} and \mathbf{F} are the solution and load vectors, respectively. A single index is used in the global numbering scheme for the entire computational domain. The subscripts of \mathbf{u} are based on this single-index numbering scheme, so as to ensure the continuity of the solution at inter-element boundary collocation points, and to satisfy the Dirichlet conditions. This is done by setting the coefficients

$$K_{ii} = 1$$

and the loads

$$F_i = \bar{u}$$

where i is the global number of the collocation point on the boundary, and \bar{u} is the prescribed function value.

2.9 Treatment of Corners

As mentioned earlier, the Legendre Collocation Method is very well suited for rectangular domains or L-shaped regions that can be broken up into three rectangular elements. Thus, a computational domain will present a series of corners which require special attention as the boundary conditions on both sides forming the corner may not be the same. For mixed boundary-value problems, two situations may occur at a corner point as depicted in Figures 2.8 and 2.9. In the first case, as in Figure 2.8, for a smooth function, the solution at the node located at a corner-point is unique; there will be only one solution at that corner. Therefore, a known value of the function is enforced as a boundary condition. While corners with different values of derivative at the two sides exist in many practical problems (see Figure 2.9), the Legendre Collocation technique provides an easy treatment as will be outlined below.

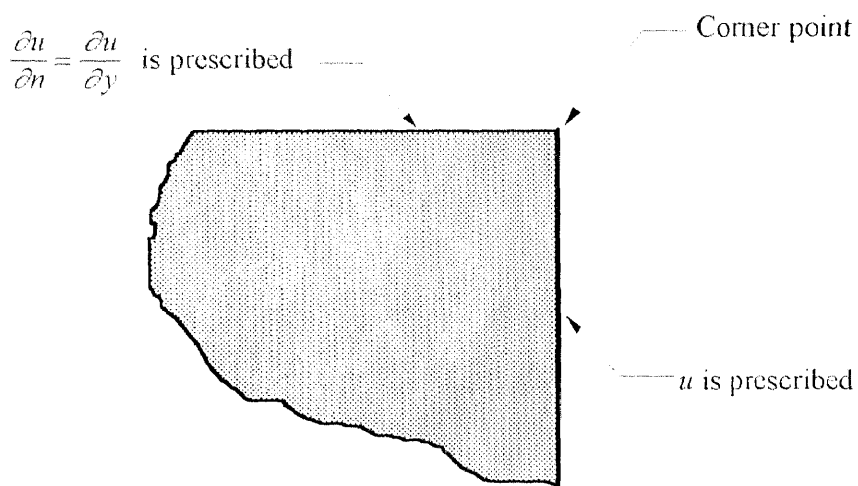


Figure 2.8 A corner with known values of the function and normal derivative.

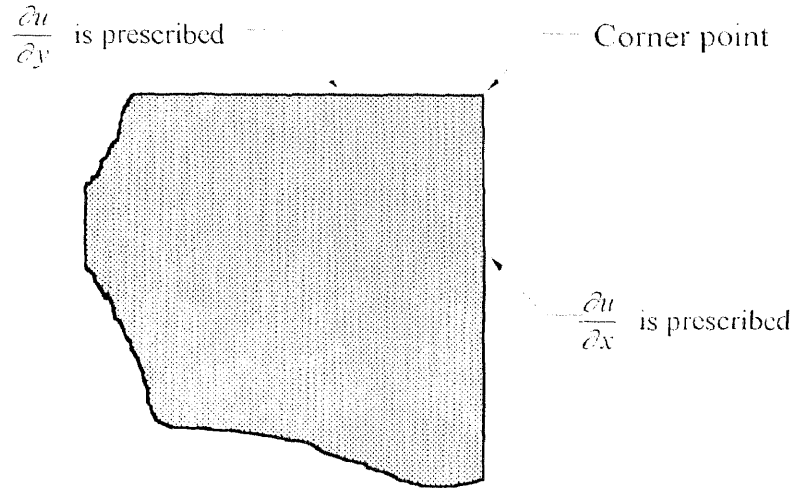


Figure 2.9 A corner with known values of normal derivative.

For example, the situation at the corner as shown in Figure 2.10 has two normal derivatives $\frac{\partial u}{\partial x}$ and $\frac{\partial u}{\partial y}$ as prescribed values. Furthermore, in this particular example, the total number of collocation points in both x and y directions is taken to be the same, $NPX = NPY = 5$. For the given node numbering scheme and reference axes as shown, Equation (2.55) gives the first derivative in the x direction for that corner (point 65) that can be written as

$$\left. \frac{\partial u}{\partial x} \right|_{\text{Point 65}} = \frac{2}{\Delta x^{(e)}} (A_{51}u_{61} + A_{52}u_{62} + A_{53}u_{63} + A_{54}u_{64} + A_{55}u_{65}) = \bar{q}_x \quad (2.58)$$

where A_{51}, \dots, A_{55} are the coefficients located in the last ($NPX = 5$) row of matrix \mathbf{A} in Equation (2.19) or (2.20). While u_{61}, \dots, u_{65} are the function values associated

with the point numbers in Figure 2.10. Similarly, from Equation (2.54), the derivative in the y direction is

$$\frac{\partial u}{\partial y} \Big|_{\text{Point 65}} = \frac{2}{\Delta y^{(e)}} (A_{51}u_{29} + A_{52}u_{38} + A_{53}u_{47} + A_{54}u_{56} + A_{55}u_{65}) = \bar{q}_y \quad (2.59)$$

Equations (2.58) and (2.59) are normalized to yield

$$\frac{2}{\Delta x^{(e)} \bar{q}_x} (A_{51}u_{61} + A_{52}u_{62} + A_{53}u_{63} + A_{54}u_{64} + A_{55}u_{65}) = 1 \quad (2.60)$$

$$\frac{1}{\Delta y^{(e)} \bar{q}_y} (A_{51}u_{29} + A_{52}u_{38} + A_{53}u_{47} + A_{54}u_{56} + A_{55}u_{65}) = 1 \quad (2.61)$$

Now both equations can be equated to give

$$\begin{aligned} & \frac{2}{\Delta y^{(e)} \bar{q}_y} (A_{51}u_{29} + A_{52}u_{38} + A_{53}u_{47} + A_{54}u_{56}) - \\ & \frac{2}{\Delta x^{(e)} \bar{q}_x} (A_{51}u_{61} + A_{52}u_{62} + A_{53}u_{63} + A_{54}u_{64}) + \left(\frac{2}{\Delta y^{(e)} \bar{q}_y} - \frac{2}{\Delta x^{(e)} \bar{q}_x} \right) u_{65} = 0 \end{aligned} \quad (2.62)$$

Equation (2.62) is the equation for point number 65, and therefore will be positioned in the row number 65 in the matrix equations for the complete problem, and the location of the coefficients in the column of the matrix corresponds to the point number of the unknown u . Thus, the boundary conditions at a corner are taken into account.

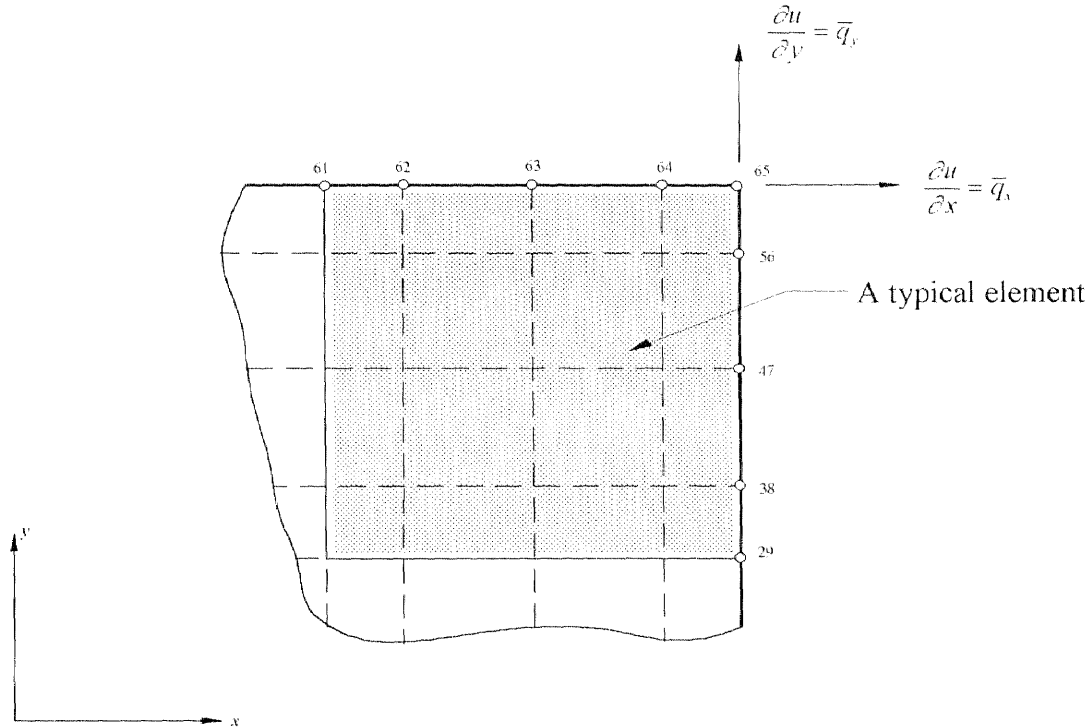


Figure 2.10 Definition at a corner for a 5×5 mesh for each element.

In general, Equation (2.62) can be written in the form

$$\frac{2}{\Delta y^{(e)} \bar{q}_y} \sum_{j=1}^{NPY} AY_{NPY,j} u_{NPX,j} - \frac{2}{\Delta x^{(e)} \bar{q}_x} \sum_{i=1}^{NPX} AX_{NPX,j} u_{i,NPY} = 0 \quad (2.63)$$

as the enforcement of conditions on the normal derivatives in the x and y directions at upper right corner point of the region. Slight modifications in Equation (2.63) are necessary for different locations of the corner point.

CHAPTER 3

TREATMENT OF BOUNDARY SINGULARITIES

3.1 Introduction

In many problems of practical importance, singularities either inside the domain or on the boundaries are encountered. In the design process, the quantities involving derivatives such as stresses, bending moments, shear forces etc. are particularly important. One type of singularity is, for example, a re-entrant corner in the torsion problem that causes high stress concentration at this corner [32]. Therefore it is important to obtain an accurate knowledge of the behavior of the derivatives in a neighborhood of the singular point.

It is generally impossible to obtain an accurate approximation in a neighborhood of a singular point, using a single standard numerical method such as finite difference, finite element or boundary element. The most common method in dealing with singular points using available computer software is to refine the mesh around the location where the singularity occurs. This procedure, if it converges, will produce slow convergence in the entire domain and especially near a singularity [33,34].

In this study, the Legendre Collocation Method applied to this type of problem also shows the same slow convergence in the neighborhood of singularity. The advantage of this method over other methods is that using a higher approximation collocated at the zeros of a high degree Legendre polynomial, will automatically provide a finer mesh near sharp re-entrant corners as depicted in Figure 3.1. Such sharp re-entrant corners give rise to singularities of various types.

Moreover, it is easy to increase the degree of the polynomial when using a computer program. However, evaluation of the accuracy of a solution obtained using such a procedure should be considered with extreme care.

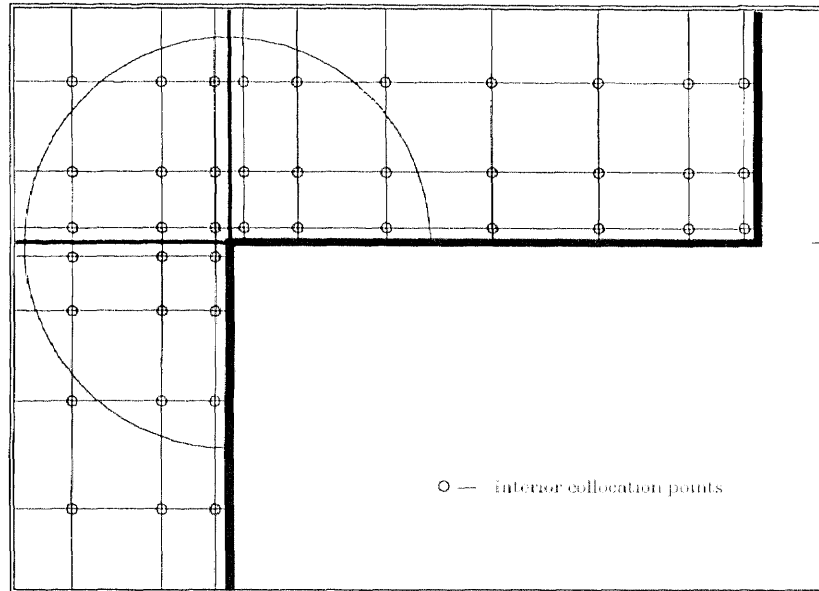


Figure 3.1 Legendre collocation points in the neighborhood of a singularity.

Hence, special treatment for problems involving singularities is highly desirable. A major purpose of this study is to further extend the use of the Legendre Collocation Method by a modification that can produce accurate results near the singularity. We begin by getting satisfactory accuracy everywhere except in a neighborhood of singularity. Once the solution at any desired point in the domain sufficiently far from the singularity can be computed satisfactorily, then these results are used in a modified procedure for obtaining a solution in a neighborhood of the singularity. The resulting solution will also be capable of giving approximate partial derivatives in a neighborhood of the singularity.

The treatment discussed below will be confined to problems involving boundary singularities, which occur frequently in practical engineering. Such singularities occur when there is a sudden change of direction of the boundary, producing a re-entrant corner or a change in boundary conditions at some point on the boundary that is not a corner.

A comprehensive review of methods for treating problems with singularities is given by Lefeber [33]. Even though the book is dedicated to the Boundary Element Method, Lefeber provides citations of numerous references on the treatment of singularities.

As a typical example of the proposed treatment in this study, we consider the problem of a bar with an L-shaped cross-section under torsion. The procedure can be outlined as follows:

1. The domain is divided into three rectangular elements forming the L-shaped region, and the solution at the collocation points for the entire domain is obtained by the Legendre Collocation Method.
2. In a neighborhood of the singularity, a circular sector with fixed radius and angle θ from 0 to 1.5π is established. In this sector, the defining equations are re-written in polar coordinates, and the solution is obtained in terms of an infinite series of eigenfunctions for the circular sector. This solution satisfies the governing differential equation and the boundary conditions at the edges of the domain forming the re-entrant corner. Note that the solution need not satisfy the boundary condition along the circular arc.
3. A selected number of points are taken along the circular arc, and solution function values are calculated at those points by interpolating the results obtained by the Legendre Collocation Method. A finite number of terms of

the homogeneous series solution in the circular sector is taken. The coefficients of the terms in this truncated series are determined by a discrete least-squares procedure to approximate the previously computed values at the selected points along the sector arc. Thus, the boundary condition at the discrete points along the sector arc is satisfied 'as accurately as possible' by the solution in the circular sector. By using the least-squares approach, the effect of the oscillation of the trigonometric functions comprising the solution along the arc is minimized. The complexity of finding the coefficients can also be avoided by selecting the points along the arc in such a way that the eigenfunctions are mutually orthogonal with respect to summation of the truncated set.

4. Once the coefficients become known, the approximate solution and its partial derivatives can be found.

As previously stated, in the above treatment of the singularity, the undetermined coefficients in the finite series solution for the circular sector are determined by the least-squares approach. The derived series solution satisfies the governing differential equation and also the boundary conditions along the two adjacent sides of the singularity. The task is now to make the values computed by the series solution agree with the previously computed values of the function along the sector arc. This becomes the boundary condition for the solution in the sector. There is another attractive approach in matching the series solution along the sector arc. This is a minimax approximation, or minimizing the maximum error [35], and it is done by simply taking the matching points along the arc at the zeros of a Chebyshev polynomial that have been transformed to coincide with the interval representing the length of the arc. As a result, a set of simultaneous linear equations has to be solved for determining the unknown coefficients in the series

solution. Thus, it is not required to find the orthogonality conditions for summation of the eigenfunctions that make up the truncated series solution. The details of reasoning about this minimax approach will also be presented in this chapter.

The combination of Legendre collocation and discrete least-squares or minimax formulation in obtaining the solution near a singularity is attractive because no numerical integration is required.

A problem previously done by Whiteman and Papamichael [36], Symm [37,38], and Lefebvre [33], termed "The Problem of Motz" [39], will next be formulated for the purpose of comparison. This problem consists of finding a numerical solution of Laplace's equation in the finite rectangular domain, with a set of mixed boundary conditions, one of which produces a singularity. Whiteman and Papamichael used a Conformal Transformation Method considered very efficient in solving singular problems in rectangular domains [33]. Symm treated the problem of Motz by a boundary integral method. In this chapter, similar procedures applied to the torsional problem will be applied to the problem of Motz.

3.2 Eigenfunctions Solution for Torsion of an L-shaped Bar

As mentioned above, the circular sector is defined in the neighborhood of a singularity, as depicted in Figure 3.2. A Fourier series solution is obtained such that it satisfies the boundary conditions along the two boundaries forming the re-entrant corner, but the boundary condition along the arc is left undetermined. Substitution of this solution into the governing differential equation yields a complementary and particular solution. This final form of the infinite series

solution, containing the undetermined coefficients of the complementary solution, is truncated and the undetermined coefficients are determined by a discrete least-squares procedure, using the orthogonality condition with respect to summation of the truncated set of eigenfunctions.

In polar coordinates, Poisson equation in a two-dimensional region is given by [40]

$$\phi_{rr} + \frac{1}{r} \phi_r + \frac{1}{r^2} \phi_{\theta\theta} = -F(r, \theta) \quad (3.1)$$

Consider a circular sector as shown in Figure 3.2. Note that the angle θ varies from 0 to $\frac{3\pi}{2}$, and the radius r from 0 to R . Differential equation (3.1) is subject to the following boundary conditions

$$\phi = 0 \text{ along } \theta = 0 \quad (3.2)$$

$$\phi = 0 \text{ along } \theta = \frac{3\pi}{2} \quad (3.3)$$

$$\phi = f(\theta) \text{ along } r = R \quad (3.4)$$

It is important to note here, based on the membrane analogy introduced by L. Prandtl [32], that the solution ϕ of the torsion problem behaves like the deflection of a homogeneous membrane supported at the edges, with the same outline as that of the L-shaped cross section of the twisted bar subjected to a uniform lateral pressure. Thus, ϕ has to be finite at the origin (See Figure 3.2).

As discussed in Appendix A., using the method of separation of variables, the general form of the solution in terms of eigenfunctions for the homogeneous part of equation (3.1) satisfying the homogeneous Dirichlet boundary conditions at the edges forming the angular sector is found to be

$$\phi(r, \theta) = \sum_{n=1}^{\infty} R_n(r) \sin \frac{n\pi}{\alpha} \theta \quad (A.18)$$

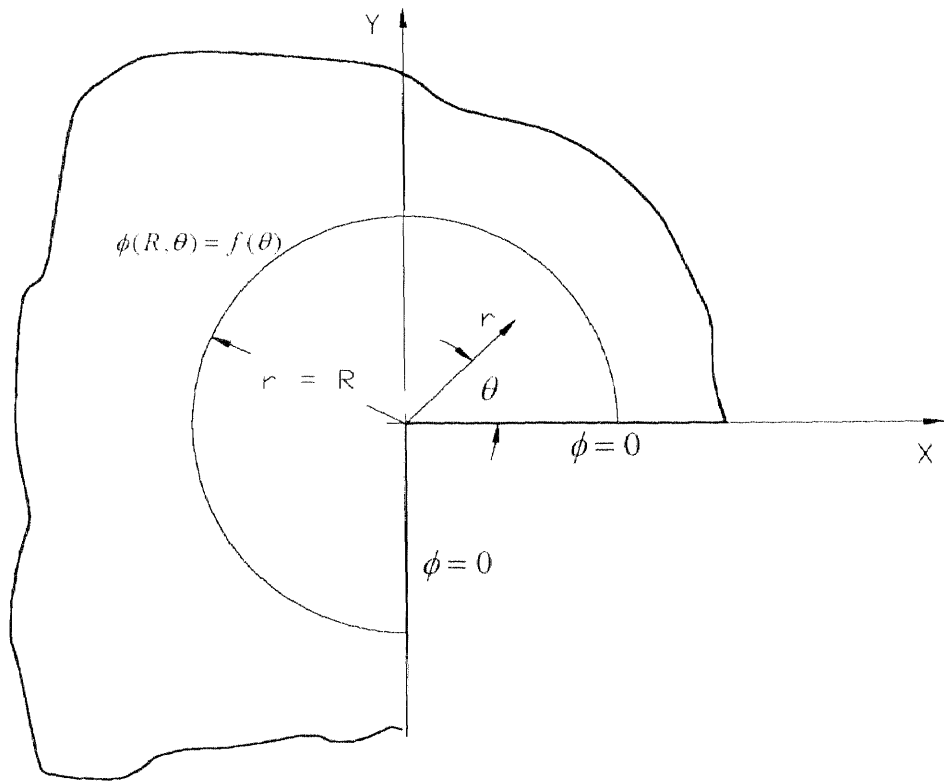


Figure 3.2 Circular sector for Poisson equation in polar coordinates.

Now, replacing $R_n(r)$ with $b_n(r)$ and taking $\alpha = \frac{3\pi}{2}$ as shown in Figure 3.2, the solution $\phi(r, \theta)$ can be written in the form

$$\phi(r, \theta) = \sum_{n=1}^{\infty} b_n(r) \sin \frac{2n}{3} \theta \quad (3.5)$$

Solution (3.5) satisfies the boundary conditions along $\theta = 0$ and $\theta = \frac{3\pi}{2}$. The coefficients $b_n(r)$ can be determined using the following formula, taking into account orthogonality and normalization

$$b_n(r) = \frac{4}{3\pi} \int_0^{\frac{3\pi}{2}} \phi(r, \theta) \sin \frac{2n}{3} \theta d\theta \quad (3.6)$$

Orthogonality conditions and normalization factors related to Equations (3.5) and (3.6) are given by

$$\int_0^{\frac{3\pi}{2}} \sin \frac{2n}{3} \theta \sin \frac{2m}{3} \theta d\theta = 0, \quad \text{for } n \neq m \quad (3.7)$$

and

$$\int_0^{\frac{3\pi}{2}} \sin^2 \frac{2n}{3} \theta d\theta = \frac{3\pi}{4} \quad (3.8)$$

To solve the inhomogeneous differential equation (3.1), $F(r, \theta)$ in the right-hand side of Equation (3.1) is expanded in terms of the eigenfunctions $\sin \frac{2n}{3} \theta$ in the form,

$$F(r, \theta) = \sum_{n=1}^{\infty} B_n(r) \sin \frac{2n}{3} \theta \quad (3.9)$$

where

$$B_n(r) = \frac{4}{3\pi} \int_0^{\frac{3\pi}{2}} F(r, \theta) \sin \frac{2n}{3} \theta d\theta \quad (3.10)$$

By substituting Equations (3.5), (3.9) and (3.10) into Equation (3.1), we obtain the ordinary differential equations whose solutions yield the $b_n(r)$.

In case of the torsional problem,

$$F(r, \theta) = 2 \quad (3.11)$$

and therefore the coefficients are given by

$$B_n(r) = \frac{4}{3\pi} \int_0^{\frac{3\pi}{2}} 2 \sin \frac{2n}{3} \theta d\theta \quad (3.12)$$

or

$$B_n(r) = -\frac{4}{n\pi} \left[(-1)^n - 1 \right] \quad (3.13)$$

Next, differentiating $\phi(r, \theta)$ with respect to r and θ , we obtain,

$$\phi_r = \sum_{n=1}^{\infty} b'_n(r) \sin \frac{2n}{3} \theta \quad (3.14)$$

$$\phi_{rr} = \sum_{n=1}^{\infty} b''_n(r) \sin \frac{2n}{3} \theta \quad (3.15)$$

$$\phi_{\theta\theta} = - \sum_{n=1}^{\infty} b_n(r) \left(\frac{2n}{3} \right)^2 \sin \frac{2n}{3} \theta \quad (3.16)$$

and then Equations (3.9), (3.14), (3.15) and (3.16) are substituted into Equation (3.1) to get

$$\sum_{n=1}^{\infty} b''_n(r) \sin \frac{2n}{3} \theta + \sum_{n=1}^{\infty} \left(\frac{b'_n(r)}{r} \right) \sin \frac{2n}{3} \theta - \sum_{n=1}^{\infty} \left(\frac{2n}{3r} \right)^2 b_n(r) \sin \frac{2n}{3} \theta = - \sum_{n=1}^{\infty} B_n(r) \sin \frac{2n}{3} \theta \quad (3.17)$$

Matching coefficients of the eigenfunctions $\sin \frac{2n}{3} \theta$ on both sides of Equation (3.17), we obtain the following differential equations which are only functions of r

$$b''_n(r) + \frac{b'_n(r)}{r} - \left(\frac{2n}{3r} \right)^2 b_n(r) = -B_n(r) \quad (3.18)$$

Each of these is a standard nonhomogeneous differential equation with solution comprised of a complementary and particular part.

To find the complementary function, it is necessary to solve the homogeneous part of Equation (3.18). Thus, the solution of equation

$$b''_{nc}(r) + \frac{b'_{nc}(r)}{r} - \left(\frac{2n}{3r} \right)^2 b_{nc}(r) = 0 \quad (3.19)$$

has to be found. Try a solution in the form

$$b_{nc}(r) = r^k \quad (3.20)$$

By substituting $b''_{nc}(r)$, $b'_{nc}(r)$ and $b_{nc}(r)$ into Equation (3.19), we have

$$k(k-1)r^{k-2} + kr^{k-2} - \left(\frac{2n}{3}\right)^2 r^{k-2} = 0,$$

and upon simplification

$$k^2 - \left(\frac{2n}{3}\right)^2 = 0.$$

Thus

$$k = \pm \frac{2n}{3},$$

and the complementary solution to Equation (3.19) is given by

$$b_{nc} = c_n r^{\frac{2n}{3}} + \tilde{c}_n r^{-\frac{2n}{3}} \quad (3.20)$$

To find a particular solution $b_{np}(r)$ of Equation (3.18), one needs to replace $B_n(r)$ with Equation (3.13), so that

$$b''_{np}(r) + \frac{b'_{np}(r)}{r} - \left(\frac{2n}{3r}\right)^2 b_{np}(r) = \frac{4}{n\pi} [(-1)^n - 1] \quad (3.21)$$

In this case, try

$$b_{np}(r) = Kr^2$$

and substitute again $b''_{np}(r)$, $b'_{np}(r)$ and $b_{np}(r)$ into Equation (3.21) getting

$$2K + 2K - \left(\frac{2n}{3r}\right)^2 K = \frac{4}{n\pi} [(-1)^n - 1]$$

or

$$K = \frac{9}{n\pi(9-n^2)} [(-1)^n - 1], \quad n \neq 3$$

K is unbounded when $n = 3$ and the particular solution is given by

$$b_{np}(r) = \frac{9r^2}{n\pi(9-n^2)} [(-1)^n - 1], \quad n \neq 3 \quad (3.22)$$

Combining Equations (3.20) and (3.22), we obtain the general solution of Equation (3.18) with $F(r, \theta) = 2$ as given by

$$b_n(r) = c_n r^{\frac{2n}{3}} + \bar{c}_n r^{-\frac{2n}{3}} + \frac{9r^2}{n\pi(9-n^2)} [(-1)^n - 1], \quad n \neq 3$$

However, it is required that $b_n(r)$ be finite when $r = 0$. Hence, $\bar{c}_n = 0$, and

$$b_n(r) = c_n r^{\frac{2n}{3}} + \frac{9r^2}{n\pi(9-n^2)} [(-1)^n - 1], \quad n \neq 3 \quad (3.23)$$

Finally, the solution for the Poisson equation (3.1) for the circular sector depicted in Figure 3.1 can be written as

$$\phi(r, \theta) = \sum_{\substack{n=1 \\ n \neq 3}}^{\infty} \left\{ c_n r^{\frac{2n}{3}} + \frac{9r^2}{n\pi(9-n^2)} [(-1)^n - 1] \right\} \sin \frac{2n}{3} \theta \quad (3.24)$$

The solution in the form of Equation (3.24) satisfies the differential equation in the domain and also the boundary conditions at both lines that form the re-entrant corner of the region. Obviously, this solution of Equation (3.24) still needs to satisfy the boundary condition at the circular arc where $r = R$.

3.3 Discrete Least-Squares Approximation for Torsion of L-shaped Bar

The Legendre Collocation Method that is used to solve numerically the torsional problem in the L-shaped region gives only the solution function at the collocation points. If an arc is drawn using the singular point as the origin and a radius equal to R , then the function values along the arc can be calculated by means of the interpolating Lagrange polynomial used previously. Thus, we can have the function values at any points along the circular arc. Now, using these values as boundary conditions along the arc, one can determine the coefficients c_n in Equation (3.24).

The discrete least squares approach will be used for determining coefficients c_n , so that the error involved as measured by the sum of the squares of the differences between the values of the approximating function and the given values at chosen discrete points is minimized. The selected points along the arc are chosen to insure orthogonality with respect to summation of the truncated set of eigenfunctions. Then the coefficients c_n can be easily computed using the formula, expressed as a summation. This eliminates the need to solve a system of linear equations, as is generally required for this approach.

For the purpose outlined above, Equation (3.24) will be re-arranged as follows

$$\phi(r, \theta) - \sum_{\substack{n=1 \\ n \neq 3}}^{\infty} \frac{9r^2}{n\pi(9-n^2)} [(-1)^n - 1] \sin \frac{2n}{3} \theta = \sum_{n=1}^{\infty} c_n r^{\frac{2n}{3}} \sin \frac{2n}{3} \theta \quad (3.25)$$

Fixing $r = R$ for the circular boundary, and using a finite number of terms M and N respectively in place of the infinite series in Equation (3.25), we have

$$\phi(R, \theta) - \sum_{\substack{n=1 \\ n \neq 3}}^M \frac{9R^2}{n\pi(9-n^2)} [(-1)^n - 1] \sin \frac{2n}{3} \theta \approx \sum_{n=1}^N c_n R^{\frac{2n}{3}} \sin \frac{2n}{3} \theta \quad (3.26)$$

Note that n should not be equal to three because this would make the left-hand side of Equation (3.26) infinite. In addition, it is independent of c_n ; therefore the upper limit of summation can be different from the right-hand side of the equation.

To calculate c_n in Equation (3.26) using a least-squares approach, the same finite number of points θ_k , $k = 1, 2, \dots, N$ will be chosen on the circular arc $r = R$. The different subscript k is used because Equation (3.26) that contains the summation should be evaluated at each point θ_k . Therefore Equation (3.26) can be written as

$$\phi(R, \theta_k) - \sum_{\substack{n=1 \\ n \neq 3}}^M \frac{9R^2}{n\pi(9-n^2)} [(-1)^n - 1] \sin \frac{2n}{3} \theta_k \approx \sum_{n=1}^N c_n R^{\frac{2n}{3}} \sin \frac{2n}{3} \theta_k \quad (3.27)$$

for $k = 1, 2, \dots, N$

where $\phi(R, \theta_k)$ are chosen points on the arc. The summation in the right-hand side of Equation (3.27) is valid only for odd numbers, and the total number of terms M in the summation is taken so that if the summation is evaluated the difference in the values with $(M-1)$ and M terms is small enough to indicate convergence. This is done in the computer program.

For simplicity of formulation, let us define

$$f(R, \theta_k) = \phi(R, \theta_k) - \sum_{\substack{n=1 \\ n \neq 3}}^M \frac{9R^2}{n\pi(9-n^2)} [(-1)^n - 1] \sin \frac{2n}{3} \theta_k \quad (3.28)$$

and

$$p_N(R, \theta_k) = \sum_{n=1}^N c_n R^{\frac{2n}{3}} \sin \frac{2n}{3} \theta_k \quad (3.29)$$

The error at a discrete point θ_k is given by

$$e(\theta_k) = f(R, \theta_k) - p_N(R, \theta_k) \quad (3.30)$$

The discrete least squares approximation requires that, for finding c_n in Equation (3.29), we minimize the quantity

$$S = \sum_{k=1}^N e^2(\theta_k).$$

which is the summation over N points of Equation (3.30), squared. In other words,

$$S = \sum_{k=1}^N \left[f(R, \theta_k) - \sum_{n=1}^N c_n R^{\frac{2n}{3}} \sin \frac{2n}{3} \theta_k \right]^2 = \text{minimum} \quad (3.31)$$

or in expanded form

$$\begin{aligned} S = & \left[f(R, \theta_1) - \sum_{n=1}^N c_n R^{\frac{2n}{3}} \sin \frac{2n}{3} \theta_1 \right]^2 + \left[f(R, \theta_2) - \sum_{n=1}^N c_n R^{\frac{2n}{3}} \sin \frac{2n}{3} \theta_2 \right]^2 \\ & + \cdots + \left[f(R, \theta_N) - \sum_{n=1}^N c_n R^{\frac{2n}{3}} \sin \frac{2n}{3} \theta_N \right]^2 = \text{minimum} \end{aligned}$$

and if Equation (3.31) is considered to be a function of c_n , for the minimum to occur, it is necessary for the c_n , $n = 1, 2, \dots, N$ to satisfy

$$\frac{\partial S}{\partial c_n} = 0, \quad n = 1, 2, \dots, N \quad (3.32)$$

Consequently,

$$\frac{\partial S}{\partial c_n} = \sum_{k=1}^N \left[f(R, \theta_k) \sin \frac{2n}{3} \theta_k - \sum_{j=1}^N c_j R^{\frac{2j}{3}} \sin \frac{2j}{3} \theta_k \sin \frac{2n}{3} \theta_k \right] = 0$$

or in expanded form

$$\begin{aligned} \frac{\partial S}{\partial c_n} = & \sum_{k=1}^N f(R, \theta_k) \sin \frac{2n}{3} \theta_k - \sum_{k=1}^N \left(c_1 R^{\frac{2}{3}} \sin \frac{2}{3} \theta_k \sin \frac{2n}{3} \theta_k + c_2 R^{\frac{4}{3}} \sin \frac{4}{3} \theta_k \sin \frac{2n}{3} \theta_k \right. \\ & \left. + \cdots + c_n R^{\frac{2n}{3}} \sin^2 \frac{2n}{3} \theta_k + \cdots + c_N R^{\frac{2N}{3}} \sin \frac{2N}{3} \theta_k \sin \frac{2n}{3} \theta_k \right) = 0 \quad (3.33) \end{aligned}$$

Thus, we have N simultaneous equations. On the other hand, we can easily calculate the coefficients c_n if there exist orthogonality conditions with respect to summation such that

$$\sum_{k=1}^N \sin \ell \varphi_k \sin m \varphi_k = 0 \quad \text{for } \ell \neq m = \text{ integers} \quad (3.34)$$

where

$$\varphi_k = \frac{2}{3} \theta_k \quad (3.35)$$

In the trigonometric identity [4]

$$\cos \varphi + \cos 3\varphi + \cos 5\varphi + \dots + \cos(2k-1)\varphi + \dots + \cos(2N-1)\varphi = \frac{1}{2} \sin 2N\varphi \csc \varphi$$

or

$$\sum_{k=1}^N \cos(2k-1)\varphi = \frac{1}{2} \sin 2N\varphi \csc \varphi, \quad (3.36)$$

the right-hand side vanishes if

$$\begin{aligned} \sin 2N\varphi &= 0, \\ 2N\varphi &= (2k-1)\pi, \quad \text{for } k = 1, 2, \dots, N \end{aligned}$$

or

$$\varphi_k = \frac{(2k-1)}{N} \frac{\pi}{2}, \quad k = 1, 2, \dots, N \quad (3.37)$$

Furthermore, the left hand side of Equation (3.34) can be written as

$$\sum_{k=1}^N \sin \ell \varphi_k \sin m \varphi_k = \frac{1}{2} \left[\sum_{k=1}^N \cos(\ell-m)\varphi_k - \sum_{k=1}^N \cos(\ell+m)\varphi_k \right] \quad (3.38)$$

To prove the orthogonality condition in Equation (3.34), it is necessary to show that each summation term of Equation (3.38) is equal to zero for $\ell \neq m$. Using the identity Equation (3.36) together with Equation (3.37), the first summation term can be written as

$$\begin{aligned}
\sum_{k=1}^N \cos(\ell - m) \varphi_k &= \sum_{k=1}^N \cos(2k-1) \frac{(\ell-m)}{N} \frac{\pi}{2} \\
&= \frac{1}{2} \sin\left(2N \frac{\ell-m}{N} \frac{\pi}{2}\right) \csc\left(\frac{\ell-m}{N} \frac{\pi}{2}\right)
\end{aligned} \tag{3.39}$$

Clearly, the right hand side of the above equation vanishes for any integer $(\ell - m)$. Similarly, the second term

$$\sum_{k=1}^N \cos(\ell + m) \varphi_k = 0, \quad \text{for } \ell \neq m$$

since $(\ell + m)$ will be an integer.

It follows that,

$$\sum_{k=1}^N \sin \ell \varphi_k \sin m \varphi_k = 0, \quad \text{for } \ell \neq m$$

At this point, we still have to take into account the case $\ell = m \neq 0$, so that the right hand side of Equation (3.34) becomes

$$\sum_{k=1}^N \sin^2 m \varphi_k$$

Using the identity

$$\sin^2 m \varphi_k = \frac{1}{2} [1 - \cos 2m \varphi_k] \tag{3.40}$$

we obtain

$$\begin{aligned}
\sum_{k=1}^N \sin^2 m \varphi_k &= \frac{1}{2} \left[\sum_{k=1}^N 1 - \sum_{k=1}^N \cos 2m \varphi_k \right] \\
&= \frac{1}{2} \left[\sum_{k=1}^N 1 - \sum_{k=1}^N \cos(2k-1) \frac{2m \pi}{N} \frac{\pi}{2} \right]
\end{aligned} \tag{3.41}$$

Note again,

$$\begin{aligned}
\sum_{k=1}^N \cos(2k-1) \frac{2m \pi}{N} \frac{\pi}{2} &= \frac{1}{2} \sin 2N \frac{2m \pi}{N} \frac{\pi}{2} \csc \frac{2m \pi}{N} \frac{\pi}{2} \\
&= 0,
\end{aligned}$$

for $m = \text{any integer}$, and

$$\sum_{k=1}^N 1 = N.$$

Hence, we have

$$\sum_{k=1}^N \sin^2 m \varphi_k = \frac{N}{2} \tag{3.42}$$

as the normalization factor when $\ell = m \neq 0$ in Equation (3.34).

In conclusion, by noting Equation (3.35) we have,

$$\sum_{k=1}^N \sin \frac{2\ell}{3} \theta_k \sin \frac{2m}{3} \theta_k = \begin{cases} 0, & \text{if } \ell \neq m; \\ \frac{N}{2}, & \text{if } \ell = m \neq 0 \end{cases} \tag{3.43}$$

where

$$\theta_k = \frac{(2k-1)}{N} \frac{3\pi}{4}, \quad k = 1, 2, \dots, N \tag{3.44}$$

Now, substituting from Equation (3.43) into Equation (3.33) we have

$$\begin{aligned} \sum_{n=1}^N f(R, \theta_k) \sin \frac{2n}{3} \theta_k - \sum_{n=1}^N c_n R^{\frac{2n}{3}} \sin^2 \frac{2n}{3} \theta_k &= 0 \\ \sum_{n=1}^N f(R, \theta_k) \sin \frac{2n}{3} \theta_k - c_n R^{\frac{2n}{3}} \frac{N}{2} &= 0, \end{aligned}$$

and finally, the coefficient c_n is given by

$$c_n = \frac{2}{NR^{\frac{2n}{3}}} \sum_{k=1}^N f(R, \theta_k) \sin \frac{2n}{3} \theta_k, \quad \text{for } n = 1, 2, \dots, N \quad (3.45)$$

where θ_k is defined as in Equation (3.44).

We conclude that in the neighborhood of a re-entrant corner, the series solution for an L-shaped bar under torsion given in Equation (3.24) is

$$\phi(r, \theta) = \sum_{n=1}^N c_n r^{\frac{2n}{3}} \sin \frac{2n}{3} \theta + \sum_{\substack{n=1 \\ n \neq 3}}^N \frac{9r^2}{n\pi(9-n^2)} [(-1)^n - 1] \sin \frac{2n}{3} \theta \quad (3.46)$$

where the c_n are defined by Equation (3.45). As mentioned earlier, we are particularly interested in derivatives that represent the shearing stresses. These derivatives can easily be obtained by differentiating $\phi(r, \theta)$ with respect to r and θ . Therefore, the radial derivative can be defined by

$$\frac{\partial \phi}{\partial r} = \sum_{n=1}^N \frac{2n}{3} c_n r^{\frac{2n-3}{3}} \sin \frac{2n}{3} \theta + \sum_{\substack{n=1 \\ n \neq 3}}^N \frac{18r}{n\pi(9-n^2)} [(-1)^n - 1] \sin \frac{2n}{3} \theta \quad (3.47)$$

and the tangential derivative is given by

$$\frac{\partial \phi}{\partial \theta} = \sum_{n=1}^N \frac{2n}{3} c_n r^{\frac{2n}{3}} \cos \frac{2n}{3} \theta + \sum_{\substack{n=1 \\ n \neq 3}}^N \frac{2n}{3} \frac{9r^2}{n\pi(9-n^2)} [(-1)^n - 1] \cos \frac{2n}{3} \theta \quad (3.48)$$

By inspecting the equation for the radial derivative, it is clear that a singularity occurs when $r = 0$ and $n = 1$.

Thus, the "best fit" mean squares approach employed above for the finite series expansion (3.45) corresponds conceptually to the orthogonal Fourier series expansion for the infinite series.

Using the above derivations as a basis, it is easy to obtain the eigensolution and its derivatives for the problems governed by Laplace's equation in an L-shaped domain. One needs only to eliminate the term

$$\sum_{\substack{n=1 \\ n \neq 3}}^N \frac{9r^2}{n\pi(9-n^2)} [(-1)^n - 1] \sin \frac{2n}{3} \theta \quad (3.49)$$

in the eigensolution Equation (3.25). Note that this term resulted from the right side of the Poisson equation

$$F(r, \theta) = 2 \quad (3.50)$$

in Equation (3.1). Thus, for Laplace's equation the coefficients c_n are given by

$$c_n = \frac{2}{NR^{\frac{2n}{3}}} \sum_{k=1}^N f(R, \theta_k) \sin \frac{2n}{3} \theta_k, \quad \text{for } n = 1, 2, \dots, N \quad (3.51)$$

where

$$f(R, \theta_k) = \phi(R, \theta_k) \quad (3.52)$$

Hence, the eigensolution for the isolated sector near the singular point is defined by

$$\phi(r, \theta) = \sum_{n=1}^N c_n r^{\frac{2n}{3}} \sin \frac{2n}{3} \theta \quad (3.53)$$

and its derivatives can be computed using the following formula:

$$\begin{aligned}\frac{\partial \phi}{\partial r} &= \sum_{n=1}^N \frac{2n}{3} c_n r^{\frac{2n-3}{3}} \sin \frac{2n}{3} \theta \\ \frac{\partial \phi}{\partial \theta} &= \sum_{n=1}^N \frac{2n}{3} c_n r^{\frac{2n}{3}} \cos \frac{2n}{3} \theta\end{aligned}\quad (3.54)$$

3.4 Minimax Fit at Chebyshev Zeros

As discussed earlier, the boundary condition at the sector arc depicted in Figure 3.2 and 3.3 are satisfied "as well as possible" using a discrete least-squares procedure. The merit of this way of obtaining the undetermined coefficients c_n in Equation (3.26) is that there is no need to solve a system of linear equations for c_n .

However, Kopal [41] has pointed out that for a system of orthogonal functions, the error of an approximation obtained by minimizing the average error will oscillate corresponding to the number of collocation points used in finding the undetermined coefficients c_n . In addition, the least-squares fit gives the greatest errors at the extreme ends of the range, and smaller errors in the middle of the range [7,42,43]. Therefore, we will now examine a procedure that can minimize the maximum error within some specified range. In this study, the range will be along the sector arc shown in Figures 3.2 and 3.3. Since the determination of the unknown coefficients c_n in Equation (3.25) will be carried out on a certain interval of variable θ with a fixed radius $r = R$, and there is complete freedom of choice in the selection of the values θ_k along the sector arc where the interpolated function values will be obtained, there are advantages in choosing θ_k in a certain way.

It is well known that if the zeros of the Chebyshev polynomial $T_{N+1}(\hat{\theta})$ are used to construct an interpolation polynomial $P_N(\theta)$ of degree at most N , then for θ in $[-1,1]$ the maximum error will have the smallest possible value [41].

The interval of the approximation is a sector arc which varies from $\theta=a$ to $\theta=b$. In most cases, $a=0$, and b is equal to some multiple of π . The transformation

$$\theta = \frac{b+a}{2} + \frac{b-a}{2} \hat{\theta} \quad (3.55)$$

is used to convert the variable θ from the interval $[a,b]$ to $[-1,1]$. The zeros of $T_{N+1}(\hat{\theta})$ are at

$$\hat{\theta}_k = \cos\left(\left(\frac{2k+1}{N+1}\right)\left(\frac{\pi}{2}\right)\right), \quad k = 0, 1, 2, \dots, N$$

and the corresponding interpolation points in $[a,b]$ are then at

$$\theta_k = \frac{b+a}{2} + \frac{b-a}{2} \hat{\theta}_k, \quad k = 0, 1, \dots, N. \quad (3.56)$$

The value of the maximum deviation from zero in the interval $[a,b]$ [44] is

$$\begin{aligned} \max_{a \leq \theta \leq b} \prod_{j=0}^N |\theta - \theta_j| &= \left| \frac{b-a}{2} \right|^{N+1} \max_{-1 \leq \hat{\theta} \leq 1} \prod_{k=0}^N |\hat{\theta} - \hat{\theta}_k| \\ &= \frac{1}{2^N} \left| \frac{b-a}{2} \right|^{N+1} \end{aligned}$$

If the derivative $f^{(N+1)}(\xi)$ in the maximum error defined by [44]

$$R_N(\theta) = f(\theta) - P_N(\theta) = \frac{f^{(N+1)}(\xi)}{(N+1)!} \prod_{j=0}^N |\theta - \theta_j|$$

is finite, and equal to C_{N+1} , then we have ensured that

$$|R_N(\theta)| \leq \frac{C_{N+1}}{2^N (N+1)!} \left| \frac{b-a}{2} \right|^{N+1} \quad (3.57)$$

in the interval $[a,b]$.

For convenience, Equation (3.26) with fixed $r = R$ is repeated here:

$$\phi(R, \theta) - \sum_{\substack{n=1 \\ n \neq 3}}^M \frac{9R^2}{n\pi(9-n^2)} [(-1)^n - 1] \sin \frac{2n}{3} \theta = \sum_{n=1}^N c_n R^{\frac{2n}{3}} \sin \frac{2n}{3} \theta \quad (3.26)$$

As discussed above, by computing the value of $\phi(R, \theta_k)$, $k = 1, 2, \dots, N$ in the interval $[a,b]$ at

$$\theta_k = \frac{b+a}{2} + \frac{b-a}{2} \cos \left(\frac{(2k-1)\pi}{N} \right) \quad (3.58)$$

where

$$\cos \left(\left(\frac{(2k-1)}{N} \right) \left(\frac{\pi}{2} \right) \right), \quad k = 1, 2, \dots, N$$

are the zeros of the Chebyshev polynomial $T_N(\hat{\theta})$ in the interval $[-1,1]$. the interpolation error is minimized in the minimax (minimum - maximum error) sense. Thus, substituting Equation (3.58) into Equation (3.26), leads to a simultaneous system of linear equations for determination of the c_n . The resulting system can be solved using any standard methods, for example, LU decomposition and back substitution.

It is important to note here, the zeros of $T_N(\hat{\theta})$, and consequently the locations of θ_k expressed in Equation (3.58), tend to be packed more densely near the ends of the interval than at the center as shown in Table 3.1. While the least-squares method gives equidistant interpolation points throughout the range except the one equidistant from the end points, use of the Chebyshev zeros as interpolation points will crowd the data points closer to both end points than in the least-squares method (see Table 3.1).

Table 3.1 Interpolation points θ_k along the sector arc from $\theta=0$ to $\theta=1.5\pi$

Point no.	Least-squares sense* θ_k	Minimax sense** θ_k
1	0.000000	0.000000
2	0.471239	0.115320
3	1.413717	0.971258
4	2.356194	2.356194
5	3.298672	3.741131
6	4.241150	4.597069
7	4.712389	4.712389

The node points, for $k = 2, \dots, 6$, are calculated by:

* - Equation (3.44)

** - Equation (3.58)

Thus, as stated by Lanczos [7], the non equidistant distribution of the data points which are strongly increased around the two ends of the range will prevent the error oscillations from becoming damaging. Note that the biggest errors usually occur in the neighborhoods of the two end points of the range. Moreover, by using the transformed Chebyshev zeros as the chosen points, the error now oscillates with the same order of magnitude, and absolutely smallest maximum error throughout the interval.

3.5 Series Solution for the Problem of Motz

The problem of Motz mentioned earlier is a problem with mixed boundary conditions satisfying Laplace's equation in a rectangular domain. This problem can

be considered as a standard example for treatment of a singularity of this type. At one side of the rectangular domain, a change in boundary conditions occurs. This leads to a singularity which is not located at an angular point, but it will be viewed as a corner with $\theta = \pi$. The singularity treatment will further be formulated by taking the point where the change of boundary conditions occurs as the center of semi-circular region with radius $r = R$. Figure 3.3 shows the geometric definition of the problem.

Consider the semi-circular region in Figure 3.3 governed by Laplace's equation:

$$\nabla^2 \phi = 0 \quad (3.59)$$

with boundary conditions

$$\frac{\partial \phi}{\partial n} = \frac{\partial \phi}{\partial \theta} = A \text{ along } \theta = 0 \quad (3.60)$$

$$\phi = B \text{ along } \theta = \pi \quad (3.61)$$

and

$$\phi = f(R, \theta) \text{ on the circular arc} \quad (3.62)$$

Recall that boundary conditions along the arc are satisfied at discrete points, and the function values at these points are given by interpolation of the solutions obtained previously through the Legendre Collocation Method. The boundary-matching will be done by the least-squares method.

Reasoning as in the previously discussed problem, and using the resulting Equation (B.14) in Appendix B., the series solution satisfying the mixed boundary conditions on the straight line except on the sector arc specified in Equations (3.60) and (3.61), and Laplace's Equation (3.59) is found to be:

$$\phi(r, \theta) = B + A(\theta - \alpha) + \sum_{n=1}^{\infty} c_n r^{\frac{2n-1}{2}} \cos \frac{2n-1}{2} \theta \quad (3.63)$$

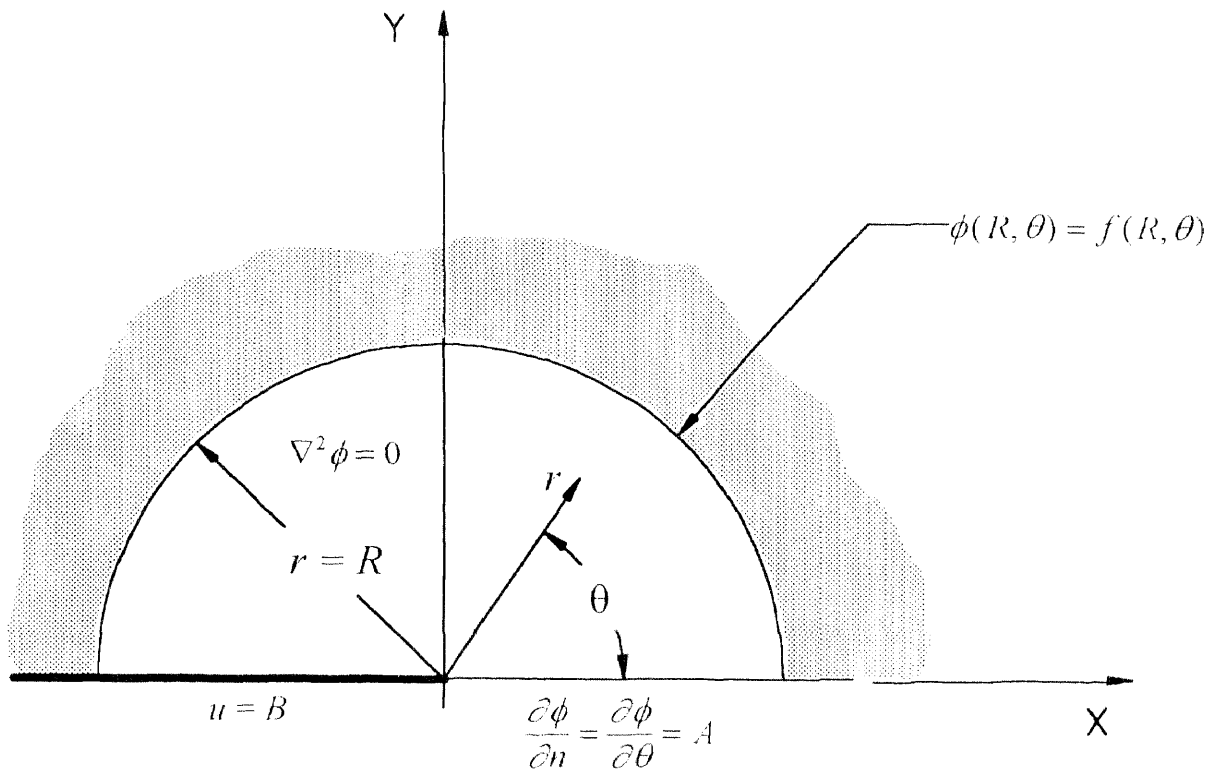


Figure 3.3 Mixed boundary conditions on a line.

The first two functions satisfy the non-homogeneous boundary conditions, while the summation term satisfies the homogeneous boundary conditions as formulated in Appendix B. Applying Equation (3.63) along the sector arc where $r = R$, for $\alpha = \pi$ (See Figure 3.3), and taking a finite number of terms for the summation, we have

$$\phi(R, \theta) \approx B + A(\theta - \pi) + \sum_{n=1}^N c_n R^{\frac{2n-1}{2}} \cos \frac{2n-1}{2} \theta \quad (3.64)$$

Re-arrange Equation (3.64) to yield

$$\phi(R, \theta) - B - A(\theta - \pi) \approx \sum_{n=1}^N c_n R^{\frac{2n-1}{2}} \cos \frac{2n-1}{2} \theta \quad (3.65)$$

To calculate the coefficients c_n by the discrete least-squares approximation method, we denote

$$f(R, \theta_k) = \phi(R, \theta_k) - B - A(\theta_k - \pi) \quad (3.66)$$

and

$$P_N(R, \theta_k) = \sum_{n=1}^N c_n R^{\frac{2n-1}{2}} \cos \frac{2n-1}{2} \theta_k \quad (3.67)$$

where $\theta_k, k = 1, 2, \dots, N$ are selected points along the arc necessary for determining c_n . Expression for the errors similar to those in Equation (3.30) are obtained at these points, and as a result, by using a least-squares method, the quantity that should be minimized is given by

$$S = \sum_{k=1}^N \left[f(R, \theta_k) - \sum_{n=1}^N c_n R^{\frac{2n-1}{2}} \cos \frac{2n-1}{2} \theta_k \right]^2 = \text{minimum} \quad (3.68)$$

Again Equation (3.32) is the necessary condition for Equation (3.68) to be a minimum. Upon minimizing Equation (3.68), we have

$$\begin{aligned} \frac{\partial S}{\partial c_n} &= \sum_{k=1}^N f(R, \theta_k) \cos \frac{2n-1}{2} \theta_k - \sum_{k=1}^N \left(c_1 R^{\frac{1}{2}} \cos \frac{1}{2} \theta_k \cos \frac{2n-1}{2} \theta_k + c_2 R^{\frac{3}{2}} \cos \frac{3}{2} \theta_k \cos \frac{2n-1}{2} \theta_k \right. \\ &\quad \left. + \dots + c_n R^{\frac{2n-1}{2}} \cos^2 \frac{2n-1}{2} \theta_k + \dots + c_N R^{\frac{2N-1}{2}} \cos \frac{2N-1}{2} \theta_k \cos \frac{2n-1}{2} \theta_k \right) = 0 \end{aligned} \quad (3.69)$$

and by observing Equation (3.69), c_n can be easily computed if there exists an orthogonality condition with respect to summation such that

$$\sum_{k=1}^N \cos \frac{2m-1}{2} \theta_k \cos \frac{2n-1}{2} \theta_k = 0, \quad \text{for } m \neq n \quad (3.70)$$

and

$$\sum_{k=1}^N \cos^2 \frac{2m-1}{2} \theta_k = \text{constant}, \quad \text{for } m = n \quad (3.71)$$

If we let

$$\varphi_k = \frac{\theta_k}{2} \quad (3.72)$$

the requirement in Equation (3.70) now becomes

$$\sum_{k=1}^N \cos(2m-1)\varphi_k \cos(2n-1)\varphi_k = 0, \quad \text{for } m \neq n \quad (3.73)$$

Equation (3.73) can be further transformed using the trigonometric identity in Equation (3.74)

$$\sum_{k=1}^N \cos(2m-1)\varphi_k \cos(2n-1)\varphi_k = \frac{1}{2} \sum_{k=1}^N [\cos 2(m-n)\varphi_k + \cos 2(m+n-1)\varphi_k] \quad (3.74)$$

In the previous section, it has been shown that

$$\sum_{k=1}^N \cos(2k-1)\varphi = \frac{1}{2} \sin 2N\varphi \csc \varphi \quad (3.75)$$

will vanish if

$$\varphi_k = \frac{(2k-1)}{N} \frac{\pi}{2}, \quad \text{for } k = 1, 2, \dots, N \quad (3.76)$$

(see Equations (3.36) and (3.37)).

Substituting φ_k in Equation (3.37) into the first term of the right-hand side of Equation (3.74) yields

$$\begin{aligned}
\sum_{k=1}^N \cos 2(m-n)\varphi_k &= \sum_{k=1}^N \cos(2k-1) \frac{(m-n)\pi}{N} \\
&= \frac{1}{2} \sin 2N \frac{(m-n)\pi}{N} \csc \frac{(m-n)\pi}{N} \\
&= 0
\end{aligned} \tag{3.77}$$

and into the second term yields

$$\begin{aligned}
\sum_{k=1}^N \cos 2(m+n-1)\varphi_k &= \sum_{k=1}^N \cos(2k-1) \frac{(m+n-1)\pi}{N} \\
&= \frac{1}{2} \sin 2N \frac{(m+n-1)\pi}{N} \csc \frac{(m+n-1)\pi}{N} \\
&= 0
\end{aligned} \tag{3.78}$$

Note that m and n are any integers. In conclusion, the orthogonality condition expressed in Equation (3.70) can be satisfied.

To find the constant, again Equation (3.70) is transformed using the trigonometric identity

$$\sum_{k=1}^N \cos^2(2n-1)\varphi_k = \frac{1}{2} \left[\sum_{k=1}^N 1 + \sum_{k=1}^N \cos 2(2n-1)\varphi_k \right] \tag{3.79}$$

and substituting the value of φ_k yields

$$\sum_{k=1}^N \cos^2(2n-1)\varphi_k = \frac{1}{2} \left[\sum_{k=1}^N 1 + \sum_{k=1}^N \cos(2k-1) \frac{(2n-1)\pi}{N} \right] \tag{3.80}$$

The first term of the right-hand side of Equation (3.80) is equal to N and the second term is

$$\sum_{k=1}^N \cos(2k-1) \frac{(2n-1)\pi}{N} = \frac{1}{2} \sin 2N \frac{(2n-1)\pi}{N} \csc \frac{(2n-1)\pi}{N} = 0$$

therefore Equation (3.80) or (3.71) can be defined by

$$\sum_{k=1}^N \cos^2(2n-1)\varphi_k = \frac{N}{2} \quad (3.81)$$

Having proved the orthogonality condition in Equation (3.70), and applying it to Equation (3.69), we have

$$\sum_{k=1}^N f(R, \theta_k) \cos \frac{(2n-1)}{2} \theta_k - \sum_{k=1}^N c_n R^{\frac{2n-1}{2}} \cos^2 \frac{(2n-1)}{2} \theta_k = 0 \quad (3.82)$$

Notice that c_n and R are independent of k , and using Equation (3.81) the coefficients c_n becomes

$$c_n = \frac{2}{NR^{\frac{2n-1}{2}}} \sum_{k=1}^N f(R, \theta_k) \cos \frac{2n-1}{2} \theta_k \quad (3.83)$$

where

$$\theta_k = 2\varphi_k = \frac{(2k-1)\pi}{N}, \quad k = 1, 2, \dots, N \quad (3.84)$$

$$f(R, \theta_k) = \phi(R, \theta_k) - A(\theta_k - \pi) - B$$

Finally, the series solution obtained for Laplace's equation for the region depicted in Figure 3.3 is

$$\phi(r, \theta) = B + A(\theta - \pi) + \sum_{n=1}^N c_n r^{\frac{2n-1}{2}} \cos \frac{2n-1}{2} \theta \quad (3.85)$$

The radial partial derivative is given by

$$\frac{\partial \phi}{\partial r} = \sum_{n=1}^N \frac{2n-1}{2} c_n r^{\frac{2n-3}{2}} \cos \frac{2n-1}{2} \theta \quad (3.86)$$

From the above equation, singularity occurs when $r = 0$ and $n = 1$. The tangential derivative is

$$\frac{\partial \phi}{\partial \theta} = A - \sum_{n=1}^N \frac{2n-1}{2} c_n r^{\frac{2n-1}{2}} \sin \frac{2n-1}{2} \theta. \quad (3.87)$$

Similar to the torsional problem of the L-shaped bar discussed in Section 3.3, the coefficients c_n in Equation (3.85), can also be determined using the minimax approach described in Section 3.4. This is a simple matter of fixing $r = R$, and replacing θ with θ_k in Equation (3.85); we then have

$$\phi(R, \theta_k) - B - A(\theta_k - \pi) = \sum_{n=1}^N c_n R^{\frac{2n-1}{2}} \cos \frac{2n-1}{2} \theta_k \quad (3.88)$$

where the value of $\phi(R, \theta_k)$, $k = 1, 2, \dots, N$ in the interval $[0, \pi]$ for the semi-circular arc (see Figure 3.3) is computed at

$$\theta_k = \frac{\pi}{2} + \frac{\pi}{2} \cos \left(\frac{(2k-1)\pi}{N} \frac{\pi}{2} \right) \quad (3.89)$$

and

$$\cos \left(\frac{(2k-1)\pi}{N} \frac{\pi}{2} \right), \quad k = 1, 2, \dots, N$$

This leads to a simultaneous system of linear equations for determination of the coefficients c_n . The resulting system can be solved using LU decomposition and back substitution.

CHAPTER 4

APPLICATIONS

4.1 Introduction

The presented formulations and solution procedures of the Legendre Collocation Method combined with an eigensolution series will now be tested on the following list of examples:

- A square bar under torsion
- The problem of Motz
- A Laplace equation for an L-shaped region

The above problems demonstrate the versatility and accuracy of the method. For a torsional problem of a square bar where there is no singularity involved, the Legendre Collocation Method developed in this study will be applied to a standard kind of two-dimensional problem most likely to be encountered in order to demonstrate its effectiveness. Not only the torsion function and its derivatives representing the shearing stress, but also the necessary torque are accurately and easily computed. The results are compared with the series solution by Timoshenko [32]. For this problem, only the Legendre Collocation Method described in Chapter 2 is applied.

In the second problem, termed the problem of Motz, the solution and its derivatives are obtained by means of procedures outlined in Chapters 2 and 3. Note that in this problem, Laplace's equation is the governing equation and the boundary conditions are mixed. The domain is rectangular and a boundary singularity occurs due to mixed boundary conditions on one side of the rectangle. This type of problem is less likely to be encountered in practical engineering

applications. The combined method developed in this study consists of the Legendre Collocation Method in combination with a series solution with its coefficients determined by least-squares or minimax approximation, for calculating the solution and its derivatives in the neighborhood of singularity. The results are compared with the available solutions obtained by previous investigators [33,36,37]. Good agreement is obtained. Furthermore, the procedures developed in this study are found easier to program, and simpler in the sense that there are no complicated mathematical formulations involved in comparison with the previous studies. The method used in the analysis of the L-shaped region is similar to that for the immediately preceding problem. This problem contains a singularity at the re-entrant corner, and is formulated in such a way that the form of the exact solution at the re-entrant corner is known. Thus, a more reliable comparison of the numerical results can be expected. Through the use of the Legendre Collocation Method alone, we find that relatively high errors occur in the neighborhood of the singularity, near the re-entrant corner. This demonstrates the need for the special treatment of the singularity. The approximate solution and its derivatives in the neighborhood of singularity are then compared with the exact solution and derivatives. Again, very good agreement is obtained. This last example has been used by several authors [16,17] in their study of the Boundary Integral Method or Boundary Element Method. Unfortunately, in their papers there are no numerical values of either the solution or its derivatives available. Thus, comparisons are not possible.

4.2 Torsion of A Square Bar

Consider a square bar under torsion as shown in Figure 4.1. We will examine the accuracy and rate of convergence of the solution, its first derivatives related to

stress or flux, and the numerical integration of the solution at the collocation points to find the torque, using the Legendre Collocation Method. This classical problem satisfies the following Poisson equation [45]

$$\nabla^2 \Psi = -2 \quad \text{in a square domain} \quad (4.1)$$

where Ψ is the Prandtl stress function. The boundary conditions on all sides of the square cross-section are $\Psi = 0$. Consequently, the values of the stress function at the boundary collocation points, including the four corner points are zero. Once the problem is solved, the solution Ψ at the interior collocation points becomes known, and the shearing stress components τ_{zx} and τ_{zy} are computed using the following formulas

$$\tau_{zx} = \frac{\partial \Psi}{\partial y} \quad (4.2)$$

and

$$\tau_{zy} = -\frac{\partial \Psi}{\partial x} \quad (4.3)$$

The application of the Legendre Collocation Method to this problem generates a $(NPX - 2) \times (NPY - 2)$ system of linear equations. Since $\Psi = 0$ on the boundary and the problem is solved for Ψ , we need only to determine Ψ at the interior collocation points. Thus, a modified Equation (2.51)

$$\left(\frac{2}{\Delta x}\right)^2 \sum_{i=2}^{NPX-1} BX_{ki} \Psi_{im} + \left(\frac{2}{\Delta y}\right)^2 \sum_{j=2}^{NPY-1} BY_{mj} \Psi_{kj} = -2 \quad (4.4)$$

that satisfies the governing equation (4.1) is applied to each interior point (x_k, y_m) for $k = 2, \dots, NPX - 1$ and $m = 2, \dots, NPY - 1$ to yield a system of equations.

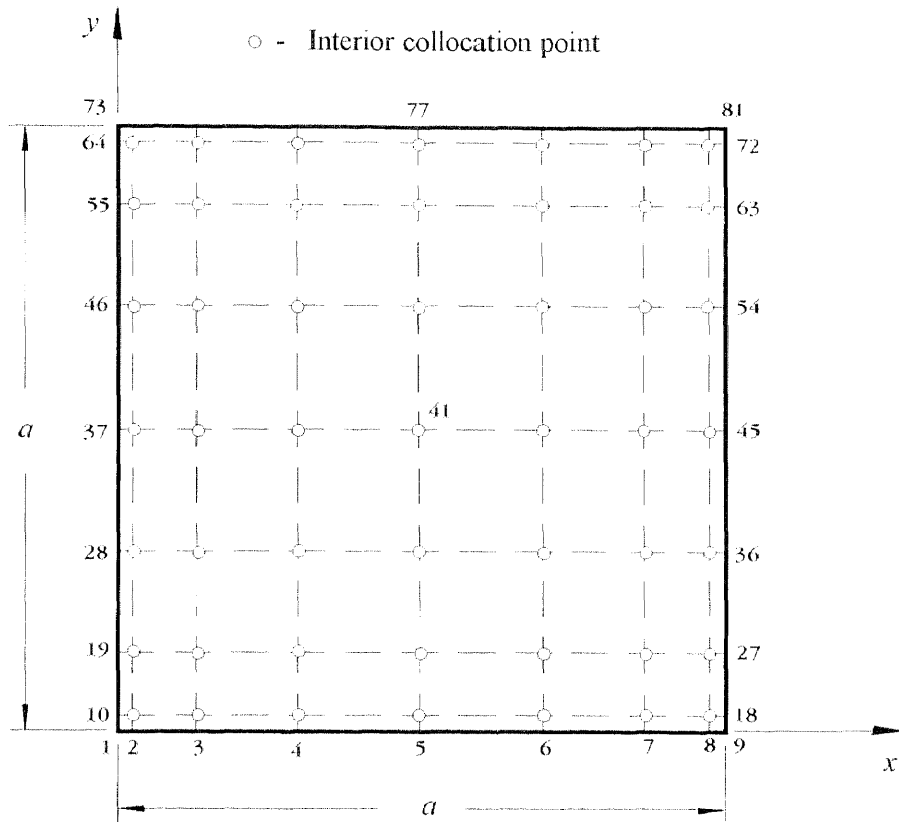


Figure 4.1 9×9 mesh for a square bar under torsion. Global numbering scheme is shown with $NPX = NPY = 9$.

Note that in the computer program, the double indices km for Ψ are replaced by single indices, and a global numbering scheme is adopted (see Figure 4.1). Also, the same number of points is taken in both the x and y directions. Hence, $NPX = NPY$, the coefficient matrix \mathbf{AX} is the same as \mathbf{AY} , and \mathbf{BX} is also equal to \mathbf{BY} .

Finally, the x component of shearing stress is defined by

$$\tau_{zx}(x_k, y_m) = \frac{2}{\Delta y} \sum_{j=1}^{NPY} A_{mj} \Psi_{kj} \quad \text{for } m = 1, \dots, NPY \quad (4.5)$$

as an approximation to Equation (4.2). In order to obtain the stresses for the entire domain, Equation (4.5) will be repeated for $k = 1, \dots, NPX$. Similarly, the shearing stress in the y direction in Equation (4.3) is computed by

$$\tau_{xy}(x_k, y_m) = -\frac{2}{\Delta x} \sum_{i=1}^{NPX} A_{ki} \Psi_{im} \quad \text{for } k = 1, \dots, NPX \quad (4.6)$$

and will also be evaluated for $m = 1, \dots, NPY$.

In the computation, the length of side a is taken as unity, therefore $\Delta x = \Delta y = a = 1$. As shown in Figure 4.1, the interior collocation points are not equally spaced. This is due to the fact that those points are the zeros of a Legendre polynomial. The figure shown is for a 9×9 mesh; therefore the interior points are the zeros of the 7th-degree Legendre polynomial.

Convergence is studied at two selected points (see Figure 4.1):

- The middle point of the cross section (Point 41) where the maximum stress is located;
- The mid-point of a side of the square (Point 5, 37, 45 and 77) where the maximum shearing stress occurs.

In order to study the convergence of the solution function and the maximum shearing stress, these two points should be kept in the same place independently of the mesh, therefore an odd number of meshes had been selected. For example, 3×3 , 5×5 etc.

Table 4.1 below gives the results of maximum value of the stress function Ψ which converges very rapidly as indicated by percentage error.

Table 4.1 Maximum Stress Function Ψ - Torsion of Square Bar

	Mesh Size				
	3 x 3	5 x 5	7 x 7	9 x 9	11 x 11
LCM	0.125	0.148148	0.147362	0.147343	0.147343
Exact	0.147343	0.147343	0.147343	0.147343	0.147343
%-Error	15.16	0.55	0.01	0	0

* Exact - Infinite Series Solution by Timoshenko [32].

* LCM - Results obtained using Legendre Collocation Method.

For 9×9 mesh size, there are 49 interior points at which the Poisson equation that governs the torsional problem, is satisfied, and the function values around the boundaries are equal to zeros. Therefore the total number of algebraic equations solved for Ψ is also 49. As indicated in Tables 4.1, various mesh sizes are used in the computation, and their corresponding numbers of equations are:

- 3×3 mesh size and one equation to be solved;
- 5×5 mesh size and nine equations to be solved, etc.

Therefore for $N \times N$ mesh size, there will be $(N - 2) \times (N - 2)$ equations to be solved, and the number of system equations would be different for different types of boundary conditions. Note that with only one equation and one unknown, the error is 15.16%. The error drops to 0.55% when 5×5 mesh size is used. From an engineering standpoint, this is a quite negligible error.

In many problems in mechanics, we are particularly interested in the first derivative of the approximate solution which represents the stress. As expected, a comparison between Table 4.1 and Table 4.2 shows the maximum shearing stress converges more slowly than the maximum stress function Ψ . It is understandable, since the maximum stress is calculated by Equation (4.5) or (4.6) which is another approximation of the approximate solution Ψ . The convergence of the stress is also quite rapid as depicted in a graphical plot in Figure 4.2.

Table 4.2 k - value for Maximum Shearing Stress - Torsion of Square Bar

	Mesh Size				
	3×3	5×5	7×7	9×9	11×11
LCM	-0.5	-0.685185	-0.674157	-0.6756	-0.675221
Exact	-0.675186	-0.675186	-0.675186	-0.675186	-0.675186
%-Error	25.95	1.48	0.15	0.06	0.01

* Maximum Shearing Stress is given by [32]:

$$\tau_{\max} = kG\theta a$$

As has been mentioned in Chapter 2, one of the advantages of taking the zeros of a Legendre polynomial as collocation points is the availability of function values needed for numerical integration employing Gauss-Legendre quadrature (see Equation (2.40)). The torque for the torsion of a square bar is obtained by summing the product of the solution Ψ at the collocation points with the associated weights, computed using Equation (C.16) in Appendix C. Table 4.3 shows again the rapid convergence of the torque.

Table 4.3 k_1 - value for Torque - Torsion of Square Bar.

	Mesh Size				
	3 x 3	5 x 5	7 x 7	9 x 9	11 x 11
LCM	0.25	0.141975	0.1406	0.140579	0.140577
Exact	0.140577	0.140577	0.140577	0.140577	0.140577
%-Error	77.84	0.55	0.01	0	0

* Torque is given by [32]:

$$M_t = k_1 G \theta a^4$$

Table 4.4 shows a comparison between Timoshenko's solution [32] and the approximate solution of the torsion function Ψ using a 9×9 mesh. Note that Timoshenko's solution which is a series solution is computed up to 10^{-9} in accuracy, with the summation ranging from 119 to 500 terms. Therefore it can be considered as the exact solution. As can be expected, due to sharp corner points, the highest relative errors of 1.23% occur at the four points nearest to the corner points. In Figure 4.1, these points are numbers 11, 17, 65 and 71. The errors at other points in the domain are extremely low, ranging from 0.00058% to 0.079%. In Figure 4.3, we have a 3-D view of the torsion function Ψ , while Figure 4.4

shows its contour plot. Both figures are based on the 9×9 mesh solution of the Legendre Collocation Method.

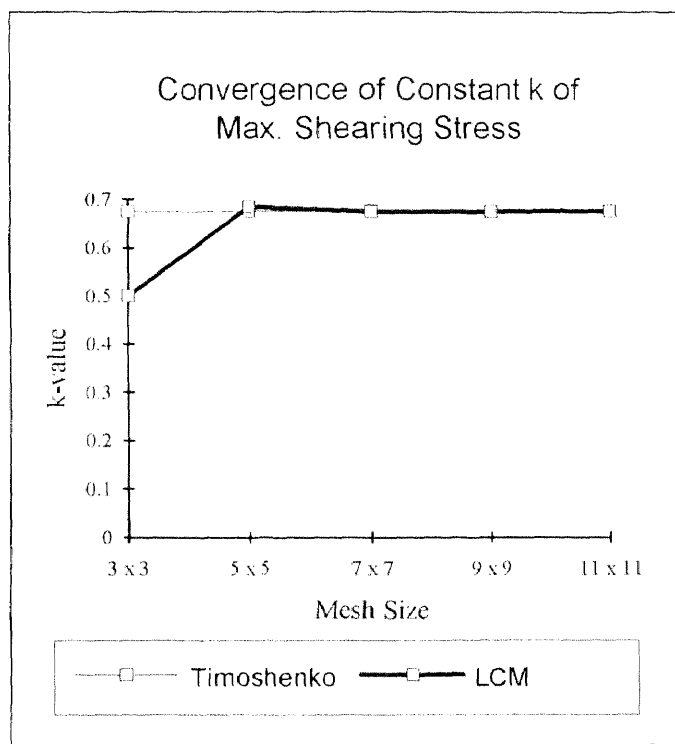


Figure 4.2 Convergence study of maximum shearing stress of square bar under torsion.

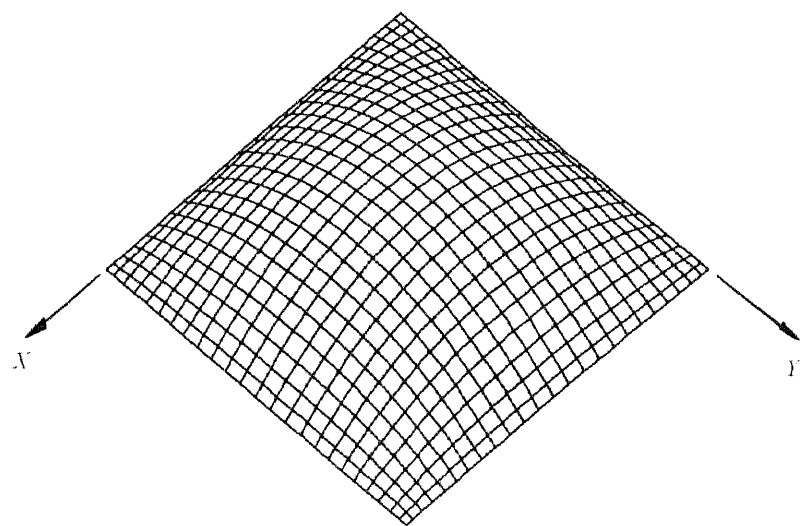


Figure 4.3 View of torsion or stress function Ψ plotted based on 9×9 mesh solution.

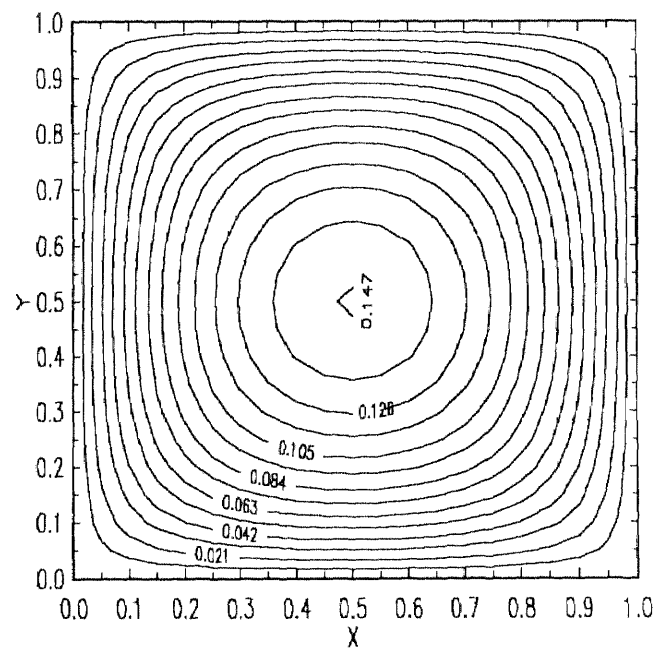


Figure 4.4 Contour plot of torsion function Ψ

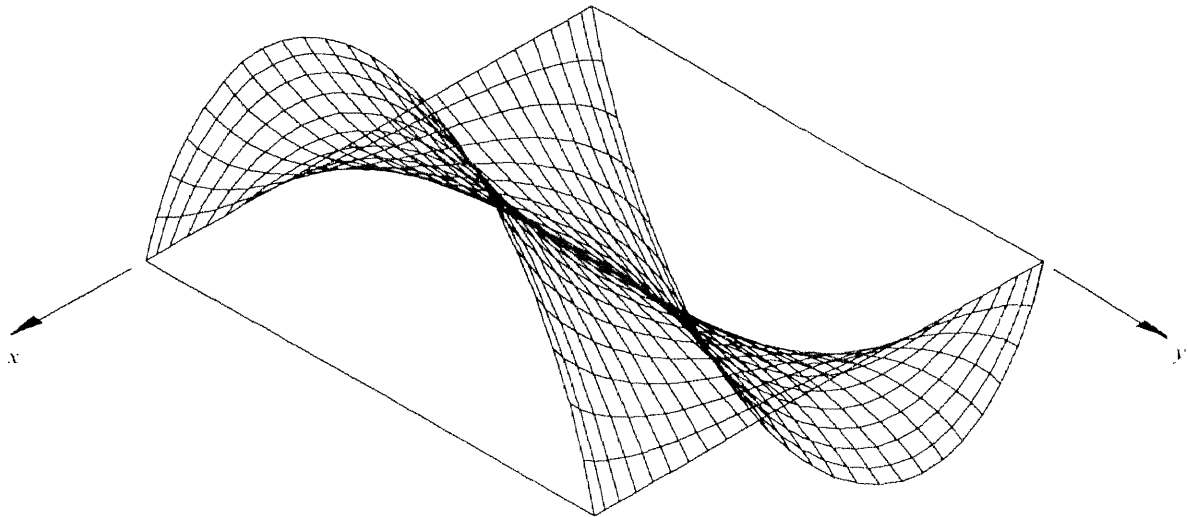


Figure 4.5 Three-dimensional plot of the shearing stress τ_{zy} obtained using 9×9 mesh size.

Also of interest is a comparison between shearing stresses τ_{zy} obtained by Timoshenko [32] and the Legendre Collocation Method utilizing Equation (4.6). Again, this comparison is performed at the collocation points (see Table 4.5). The higher relative errors occur at the collocation points nearest to the top and bottom sides of the square domain shown in Figure 4.1. Thus, on the line where point numbers 10 to 18 are located, the errors range from 2.08% to 4.19% for 9×9 mesh solution. The same magnitude of errors occurs at point numbers 64 to 72. Errors at other points are negligible, ranging from 0.007% to 0.25%. It is important to note here, that the locations of the maximum shearing stress components are correctly located by this method. As indicated in Table 4.2 and can be calculated from results in Table 4.5, the error of the maximum shearing stress is 0.06% - a negligible number. Figure 4.5 shows a 3-D plot of the shearing stress τ_{zy} . Figure 4.6 shows another 3-D plot of the magnitude of the resultant shearing stress where

one can immediately find the location of the maximum shearing stress. A contour plot of the magnitude of the resultant shearing stress is given in Figure 4.7.

The above torsion problem illustrates the general applicability and accuracy of the Legendre Collocation Method when applied to the most common types of problems. Further illustrations, typical of real situations containing singularities are included in the next sections.

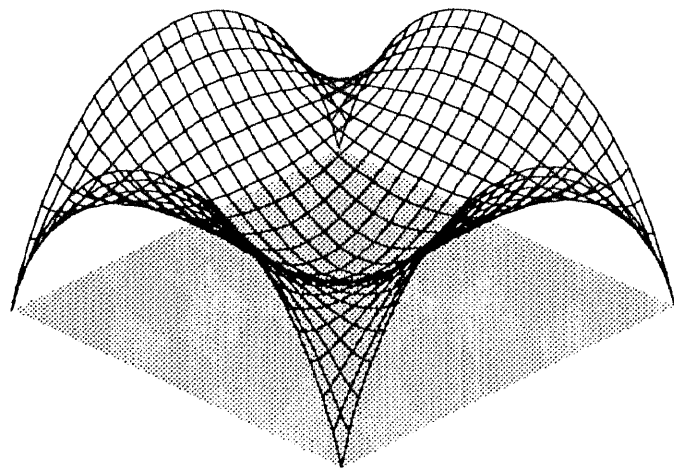


Figure 4.6 Three dimensional plot of the magnitude of resultant shearing stress.

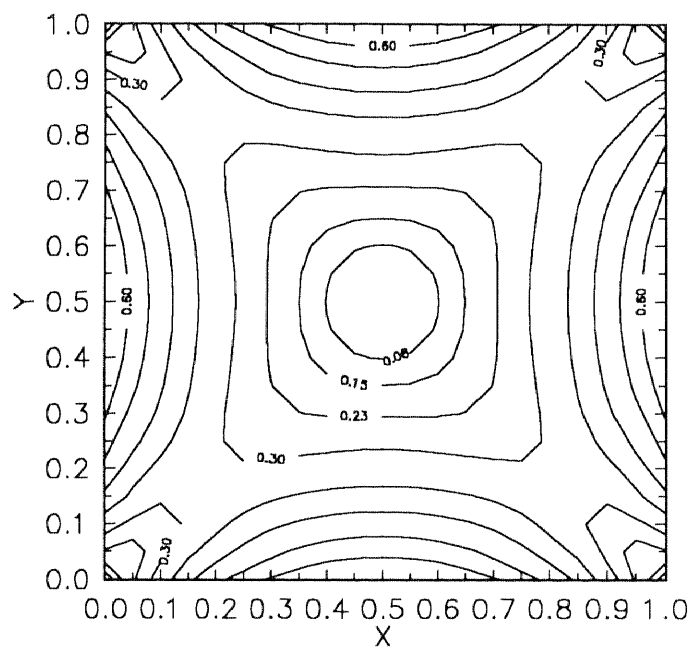


Figure 4.7 Contour plot of the magnitude of resultant of shearing stress.

Table 4.4 Comparison of torsion function Ψ at the collocation points (see Figure 4.1)

The numbers in the table have the following significance:

1st value - Legendre Collocation Method result (9×9)

2nd value - Timoshenko's result [32]

0.000000	0.000000	0.000000	0.000000	0.000000	0.000000	0.000000	0.000000	0.000000
0.000000	0.000000	0.000000	0.000000	0.000000	0.000000	0.000000	0.000000	0.000000
0.000000	0.002856	0.009556	0.014706	0.016551	0.014706	0.009556	0.002856	0.000000
0.000000	0.002821	0.009548	0.014712	0.016546	0.016546	0.009548	0.002821	0.000000
0.000000	0.009556	0.038210	0.062810	0.071762	0.062810	0.038210	0.009556	0.000000
0.000000	0.009549	0.038210	0.062812	0.071760	0.062812	0.038210	0.009549	0.000000
0.000000	0.014706	0.062810	0.108646	0.126135	0.108646	0.062810	0.014706	0.000000
0.000000	0.014712	0.062812	0.108645	0.126136	0.108645	0.062812	0.014712	0.000000
0.000000	0.016551	0.071762	0.126135	0.147343	0.126135	0.071762	0.016551	0.000000
0.000000	0.016546	0.071760	0.126136	0.147343	0.126136	0.071760	0.016546	0.000000
0.000000	0.014706	0.062810	0.108646	0.126135	0.108646	0.062810	0.014706	0.000000
0.000000	0.014712	0.062812	0.108645	0.126136	0.108645	0.062812	0.014712	0.000000
0.000000	0.009556	0.038210	0.062810	0.071762	0.062810	0.038210	0.009556	0.000000
0.000000	0.009549	0.038210	0.062812	0.071760	0.062812	0.038210	0.009549	0.000000
0.000000	0.002856	0.009556	0.014706	0.016551	0.014706	0.009556	0.002856	0.000000
0.000000	0.002821	0.009548	0.014712	0.016546	0.014712	0.009548	0.002821	0.000000
0.000000	0.000000	0.000000	0.000000	0.000000	0.000000	0.000000	0.000000	0.000000
0.000000	0.000000	0.000000	0.000000	0.000000	0.000000	0.000000	0.000000	0.000000

Table 4.5 Shearing stress τ_{xy} at the collocation points:

The number in the table have the following significance:

1st value - Legendre Collocation Method result (9 × 9)

2nd value - Timoshenko's result [32]

0.000000	0.000000	0.000000	0.000000	0.000000	0.000000	0.000000	0.000000	0.000000
0.000000	0.000000	0.000000	0.000000	0.000000	0.000000	0.000000	0.000000	0.000000
-0.128484	-0.097819	-0.044136	-0.019729	0.000000	0.019729	0.044136	0.097819	0.128484
-0.131211	-0.094685	-0.046066	-0.018986	0.000000	0.018986	0.046066	0.094685	0.131211
-0.400485	-0.351858	-0.213433	-0.092273	0.000000	0.092273	0.213433	0.351858	0.400485
-0.399502	-0.351932	-0.213416	-0.092260	0.000000	0.092260	0.213416	0.351932	0.399502
-0.602778	-0.553529	-0.380708	-0.178391	0.000000	0.178391	0.380708	0.553529	0.602778
-0.603005	-0.553699	-0.380594	-0.178426	0.000000	0.178426	0.380594	0.553699	0.603005
-0.675600	-0.625620	-0.444132	-0.215113	0.000000	0.215113	0.444132	0.625620	0.675600
-0.675186	-0.625523	-0.444197	-0.215098	0.000000	0.215098	0.444197	0.625523	0.675186
-0.602778	-0.553529	-0.380708	-0.178391	0.000000	0.178391	0.380708	0.553529	0.602778
-0.603005	-0.553699	-0.380594	-0.178426	0.000000	0.178426	0.380594	0.553699	0.603005
0.400485	-0.351858	-0.213433	-0.092273	0.000000	0.092273	0.213433	0.351858	0.400485
-0.399502	-0.351932	-0.213416	-0.092260	0.000000	0.092260	0.213416	0.351932	0.399502
-0.128484	-0.097819	-0.044136	-0.019729	0.000000	0.019729	0.044136	0.097819	0.128484
-0.131211	-0.094685	-0.046066	-0.018986	0.000000	0.018986	0.046066	0.094685	0.131211
0.000000	0.000000	0.000000	0.000000	0.000000	0.000000	0.000000	0.000000	0.000000
0.000000	0.000000	0.000000	0.000000	0.000000	0.000000	0.000000	0.000000	0.000000

4.3 The Problem of Motz

The problem of Motz [33,39] is a problem that satisfies Laplace's equation

$$\nabla^2 u = 0 \quad (4.7)$$

and is subject to mixed-boundary conditions as depicted in Figure 4.8, where ABCD is a rectangle with the dimensions AO = OB = BC. This problem has been solved by several other investigators using different approximation techniques [33,36,37,46]. The most accurate results were obtained by Whiteman and Papamichael [36] using a Conformal Transformation Method; Symm [37] treated the problem using an Integral Equation Method, Lefebvre [33] obtained exactly the same values as those of Whiteman and Papamichael by using a Boundary Element Method specifically formulated for this problem. The mathematical complexity of these previous works makes the procedure proposed below, a combination of the Legendre Collocation Method and an Eigenfunctions solution in the neighborhood of the singular point, very attractive.

Observation of Figure 4.8 reveals that this problem contains a boundary singularity at point O. Note that along boundary AO, $u = 0.5$ is prescribed, and the normal derivative on boundary OB is zero. Thus at point O there is a change in the boundary condition, and that gives rise to a singularity. Two major steps will be implemented. First, the formulation described in Chapter 2 will be used to obtain the solution u at the collocation points in the entire computational domain; then the special treatment outlined in Chapter 3 will be applied, so that an accurate solution of u , including its derivatives in a neighborhood of singularity, are obtained.

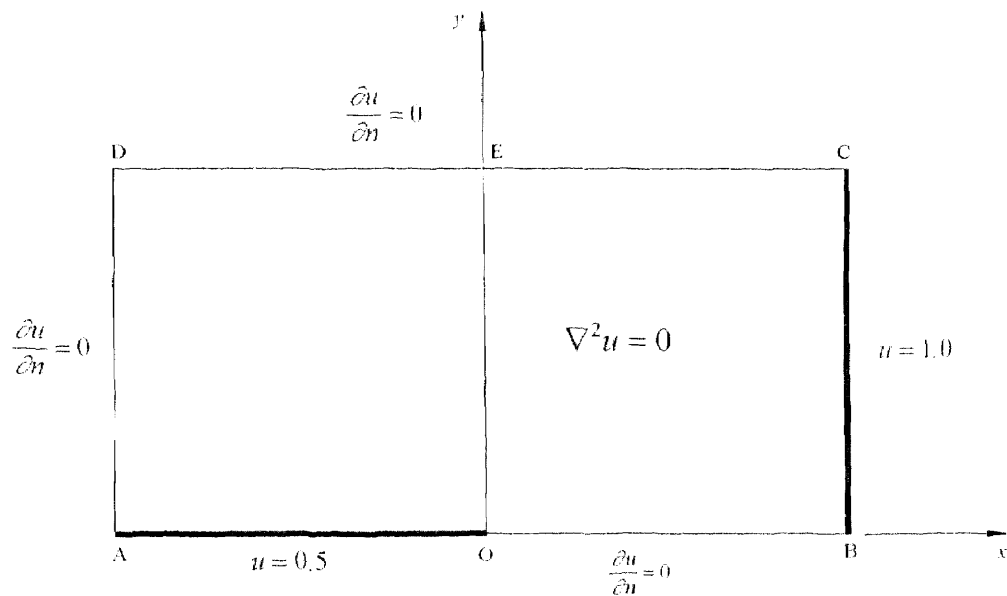


Figure 4.8 Geometric definitions for the problem of Motz

For convenience in comparison with the results obtained by the other authors [33,36,37], the dimensions of the rectangle domain depicted in Figure 4.8 are taken to be 14×7 . The use of the p -version of the Legendre Collocation Method requires that the computational domain be broken up into two fixed elements: AOED and OBCE, both are square elements 7×7 in size. The accuracy of the solution u is achieved by increasing the number of collocation points, which are determined by the degree of Legendre polynomial used in the x and y directions.

As shown in Figure 4.9, a global numbering scheme using a single index is adopted for the entire domain. Thus, in computation, the continuity of the value of the function at the collocation points located at the junction between the two elements is automatically ensured. The most obvious example of these points are the interelement boundary points along line OE. But, for convenience in writing

the formulas, the double subscript numbering scheme is used in Chapter 2, and will be used here.

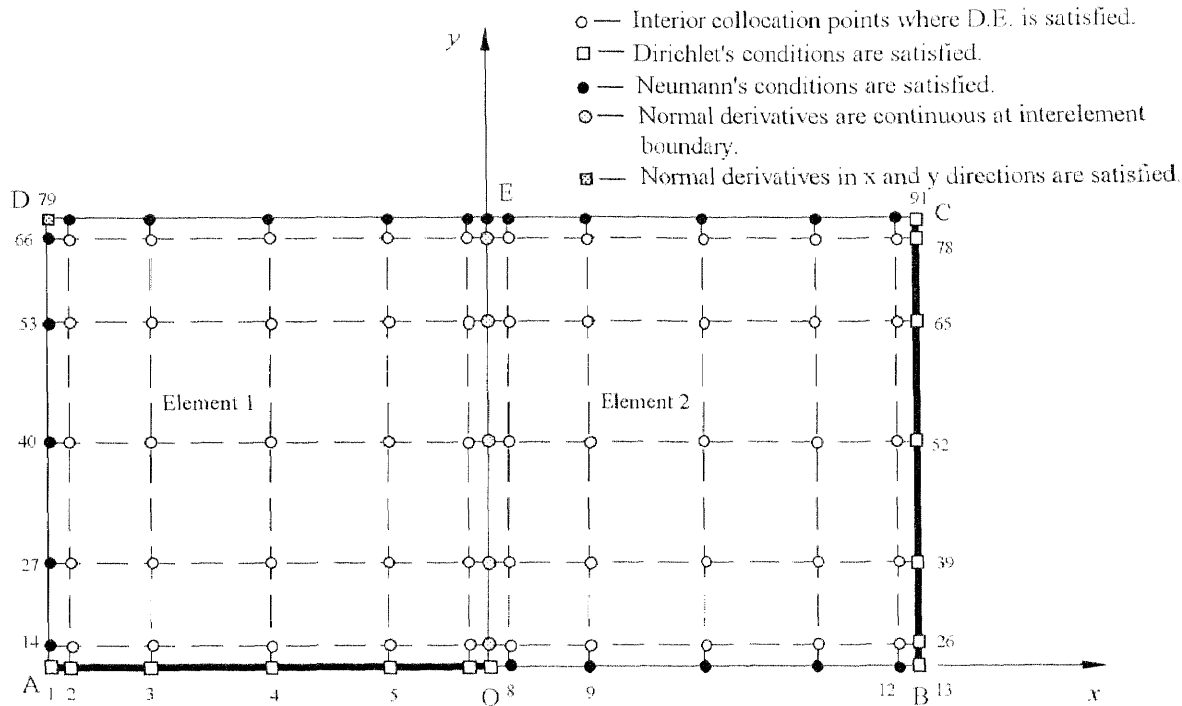


Figure 4.9 The domain is divided into two elements, and 7×7 - Legendre collocation grids for each element are shown.

In this example, the same number of collocation points in the x and y directions, $NPX = NPY$ is taken. Thus, the coefficient matrices for the first derivative is $\mathbf{AX} = \mathbf{AY}$, and for the second derivative is $\mathbf{BX} = \mathbf{BY}$. Figure 4.9 shows the domain with two macro elements, and for each element $NPX = NPY = 7$. Hence, the interior collocation points are the zeros of the 5th - degree Legendre polynomial, and there will be a total of 91 nodes for the entire domain as shown. These are the nodes where the solution u has either to be determined or prescribed.

As mentioned earlier, the first step in handling this problem containing a boundary singularity is to determine the solution u at the collocation points in the entire domain. As a result of the application of the Legendre Collocation Method, a set of simultaneous equations has to be solved. This set of algebraic linear equations is generated by the following requirements:

- (a) The **interior** collocation equations from the differential equation, namely

$$\left(\frac{2}{\Delta x^{(e)}}\right)^2 \sum_{i=1}^{NPX} BX_{ki} u_{im} + \left(\frac{2}{\Delta y^{(e)}}\right)^2 \sum_{j=1}^{NPY} BY_{mj} u_{kj} = 0 \quad (4.8)$$

have to be satisfied at each of the interior nodes of each element (See Figure 4.9). Note that Equation (4.8) is a modification of Equation (2.51) to suit this problem. The superscript in parentheses denotes the element number, here $e = 1, 2$.

- (b) The **boundary** collocation equations stem from satisfying:

- Dirichlet conditions along lines AO and BC. Thus,

$$\sum_{i=1}^{NPX} u_{ij}^{(1)} = 0.5 \quad \text{along line AO} \quad (4.9)$$

and

$$\sum_{j=1}^{NPY} u_{NPX,j}^{(2)} = 1.0 \quad \text{along line BC} \quad (4.10)$$

Since a single index is used in the computer program, in the assembled matrix Equation (2.57), the elements of the matrix \mathbf{K} that correspond to the node number n of the global numbering scheme will be equal to unity, i.e. $K_{nn} = 1$, and the corresponding load vector \mathbf{F} has components equal to either 0.5 or 1.0,

depending on which boundary line (OA or BC) is considered. Note that this satisfaction of the function values on the boundaries AO and BC not only includes the corner points A, B, and C, but also the inter-element boundary point O.

- Neumann conditions along OB, CD, and DA boundaries. For boundary lines OB and CD, it is only necessary to satisfy the prescribed normal derivative, i.e. $\frac{\partial u}{\partial y} = 0$ at the interior boundary collocation points. At points O, B, and C, the function values are to be satisfied. Thus, on line OB

$$\left(\frac{2}{\Delta y^{(2)}}\right) \sum_{j=1}^{NPY} A Y_{1,j} u_j = 0 \quad \text{for } i = 2, \dots, NPX - 1 \quad (4.11)$$

Similarly, at the interior nodes on line EC, one has

$$\left(\frac{2}{\Delta y^{(2)}}\right) \sum_{j=1}^{NPY} A Y_{NPY,j} u_j = 0 \quad \text{for } i = 2, \dots, NPX - 1 \quad (4.12)$$

For line DE

$$\left(\frac{2}{\Delta y^{(1)}}\right) \sum_{j=1}^{NPY} A Y_{NPY,j} u_j = 0 \quad \text{for } i = 2, \dots, NPX - 1 \quad (4.13)$$

at point E, the enforcement can be done by either one of the following equations

$$\left(\frac{2}{\Delta y^{(1)}}\right) \sum_{j=1}^{NPY} A Y_{NPY,j} u_{NPX,j} = 0 \quad (4.14a)$$

or

$$\left(\frac{2}{\Delta y^{(2)}} \right) \sum_{j=1}^{NPY} A Y_{NPY,j} u_{ij} = 0 \quad (4.14b)$$

The satisfaction of prescribed normal derivative, i.e. $\frac{\partial u}{\partial n} = 0$, at the interior nodes on line AD gives

$$\left(\frac{2}{\Delta x^{(1)}} \right) \sum_{i=1}^{NPA} A X_{i,j} u_{ij} = 0 \quad \text{for } j = 2, \dots, NPY - 1 \quad (4.15)$$

Note that the resulting Equations (4.11), (4.12), (4.13), (4.14a), and (4.14b) are based on Equations (2.54) and (2.56), while Equation (4.15) stems from Equation (2.53).

- (c) The **normal derivative continuity** equations at interior nodes along line OE, the interelement boundary are given by

$$\left(\frac{2}{\Delta x^{(1)}} \right) \sum_{i=1}^{NPA} A X_{NPA,i} u_{ij} - \left(\frac{2}{\Delta x^{(2)}} \right) \sum_{i=1}^{NPX} A X_{i,j} u_{ij} = 0 \quad (4.16)$$

for $j = 2, \dots, NPY - 1$

as in Equation (2.52).

- (d) The **corner** equation at corner point D in Figure 4.9: Both normal derivatives in the x and y directions are zero. The equation similar to Equation (2.63) applied to corner D is given by

$$\left(\frac{2}{\Delta y^{(1)}} \right) \sum_{j=1}^{NPY} A Y_{NPY,j} u_{ij} - \left(\frac{2}{\Delta x^{(1)}} \right) \sum_{i=1}^{NPA} A X_{i,NPY} u_{i,NPY} = 0 \quad (4.17)$$

Solving a set of algebraic equations resulting from the Legendre Collocation technique outlined above gives the solution u at the collocation points. The solution is remarkably accurate except in a neighborhood of singular point. Thus, a special treatment as described in Chapter 3 will be applied as follows:

- Once a half circle sector for isolating the singular point O has been established (see Figure 4.10), Equation (3.88) derived in Chapter 3 is applied along the sector arc of this isolated region. Thus, the resulting equation can be written as

$$\phi(R, \theta) - 0.5 = \sum_{n=1}^N c_n R^{\frac{2n-1}{2}} \cos \frac{2n-1}{2} \theta \quad (4.18)$$

where A and B in Equation (3.88) have been replaced with the known values of $A = 0$, $B = 0.5$, and R is a fixed radius (see also Figure 3.3). Furthermore, Equation (4.18) not only satisfies the Laplace equation (4.7), but also both the Neumann conditions on line OB and Dirichlet conditions on line AO.

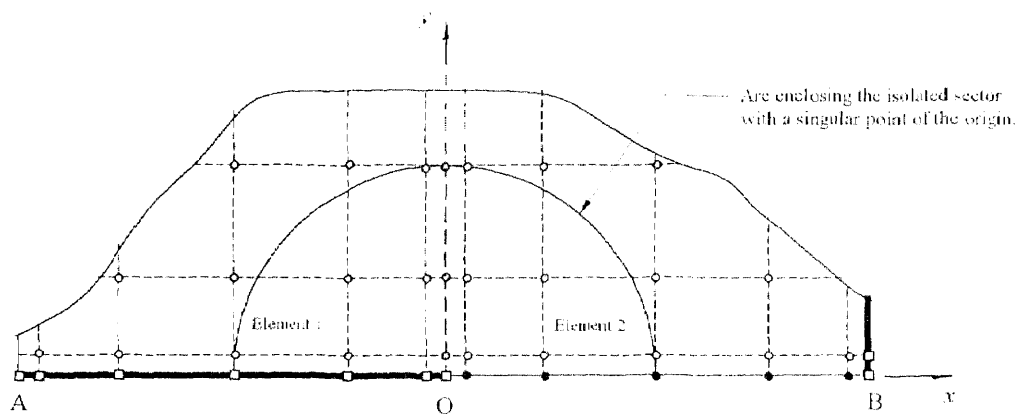


Figure 4.10 An half circle sector isolated for a special treatment in the neighborhood of a singular point O

If Equation (4.18) is made equal to the solution function that was obtained by the Legendre Collocation Method along the arc, then the coefficients c_n can be determined. Note that Equation (4.18) is expressed in polar coordinates (r, θ) with the origin at point O. The function u obtained by the Legendre Collocation Method is now replaced by ϕ in the half sector domain. To ensure accurate results of solution, the radius R of the half sector must be taken sufficiently large so that, outside the sector, the solution u obtained by the Legendre Collocation Method is virtually unaffected by the singular point O. Thus, as a general rule, to be on a safe side, the fixed radius R will be half the length of the longer side of the rectangular element.

- b. In this study, the determination of the coefficients c_n in Equation (4.18) can be performed by the following two alternative methods:
 - **A discrete least-square approximation.**

As outlined in Chapter 3, Equation (3.83) is used to determine c_n such that

$$c_n = \frac{2}{NR^{\frac{2n-1}{2}}} \sum_{k=1}^N f(R, \theta_k) \cos \frac{2n-1}{2} \theta_k \quad (4.19)$$

where $R = 3.5$

$$\theta_k = \frac{(2k-1)\pi}{N} \quad k = 1, 2, \dots, N$$

$$f(R, \theta_k) = \phi(R, \theta_k) - 0.5$$

and n is the number of selected discrete points on the arc. Note that the solution $\phi(R, \theta_k)$ is the value of the function on the arc, computed by interpolating the solution u previously obtained

through the Legendre Collocation Method. It is clear that before the interpolation can be done, the polar coordinates (r, θ) have to be transformed into cartesian coordinates (x, y) .

- **Minimax approximation at Chebyshev zeros.**

In this alternate procedure, in order to determine c_n , it is necessary to solve a set of simultaneous equations generated by Equation (4.18) such that

$$\sum_{n=1}^N c_n R^{\frac{2n-1}{2}} \cos \frac{2n-1}{2} \theta = \phi(R, \theta) - 0.5 \quad (4.20)$$

where $R = 3.5$, and

$$\theta_k = \frac{\pi}{2} + \frac{\pi}{2} \cos \left(\frac{(2k-1)}{N} \frac{\pi}{2} \right), \quad k = 1, 2, \dots, N.$$

Note that θ_k are the zeros of a Chebyshev polynomial that have been mapped onto the real interval $[0, \pi]$ (see Figure 4.10). The function values $\phi(R, \theta_k)$ in Equation (4.20) have the same meaning as $\phi(R, \theta_k)$ in the discrete least-squares approximation described above.

- Once the constant coefficients c_n in Equation (4.18) are determined through either one of the methods described above, Equation (3.50) now takes the form

$$\phi(r, \theta) = 0.5 + \sum_{n=1}^N c_n r^{\frac{2n-1}{2}} \cos \frac{2n-1}{2} \theta \quad (4.21)$$

and will satisfy Laplace's equation (4.7). In addition to that, Equation (4.21) identically satisfies the boundary conditions along the straight line

AB containing the singularity at point O, and approximately satisfies the values of the function along the sector arc. Thus, Equation (4.21) not only gives the approximate solution in this isolated sector, but also can be used to calculate the derivative with respect to the radius r

$$\frac{\partial \phi}{\partial r} = \sum_{n=1}^N \frac{2n-1}{2} c_n r^{\frac{2n-3}{2}} \cos \frac{2n-1}{2} \theta \quad (4.22)$$

and the derivative with respect to θ

$$\frac{\partial \phi}{\partial \theta} = - \sum_{n=1}^N \frac{2n-1}{2} c_n r^{\frac{2n-1}{2}} \sin \frac{2n-1}{2} \theta \quad (4.23)$$

From Equation (4.22), it is obvious that $\frac{\partial \phi}{\partial r} \rightarrow \infty$, when $n = 1$ and $r \rightarrow 0$.

This establishes the existence of the singularity at point O in Figures 4.8, 4.9 and 4.10.

The convergence of the approximate solution u obtained through the Legendre Collocation Method is shown in Table 4.6. Table 4.7 shows the comparison with previous results obtained by Lefeber [33], Symm [37], and Whiteman and Papamichael [36]. It is important to note here that the Legendre Collocation Method produces the solution at the collocation points which are the corresponding zeros of the Legendre polynomial plus the two endpoints of the interval. The solutions at a unit mesh point in Table 4.7 are obtained by two-dimensional interpolation of the Legendre Collocation Method results on each element. Thus, a certain degree of accuracy may be lost during the interpolation process. But, as indicated in Table 4.7, all data appear to be in good agreement. The conclusion can be drawn that the Legendre Collocation Method gives a very accurate result at the collocation points. A smooth three-dimensional plot of the

approximate solution u using 9×9 mesh size for the entire domain is displayed in Figure 4.12.

As mentioned previously, the neighborhood of the singularity is treated as an isolated circular sector, and the series solution for this sector is then formulated. Table 4.8 shows the rapid convergence of the coefficient c_n obtained by both methods, namely the least-squares and minimax approximation applied on the arc in computing the coefficients. Thus, by taking five points along the sector arc, c_5 has been reduced to the order of 10^{-7} . The results presented in the study are based on five coefficients in the series solution Equations (4.21), (4.22), and (4.23). Furthermore, by inspecting the coefficients in Table 4.8 for both approximation methods, one sees that there is not much difference in convergence for the series solutions. Either one of the methods can be used for accurate results. To ensure the validity of the least-squares and minimax approximation methods, the solution u along the arc is calculated at eleven equally spaced points, and as shown in Table 4.9 and Figure 4.11, the results are in good agreement. Note that the notation used for the solution in cartesian coordinates is u ; ϕ is for solution in polar coordinates.

In the neighborhood of the singularity, computed results for the solution u or ϕ and corresponding values from previous studies are compared in Table 4.10. Good agreement is seen; this establishes the validity of the method proposed in this study. Tables 4.11 and 4.12 show the derivatives in the x and y directions. Unfortunately, comparison is not possible since no published results for the derivatives in this important region are available. Figures 4.13, 4.14 and 4.15 show the contour lines representing the approximate solution u and the derivatives $\frac{\partial u}{\partial x}$ and $\frac{\partial u}{\partial y}$, using the series solution with five coefficients.

Tables 4.13 - 4.18 show the convergence of the solution u and its derivatives obtained by both the least-squares and minimax approximation methods in the series solution. Good convergence is observed.

Table 4.6 Pointwise convergence of a solution u on a square grid points of 3.5×3.5 . The results shown are based on a mesh size on each element: 3×3 , 5×5 , 7×7 , 9×9

0.595238	0.642857	0.785714	0.857143	1.000000
0.594195	0.622162	0.714702	0.844223	1.000000
0.592566	0.620119	0.707747	0.842104	1.000000
0.592016	0.619413	0.705947	0.841472	1.000000
0.571429	0.607143	0.714286	0.857143	1.000000
0.568003	0.591688	0.682206	0.835286	1.000000
0.566450	0.589772	0.666509	0.832536	1.000000
0.566032	0.589164	0.677404	0.831747	1.000000
0.500000	0.500000	0.500000	0.857143	1.000000
0.500000	0.500000	0.500000	0.823763	1.000000
0.500000	0.500000	0.500000	0.819743	1.000000
0.500000	0.500000	0.500000	0.818540	1.000000
SINGULAR POINT				

Table 4.7 Comparison results of solution u of the problem of Motz on a unit mesh

The numbers in the table have the following significance:

1st value - Interpolated results of the Legendre Collocation Method with 9×9 mesh size

2nd value - By Lefeber in Reference [33]

3rd value - By Symm in Reference [37]

4th value - By Whiteman and Papamichael in Reference [36]

0.592016 0.591360	0.594203 0.593537	0.600828 0.600123	0.612085 0.611268	0.627943 0.627168	0.648925 0.647990	0.674768 0.673769	0.705947 0.704320	0.740272 0.739197	0.778701 0.777739	0.819874 0.819173	0.863473 0.862738	0.908197 0.907758	0.953890 0.953669	1.000000 1.000000
0.589839 0.589192	0.591998 0.591341	0.598546 0.597849	0.609676 0.608888	0.625500 0.624696	0.646423 0.645492	0.672341 0.671360	0.703770 0.702138	0.738452 0.737356	0.777289 0.776294	0.818835 0.818116	0.862777 0.862020	0.907770 0.907320	0.953689 0.953463	1.000000 1.000000
0.583354 0.582748	0.585421 0.584804	0.591716 0.591054	0.602519 0.601737	0.617986 0.617215	0.638833 0.637877	0.665041 0.663987	0.697180 0.695470	0.732966 0.731777	0.773046 0.771971	0.815793 0.814998	0.860735 0.859930	0.906541 0.906057	0.953115 0.952873	1.000000 1.000000
0.572793 0.572211	0.574705 0.574100	0.580484 0.579848	0.590241 0.589803	0.605665 0.604530	0.625604 0.624756	0.652237 0.651155	0.681075 0.683908	0.723066 0.722292	0.765817 0.764842	0.811827 0.810017	0.856899 0.856677	0.904768 0.904129	0.952334 0.951981	1.000000 1.000000
0.558385 0.557974	0.559965 0.559564	0.564941 0.564471	0.574058 0.573129	0.586656 0.586345	0.606485 0.605381	0.633075 0.631800	0.673433 0.666572	0.710864 0.708639	0.756913 0.755171	0.803809 0.803628	0.854374 0.852680	0.902328 0.901829	0.951145 0.950933	1.000000 1.000000
0.540916 0.540590	0.542111 0.541760	0.545789 0.545405	0.552349 0.551974	0.563138 0.562413	0.579410 0.578559	0.605056 0.603694	0.641975 0.641560	0.692500 0.690637	0.745530 0.743812	0.798520 0.796778	0.849466 0.848644	0.900306 0.899582	0.950302 0.949931	1.000000 1.000000
0.521113 0.520907	0.521764 0.52149	0.523736 0.523492	0.527010 0.527090	0.533838 0.533030	0.543486 0.543019	0.563100 0.561952	0.603446 0.603768	0.672188 0.669540	0.735337 0.733218	0.793299 0.791154	0.846335 0.845546	0.898728 0.897920	0.949603 0.949201	1.000000 1.000000
0.500000 0.500000	0.656001 0.655482	0.728904 0.728474	0.798132 0.788908	0.839966 0.844368	0.898886 0.897303	0.950074 0.948933	1.000000 1.000000							
0.500000 0.500000	0.669540 0.655482	0.72848 0.72848	0.791154 0.78891	0.84438 0.84438	0.89732 0.89732	0.94895 0.94893								
0.500000 0.500000	0.728474 0.728474	0.78891	0.84437 0.84437											

Table 4.8 The coefficients c_n computed from interpolated results obtained through the Legendre Collocation Method with 9×9 mesh size

N	c_n	Least-Squares Approx.	Minimax Approx.
2	$c_1 =$	0.152249E+00	0.155735E+00
	$c_2 =$	0.424141E-02	0.403734E-02
3	$c_1 =$	0.152953E+00	0.152170E+00
	$c_2 =$	0.473627E-02	0.460635E-02
	$c_3 =$	0.185410E-03	0.158638E-03
4	$c_1 =$	0.153098E+00	0.152702E+00
	$c_2 =$	0.470106E-02	0.467300E-02
	$c_3 =$	0.131639E-03	0.115928E-03
	$c_4 =$	-0.137679E-04	-0.709591E-05
5	$c_1 =$	0.152633E+00	0.152487E+00
	$c_2 =$	0.471037E-02	0.468686E-02
	$c_3 =$	0.138776E-03	0.135949E-03
	$c_4 =$	-0.969339E-05	-0.581385E-05
	$c_5 =$	0.489977E-06	-0.424645E-06
6	$c_1 =$	0.152304E+00	0.153066E+00
	$c_2 =$	0.470320E-02	0.471379E-02
	$c_3 =$	0.131855E-03	0.149621E-03
	$c_4 =$	-0.460547E-05	-0.228528E-04
	$c_5 =$	0.168264E-05	-0.289098E-05
	$c_6 =$	0.198979E-08	0.515987E-06

Table 4.9 Comparison the solution u or ϕ on the sector arc of the problem of Motz (see Figure 4.10)

Point No.	Angle θ	Interpolated LCM results (9×9)	Least-squares Approx. (5 coeffs.)	Minimax Approx. (5 coeffs.)
1	0.000000	0.818540	0.818934	0.818496
2	0.314159	0.811433	0.811433	0.811082
3	0.628319	0.789953	0.790030	0.789741
4	0.942478	0.757709	0.757709	0.757296
5	1.256637	0.719010	0.718655	0.718243
6	1.570796	0.677404	0.677404	0.677404
7	1.884956	0.637786	0.637688	0.638121
8	2.199115	0.601179	0.601179	0.601438
9	2.513274	0.566908	0.567139	0.566784
10	2.827433	0.533745	0.533745	0.533195
11	3.141593	0.500000	0.500000	0.500000

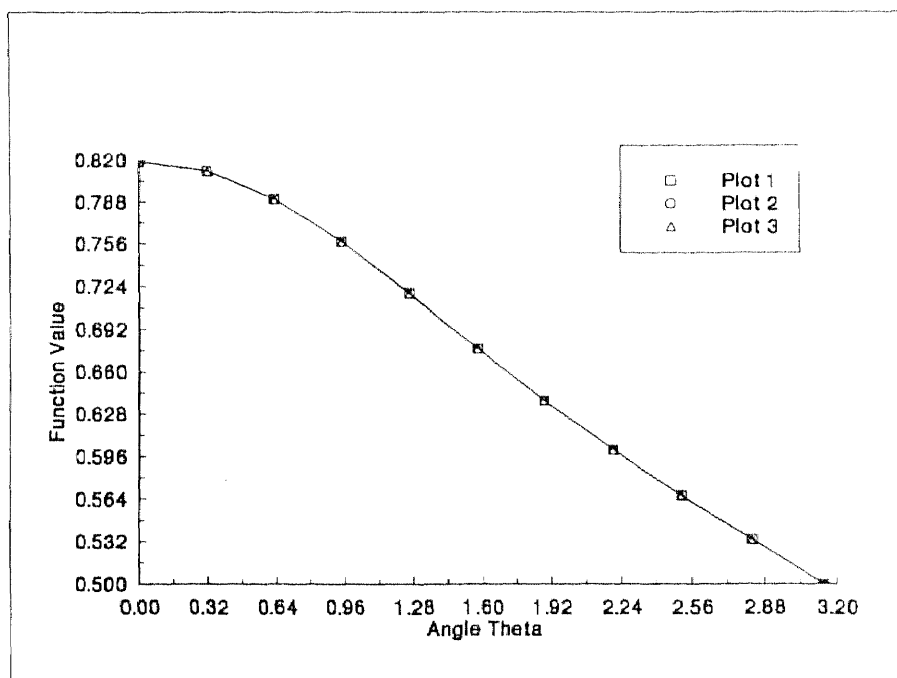


Figure 4.11 Plot of the solution values along the arc from 0 to π as shown in Table 4.9:

Plot 1 - Interpolated value from the Legendre Collocation Method

Plot 2 - Least-squares approximation value

Plot 3 - Minimax approximation value.

Table 4.10 Comparison results of the solution u of the problem of Motz on a 0.25 unit mesh in the neighborhood of the singular point O:

1st value - 5 points Least-squares approximation result on the Legendre Collocation Method

2nd value - 5 points Minimax approximation result on the Legendre Collocation Method

3rd value - Lefeber's result in Reference [33]

4th value - Symm's result in Reference [37]

5th value - Whiteman and Papamicheal's result in Reference [36]

0.562459	0.570014	0.579358	0.590825	0.604492	0.619997	0.636626	0.653666	0.670629
0.562420	0.569973	0.579309	0.590761	0.604410	0.619891	0.636496	0.653511	0.670448
0.561952	0.569473	0.578770	0.590176	0.603768	0.619186	0.635724	0.652670	0.669540
0.56195	0.56947	0.57877	0.59017	0.60376	0.61918	0.63572	0.65267	0.66954
0.56195	0.56947	0.57877	0.59018	0.60377	0.61919	0.63572	0.65267	0.66954
0.548811	0.555555	0.564431	0.576189	0.591255	0.609033	0.628077	0.647146	0.665642
0.548774	0.555517	0.564386	0.576131	0.591178	0.608933	0.627953	0.646996	0.665465
0.548417	0.555128	0.563958	0.575650	0.590629	0.608304	0.627239	0.646199	0.664591
0.54841	0.55512	0.56395	0.57565	0.59063	0.60830	0.62724	0.64620	0.66459
0.54842	0.55513	0.56396	0.57565	0.59063	0.60830	0.62724	0.64620	0.66459
0.533695	0.538994	0.546584	0.558046	0.575121	0.596870	0.619631	0.641270	0.661421
0.533667	0.538964	0.546549	0.557999	0.575054	0.596778	0.619511	0.641124	0.661249
0.533424	0.538696	0.546245	0.557640	0.574612	0.596229	0.618854	0.640366	0.660402
0.53342	0.53869	0.54624	0.55764	0.57461	0.59623	0.61885	0.64037	0.66040
0.53342	0.53870	0.54624	0.55764	0.57461	0.59623	0.61885	0.64037	0.66040
0.517258	0.520262	0.524989	0.533826	0.553544	0.584223	0.612592	0.636944	0.658519
0.517243	0.520245	0.524969	0.533797	0.553495	0.584141	0.612478	0.636801	0.658349
0.517120	0.520108	0.524808	0.533591	0.553186	0.583671	0.611865	0.636072	0.657521
0.51712	0.52011	0.52481	0.53359	0.55318	0.58367	0.61186	0.63607	0.65752
0.51712	0.52011	0.52481	0.53359	0.55319	0.58367	0.61186	0.63607	0.65752
0.500000	0.500000	0.500000	0.500000	0.500000	0.576910	0.609617	0.635308	0.657473
0.500000	0.500000	0.500000	0.500000	0.500000	0.576834	0.609505	0.635166	0.657304
0.500000	0.500000	0.500000	0.500000	0.500000	0.576408	0.608911	0.634447	0.656482
0.50000	0.50000	0.50000	0.50000	0.50000	0.57641	0.60891	0.63445	0.65648
0.50000	0.50000	0.50000	0.50000	0.50000	0.57641	0.60891	0.63445	0.65648

Table 4.11 The derivative $\frac{\partial u}{\partial x}$ of the problem of Motz on a 0.25 unit mesh in the neighborhood of the singular point O:

1st value - 5 points Least-squares approximation result on the Legendre Collocation Method

2nd value - 5 points Minimax approximation result on the Legendre Collocation Method

0.027157	0.033539	0.041450	0.050351	0.058740	0.064791	0.067754	0.068241	0.067299
0.027164	0.033519	0.041405	0.050285	0.058656	0.064695	0.067652	0.068138	0.067200
0.023622	0.030755	0.040783	0.053628	0.066492	0.074673	0.076833	0.075342	0.072526
0.023628	0.030737	0.040743	0.053565	0.066408	0.074575	0.076730	0.075238	0.072426
0.017992	0.024981	0.036801	0.056293	0.079767	0.091315	0.089421	0.083539	0.077813
0.017995	0.024967	0.036766	0.056231	0.079676	0.091208	0.089310	0.083432	0.077710
0.009907	0.014627	0.024565	0.050655	0.110396	0.122489	0.104591	0.091128	0.082036
0.009909	0.014619	0.024541	0.050602	0.110281	0.122355	0.104469	0.091016	0.081931
0.000000	0.000000	0.000000	0.000000	SINGULAR POINT	0.156208	0.113041	0.094451	0.083697
0.000000	0.000000	0.000000	0.000000		0.156044	0.112912	0.094337	0.083591

Table 4.12 The derivative $\frac{\partial u}{\partial y}$ of the problem of Motz on a 0.25 unit mesh in the neighborhood of the singular point O:

1st value - 5 points Least-squares approximation result on the Legendre Collocation Method

2nd value - 5 points Minimax approximation result on the Legendre Collocation Method

0.051712	0.054029	0.054960	0.053411	0.048700	0.041509	0.033627	0.026561	0.020876	
0.051715	0.054029	0.054955	0.053400	0.048685	0.041492	0.033608	0.026541	0.020855	
0.057533	0.061866	0.064964	0.064442	0.057815	0.046282	0.034485	0.025258	0.018744	
0.057510	0.061842	0.064936	0.064411	0.057784	0.046255	0.034463	0.025239	0.018728	
0.063307	0.070704	0.078431	0.082313	0.72693	0.050744	0.032280	0.021145	0.014641	
0.063262	0.070659	0.078380	0.082256	0.072641	0.050708	0.032257	0.021129	0.014629	
0.067856	0.078752	0.094314	0.114724	0.105398	0.047444	0.022152	0.012642	0.008197	
0.067798	0.078691	0.094242	0.114630	0.105309	0.047406	0.022135	0.012632	0.008190	
0.069634	0.082246	0.103061	0.149145	SINGULAR POINT	0.000000	0.000000	0.000000	0.000000	
0.069572	0.082180	0.102977	0.149015		0.000000	0.000000	0.000000	0.000000	

Table 4.13 Pointwise convergence of Least-squares approximation on the eigensolution u in the neighborhood of the singular point O. The results are on a 0.25 unit mesh and based on 9×9 mesh size for each element in the Legendre Collocation Method solution:

- 1st value - two coefficients in the eigensolution Equation (4.21)
- 2nd value - three coefficients in the eigensolution Equation (4.21)
- 3rd value - four coefficients in the eigensolution Equation (4.21)
- 4th value - five coefficients in the eigensolution Equation (4.21)

0.562697	0.570293	0.579641	0.591070	0.604657	0.620035	0.636491	0.653310	0.670004
0.562656	0.570202	0.579538	0.591002	0.604674	0.620191	0.636843	0.653917	0.670926
0.562676	0.570250	0.579621	0.591121	0.604829	0.620380	0.637058	0.654147	0.671155
0.562459	0.570014	0.579358	0.590825	0.604492	0.619997	0.636626	0.653666	0.670629
0.548955	0.556724	0.564593	0.576307	0.591285	0.608930	0.627794	0.646637	0.664859
0.548958	0.555700	0.564577	0.576343	0.591425	0.609230	0.628313	0.647431	0.665986
0.548980	0.555742	0.564643	0.576435	0.591545	0.609374	0.628473	0.647593	0.666135
0.548811	0.555455	0.564431	0.576189	0.591255	0.609033	0.628077	0.647146	0.665642
0.533774	0.539085	0.546663	0.558080	0.575064	0.596673	0.619246	0.640653	0.660527
0.533794	0.539094	0.546690	0.558166	0.575269	0.597061	0.619875	0.641575	0.661798
0.533811	0.539125	0.546737	0.558232	0.575356	0.597168	0.619992	0.641688	0.661888
0.533695	0.538994	0.546584	0.558046	0.575121	0.596870	0.619631	0.641270	0.661421
0.517292	0.520300	0.525018	0.533820	0.553453	0.583978	0.612149	0.636264	0.657559
0.517308	0.520313	0.525046	0.533896	0.553654	0.584399	0.612837	0.637261	0.658915
0.517317	0.520329	0.525070	0.533933	0.553710	0.584478	0.612926	0.637343	0.658969
0.517258	0.520262	0.524989	0.533826	0.553544	0.584223	0.612592	0.636944	0.658519
0.500000	0.500000	0.500000	0.500000	0.500000	0.576655	0.609156	0.634607	0.656491
0.500000	0.500000	0.500000	0.500000	0.500000	0.577074	0.609861	0.635628	0.657875
0.500000	0.500000	0.500000	0.500000	0.500000	0.577140	0.609941	0.635699	0.657917
0.500000	0.500000	0.500000	0.500000	0.500000	0.576910	0.609617	0.635308	0.657473

Table 4.14 Pointwise convergence of Minimax approximation on the eigensolution u in the neighborhood of the singular point O. The results are on a 0.25 unit mesh and based on 9×9 mesh size for each element in the Legendre Collocation Method solution:

1st value - two coefficients in the eigensolution Equation (4.21)

2nd value - three coefficients in the eigensolution Equation (4.21)

3rd value - four coefficients in the eigensolution Equation (4.21)

4th value - five coefficients in the eigensolution Equation (4.21)

0.564600	0.572316	0.581818	0.593443	0.607266	0.622911	0.639648	0.656744	0.673702
0.562442	0.569955	0.579243	0.590642	0.604231	0.619648	0.636186	0.653133	0.670007
0.562496	0.570072	0.579433	0.590911	0.604585	0.620091	0.636717	0.653748	0.670695
0.562420	0.569973	0.579309	0.590761	0.604410	0.619891	0.636496	0.653511	0.670448
0.550421	0.557304	0.566328	0.578256	0.593513	0.611487	0.630695	0.649868	0.668393
0.548784	0.555494	0.564324	0.576023	0.591015	0.608708	0.627663	0.646643	0.665055
0.548833	0.555594	0.564483	0.576251	0.591322	0.609102	0.628144	0.647204	0.665684
0.548774	0.555517	0.564386	0.576131	0.591178	0.608933	0.627953	0.646996	0.665465
0.534775	0.540179	0.547897	0.559535	0.576858	0.598897	0.621907	0.643709	0.663929
0.533670	0.538944	0.546499	0.557910	0.574914	0.596574	0.619242	0.640791	0.660861
0.533708	0.539018	0.546618	0.558087	0.575168	0.596920	0.619679	0.641310	0.661446
0.533667	0.538964	0.546549	0.557999	0.575054	0.596778	0.619511	0.641124	0.661249
0.517801	0.520863	0.525671	0.534653	0.554704	0.585876	0.614620	0.639196	0.660872
0.517243	0.520234	0.524940	0.533742	0.553390	0.583960	0.612223	0.636483	0.657975
0.517264	0.520273	0.525005	0.533847	0.553573	0.584258	0.612627	0.636973	0.658533
0.517243	0.520245	0.524969	0.533797	0.553495	0.584141	0.612478	0.636801	0.658349
0.500000	0.500000	0.500000	0.500000	0.500000	0.578372	0.611549	0.637493	0.659772
0.500000	0.500000	0.500000	0.500000	0.500000	0.576666	0.609257	0.634852	0.656935
0.500000	0.500000	0.500000	0.500000	0.500000	0.576939	0.609649	0.635333	0.657484
0.500000	0.500000	0.500000	0.500000	0.500000	0.576834	0.609505	0.635166	0.657304

Table 4.15 Pointwise convergence of $\frac{\partial u}{\partial x}$ of Least-squares approximation on the eigensolution u in the neighborhood of the singular point O. The results are on a 0.25 unit mesh and based on 9×9 mesh size for each element in the Legendre Collocation Method solution:

1st value - x - derivative based on two coefficients in the eigensolution Equation (4.21)

2nd value - x - derivative based on three coefficients in the eigensolution Equation (4.21)

3rd value - x - derivative based on four coefficients in the eigensolution Equation (4.21)

4th value - x - derivative based on five coefficients in the eigensolution Equation (4.21)

0.027392	0.033631	0.041386	0.050119	0.058327	0.064191	0.066964	0.067262	0.066130	
0.027123	0.033505	0.041428	0.050352	0.058773	0.064861	0.067866	0.068401	0.067517	
0.027225	0.033631	0.041570	0.050501	0.058916	0.064983	0.067950	0.068430	0.067473	
0.027157	0.033539	0.041450	0.050351	0.058740	0.064791	0.067754	0.068241	0.067299	
0.023781	0.030794	0.040684	0.053368	0.066052	0.074044	0.076019	0.074343	0.071342	
0.023610	0.030749	0.040797	0.053674	0.066580	0.074804	0.077005	0.075558	0.072797	
0.023682	0.030839	0.040900	0.053784	0.066686	0.074887	0.077046	0.075538	0.072698	
0.023622	0.030755	0.040783	0.053628	0.066492	0.074673	0.076833	0.075342	0.072526	
0.018086	0.024985	0.036691	0.056028	0.079306	0.090656	0.088580	0.082521	0.076616	
0.017992	0.024991	0.036835	0.056374	0.079913	0.091511	0.089648	0.083803	0.078124	
0.018038	0.025050	0.036906	0.056456	0.079998	0.091575	0.089664	0.083751	0.077989	
0.017992	0.024981	0.036801	0.056293	0.079767	0.091315	0.089421	0.083539	0.077813	
0.009950	0.014620	0.024485	0.050441	0.109906	0.121776	0.103721	0.090094	0.080829	
0.009911	0.014638	0.024597	0.050746	0.110625	0.122767	0.104868	0.091425	0.082373	
0.009933	0.014668	0.024636	0.050804	0.110722	0.122841	0.104876	0.091357	0.082217	
0.009907	0.014627	0.024565	0.050655	0.110396	0.122489	0.104591	0.091128	0.082036	
0.000000	0.000000	0.000000	0.000000	SINGULAR	0.155430	0.112155	0.093411	0.082487	
0.000000	0.000000	0.000000	0.000000	POINT	0.156563	0.113341	0.094761	0.084044	
0.000000	0.000000	0.000000	0.000000		0.156663	0.113350	0.094688	0.083881	
0.000000	0.000000	0.000000	0.000000		0.156208	0.113041	0.094451	0.083697	

Table 4.16 Pointwise convergence of $\frac{\partial^y u}{\partial y^y}$ of Least-squares approximation on the eigensolution u in the neighborhood of the singular point O. The results are on a 0.25 unit mesh and based on 9×9 mesh size for each element in the Legendre Collocation Method solution:

1st value - y - derivative based on two coefficients in the eigensolution Equation (4.21)

2nd value - y - derivative based on three coefficients in the eigensolution Equation (4.21)

3rd value - y - derivative based on four coefficients in the eigensolution Equation (4.21)

4th value - y - derivative based on five coefficients in the eigensolution Equation (4.21)

0.052150	0.054538	0.055520	0.054008	0.049330	0.042168	0.034313	0.027269	0.021601	
0.051906	0.054193	0.055086	0.053490	0.048726	0.041474	0.033529	0.026401	0.020657	
0.051890	0.054213	0.055146	0.053595	0.048875	0.041671	0.033776	0.026703	0.021019	
0.051712	0.054029	0.054960	0.053411	0.048700	0.041509	0.033627	0.026561	0.020876	
0.057846	0.062236	0.065368	0.064866	0.058260	0.046753	0.034984	0.025779	0.019282	
0.057726	0.062039	0.065111	0.064555	0.057879	0.046287	0.034431	0.025149	0.018586	
0.057733	0.062077	0.065183	0.064660	0.058016	0.046453	0.034629	0.025384	0.018864	
0.057533	0.061866	0.064964	0.064442	0.057815	0.046282	0.034485	0.025258	0.018744	
0.063521	0.070959	0.078694	0.082563	0.072944	0.051027	0.032596	0.021485	0.014995	
0.063502	0.070891	0.078610	0.082474	0.072808	0.050789	0.032263	0.021082	0.014540	
0.063526	0.070943	0.078692	0.082584	0.072935	0.050921	0.032405	0.021244	0.014729	
0.063307	0.070704	0.078431	0.082313	0.072693	0.050744	0.032280	0.021145	0.014641	
0.068007	0.078927	0.094462	0.114786	0.105407	0.047546	0.022299	0.012808	0.008372	
0.068056	0.078954	0.094529	0.114962	0.105601	0.047513	0.022156	0.012614	0.008148	
0.068091	0.079016	0.094623	0.115091	0.105733	0.047601	0.022234	0.012698	0.008244	
0.067856	0.078752	0.094314	0.114724	0.105398	0.047444	0.022152	0.012642	0.008197	
0.069763	0.082391	0.103158	0.149068	SINGULAR POINT	0.000000	0.000000	0.000000	0.000000	
0.069836	0.082456	0.103294	0.149459		0.000000	0.000000	0.000000	0.000000	
0.069875	0.082521	0.103395	0.149615		0.000000	0.000000	0.000000	0.000000	
0.069634	0.082246	0.103061	0.149145		0.000000	0.000000	0.000000	0.000000	

Table 4.17 Pointwise convergence of $\frac{\partial^2 u}{\partial x^2}$ of Minimax approximation on the eigensolution u in the neighborhood of the singular point O. The results are on a 0.25 unit mesh

and based on 9×9 mesh size for each element in the Legendre Collocation Method solution:

1st value - x - derivative based on two coefficients in the eigensolution Equation (4.21)

2nd value - x - derivative based on three coefficients in the eigensolution Equation (4.21)

3rd value - x - derivative based on four coefficients in the eigensolution Equation (4.21)

4th value - x - derivative based on five coefficients in the eigensolution Equation (4.21)

0.027814	0.034175	0.042083	0.050984	0.059343	0.065299	0.068091	0.068350	0.067148
0.027012	0.033343	0.041204	0.050057	0.058406	0.064429	0.067383	0.067877	0.066956
0.027255	0.033615	0.041505	0.050388	0.058757	0.064788	0.067729	0.068192	0.067226
0.027255	0.033615	0.041505	0.050388	0.058757	0.064788	0.067729	0.068192	0.067226
0.024165	0.031321	0.041413	0.054355	0.067287	0.075414	0.077381	0.075615	0.072496
0.023507	0.030595	0.040572	0.053361	0.066172	0.074320	0.076473	0.074994	0.072204
0.023697	0.030814	0.040828	0.053659	0.066508	0.074671	0.076810	0.075294	0.072453
0.023697	0.030814	0.040828	0.053659	0.066508	0.074671	0.076810	0.075294	0.072453
0.018391	0.025433	0.037385	0.057133	0.080895	0.092444	0.090257	0.084000	0.077905
0.017910	0.024862	0.036631	0.056051	0.079441	0.090944	0.089052	0.083195	0.077502
0.018043	0.025022	0.036833	0.056319	0.079786	0.091319	0.089401	0.083493	0.077740
0.018043	0.025022	0.036833	0.056319	0.079786	0.091319	0.089401	0.083493	0.077740
0.010122	0.014891	0.024968	0.051493	0.112262	0.124315	0.105767	0.091760	0.082224
0.009865	0.014562	0.024461	0.050463	0.110008	0.122047	0.104195	0.090778	0.081729
0.009934	0.014649	0.024583	0.050676	0.110430	0.122507	0.104577	0.091085	0.081963
0.009934	0.014649	0.024583	0.050676	0.110430	0.122507	0.104577	0.091085	0.081963
0.000000	0.000000	0.000000	0.000000	SINGULAR	0.158763	0.114403	0.095158	0.083923
0.000000	0.000000	0.000000	0.000000	POINT	0.155675	0.112627	0.094097	0.083391
0.000000	0.000000	0.000000	0.000000		0.156242	0.113031	0.094409	0.083625
0.000000	0.000000	0.000000	0.000000		0.156242	0.113031	0.094409	0.083625

Table 4.18 Pointwise convergence of $\frac{\partial u}{\partial y}$ of Minimax approximation on the eigensolution u in the neighborhood of the singular point O. The results are on a 0.25 unit mesh and based on 9×9 mesh size for each element in the Legendre Collocation Method solution:

1st value - y - derivative based on two coefficients in the eigensolution Equation (4.21)

2nd value - y - derivative based on three coefficients in the eigensolution Equation (4.21)

3rd value - y - derivative based on four coefficients in the eigensolution Equation (4.21)

4th value - y - derivative based on five coefficients in the eigensolution Equation (4.21)

0.053841	0.056238	0.057197	0.055606	0.050778	0.043416	0.035350	0.028119	0.022301
0.051773	0.054058	0.054953	0.053371	0.048634	0.041423	0.033522	0.026434	0.020723
0.051779	0.054114	0.055058	0.053516	0.048809	0.041619	0.033736	0.026669	0.020984
0.051715	0.054029	0.054955	0.053400	0.048685	0.041492	0.033608	0.026541	0.020855
0.059649	0.064090	0.067242	0.066677	0.059870	0.048058	0.035987	0.026547	0.019883
0.057547	0.061845	0.064905	0.064352	0.057710	0.046176	0.034381	0.025148	0.018622
0.057580	0.061933	0.065045	0.064531	0.057906	0.046371	0.034571	0.025342	0.018827
0.057510	0.061842	0.064936	0.064411	0.057784	0.046255	0.034463	0.025239	0.018728
0.065440	0.072994	0.080847	0.084740	0.074839	0.052372	0.033488	0.022101	0.015448
0.063281	0.070638	0.078316	0.082155	0.072531	0.050619	0.032184	0.021060	0.014553
0.063339	0.070759	0.078502	0.082392	0.072771	0.050813	0.032341	0.021203	0.014698
0.063262	0.070659	0.078380	0.082256	0.072641	0.050708	0.032257	0.021129	0.014629
0.070019	0.081130	0.096953	0.117662	0.107980	0.048737	0.022888	0.013166	0.008620
0.067804	0.078649	0.094139	0.114455	0.105123	0.047319	0.022087	0.012594	0.008150
0.067881	0.078800	0.094381	0.114804	0.105472	0.047489	0.022185	0.012672	0.008225
0.067798	0.078691	0.094242	0.114630	0.105309	0.047406	0.022135	0.012632	0.008190
0.071811	0.084669	0.105839	0.152707	SINGULAR	0.000000	0.000000	0.000000	0.000000
0.069572	0.082129	0.102855	0.148765	POINT	0.000000	0.000000	0.000000	0.000000
0.069656	0.082292	0.103127	0.149234		0.000000	0.000000	0.000000	0.000000
0.069572	0.082180	0.102977	0.149015		0.000000	0.000000	0.000000	0.000000

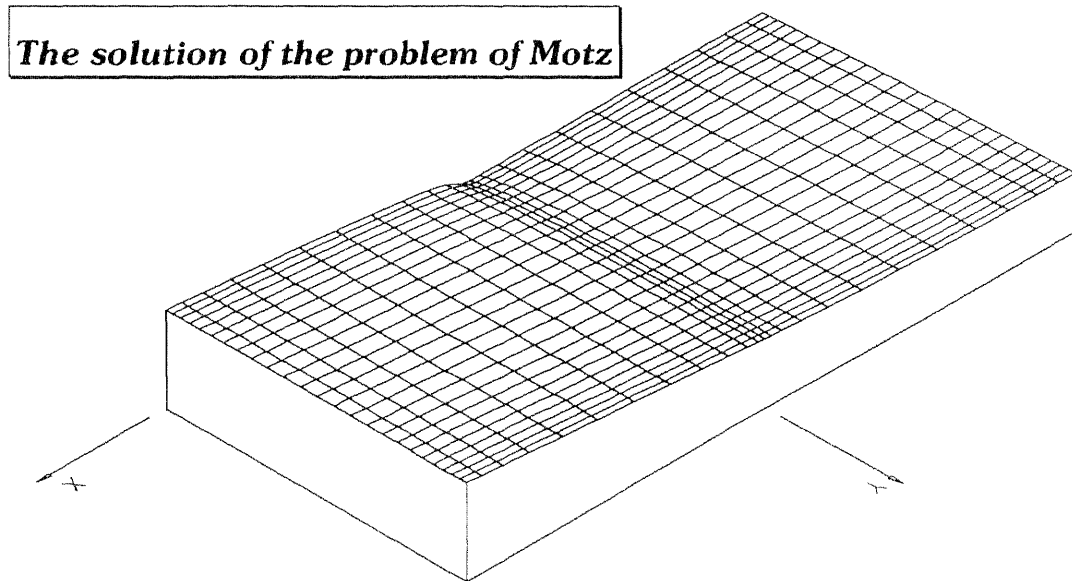


Figure 4.12 Three-dimensional plot of the solution u obtained through the Legendre Collocation Method.

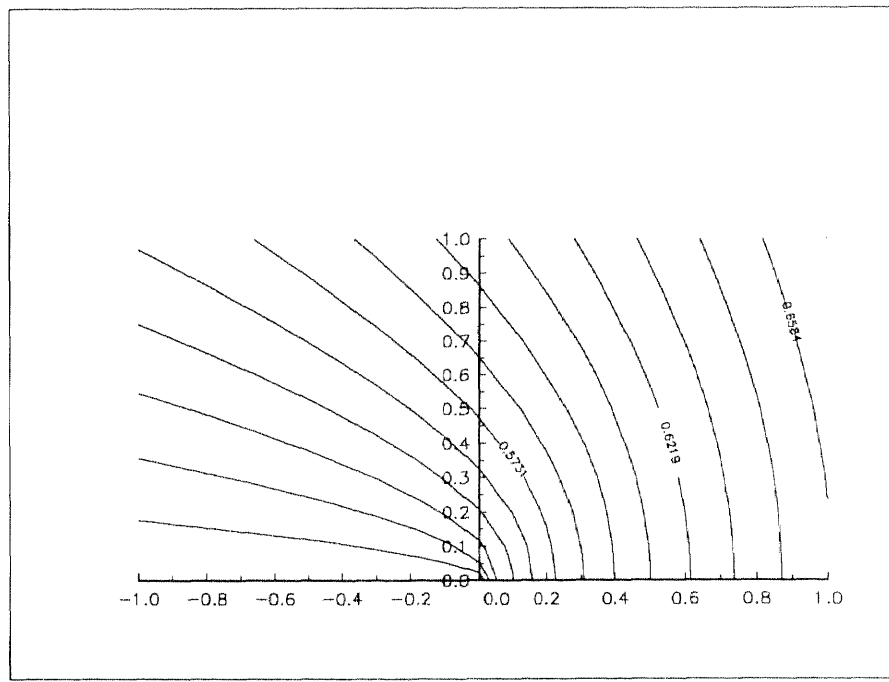


Figure 4.13 Contour plot of solution u in the neighborhood of singularity

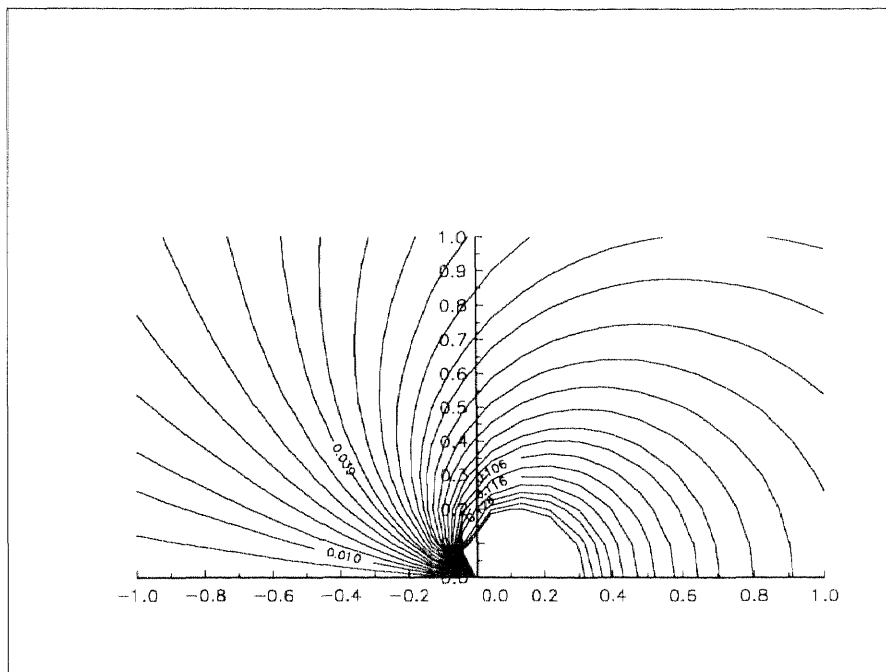


Figure 4.14 Contour plot of $\frac{\partial u}{\partial x}$ in the neighborhood of singularity

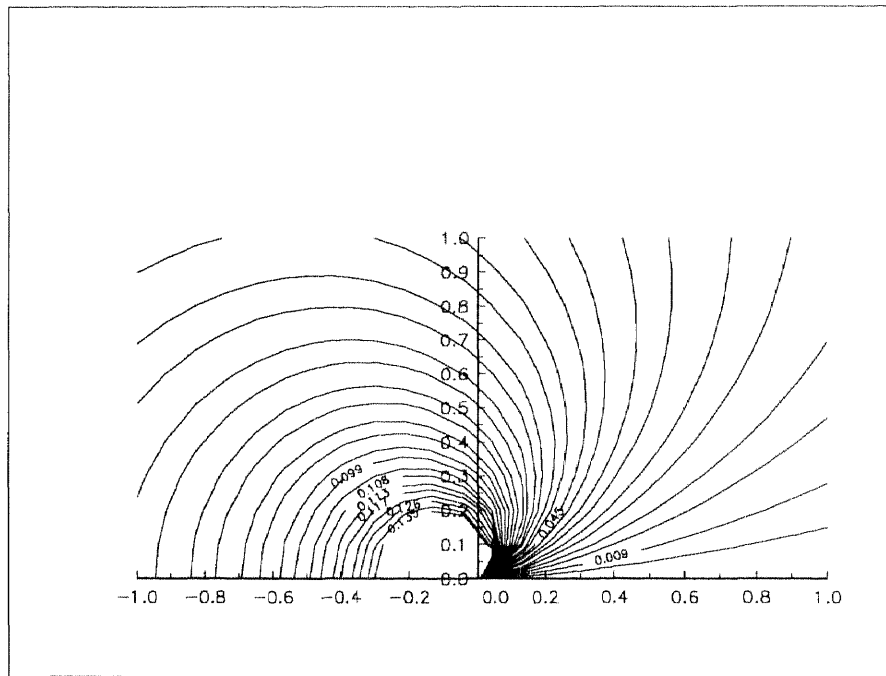


Figure 4.15 Contour plot of $\frac{\partial u}{\partial y}$ in the neighborhood of singularity

4.4 Solution of Laplace's Equation in L-shaped Domain

As a third example of the application of the method in this study, consider the problem of finding the approximate solution ϕ in an L-shaped region that satisfies Laplace's equation and is subjected to mixed boundary conditions as depicted in Figure 4.16.

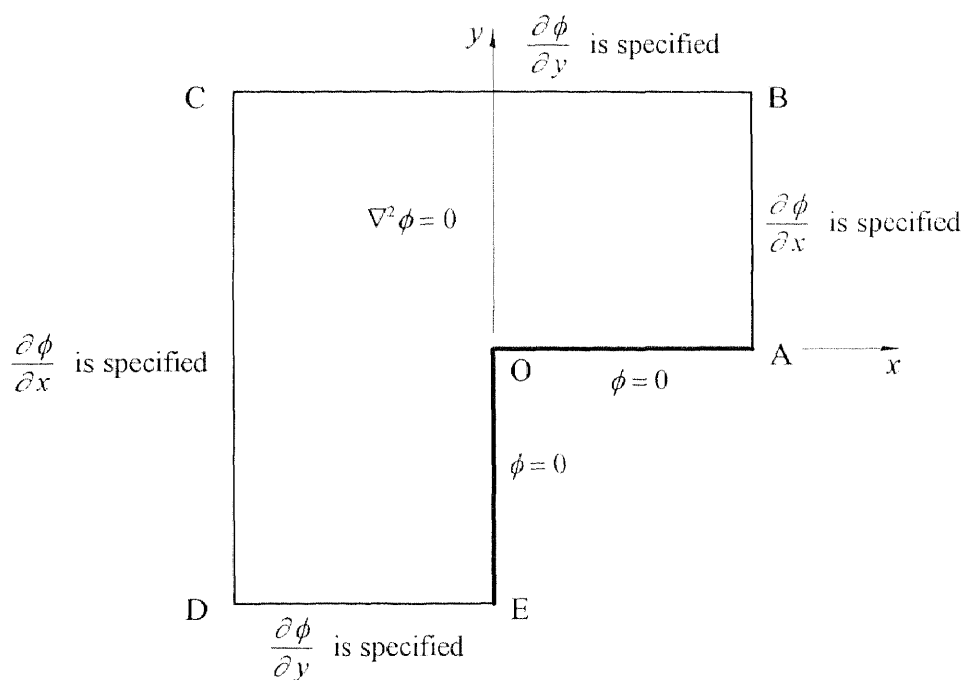


Figure 4.16 L-shaped domain and boundary conditions for Laplace's equation.

The length of side OA = AB = DE = EO = 1, while BC = CD = 2. Thus, the region can be easily broken into three square elements with sides equal to unity.

The differential equation has the known exact solution ϕ in polar coordinates (r, ϕ) in the form

$$\phi = r^{\frac{2}{3}} \sin \frac{2}{3} \theta \quad (4.24)$$

satisfying Laplace's equation in polar coordinates

$$\frac{\partial^2 \phi}{\partial r^2} + \frac{1}{r^2} \frac{\partial^2 \phi}{\partial \theta^2} + \frac{1}{r} \frac{\partial \phi}{\partial r} = 0$$

as shown in Appendix A. Equation (4.24) reveals that the radial derivative of ϕ approaches infinity if $r \rightarrow 0$. Thus, singularity occurs at the origin O in Figure 4.16.

As indicated in Figure 4.16, it is necessary to derive the equations for the prescribed normal derivatives $\frac{\partial \phi}{\partial x}$ and $\frac{\partial \phi}{\partial y}$ from Equation (4.24), and apply the boundary conditions along the boundary lines AB, BC, CD and DE. Clearly, Equation (4.24) satisfies the conditions along EO and OA lines. Since Equation (4.24) is defined in polar coordinates, and the normal derivatives have to be formulated in cartesian coordinates, the following transformation formulas (see Figure 4.17)

$$\begin{aligned} r &= \sqrt{x^2 + y^2} \\ \theta &= \tan^{-1} \frac{y}{x} \end{aligned} \quad (4.25)$$

will be used.

The derivative of ϕ with respect to x is given by

$$\frac{\partial \phi}{\partial x} = \frac{\partial \phi}{\partial r} \frac{\partial r}{\partial x} + \frac{\partial \phi}{\partial \theta} \frac{\partial \theta}{\partial x} \quad (4.26)$$

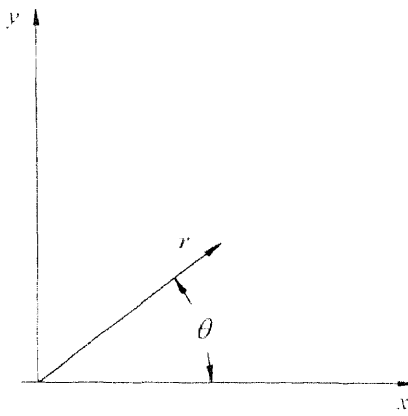


Figure 4.17 Polar coordinates (r, θ) related to cartesian coordinates (x,y)

and with respect to y :

$$\frac{\partial \phi}{\partial y} = \frac{\partial \phi}{\partial r} \frac{\partial r}{\partial y} + \frac{\partial \phi}{\partial \theta} \frac{\partial \theta}{\partial y} \quad (4.27)$$

From Equation (4.25), one has

$$\frac{\partial r}{\partial x} = \frac{x}{\sqrt{x^2 + y^2}} = \cos \theta \quad (.4.28)$$

$$\frac{\partial r}{\partial y} = \frac{y}{\sqrt{x^2 + y^2}} = \sin \theta \quad (4.29)$$

$$\frac{\partial \theta}{\partial x} = \frac{-y}{x^2 + y^2} = -\frac{\sin \theta}{r} \quad (4.30)$$

and

$$\frac{\partial \theta}{\partial y} = \frac{x}{x^2 + y^2} = \frac{\cos \theta}{r} \quad (4.31)$$

Differentiation of Equation (4.24) gives

$$\frac{\partial \phi}{\partial r} = \frac{2}{3} r^{-\frac{1}{3}} \sin \frac{2}{3} \theta \quad (4.32)$$

and

$$\frac{\partial \phi}{\partial \theta} = \frac{2}{3} r^{\frac{2}{3}} \cos \frac{2}{3} \theta \quad (4.33)$$

Again, it is clear from Equation (4.32) that $\frac{\partial \phi}{\partial r} \rightarrow \infty$, when $r \rightarrow 0$. This confirms the occurrence of a singularity at the origin O of Figure 4.16.

Substitution of Equations (4.28), (4.30), (4.32) and (4.33) into Equation (4.26) gives

$$\frac{\partial \phi}{\partial x} = -\frac{2}{3} r^{-\frac{1}{3}} \sin \frac{1}{3} \theta \quad (4.34)$$

and Equations (4.29), (4.31), (4.32) and (4.33) into Equation (4.27) yields

$$\frac{\partial \phi}{\partial y} = \frac{2}{3} r^{-\frac{1}{3}} \cos \frac{1}{3} \theta \quad (4.35)$$

where r and θ in Equations (4.34) and (4.35) are defined by Equation (4.25). Thus, in Figure 4.16, Equation (4.34) is the Neumann boundary condition along the AB and CD lines; the Dirichlet condition in Equation (4.35) will be applied along the DE and BC lines.

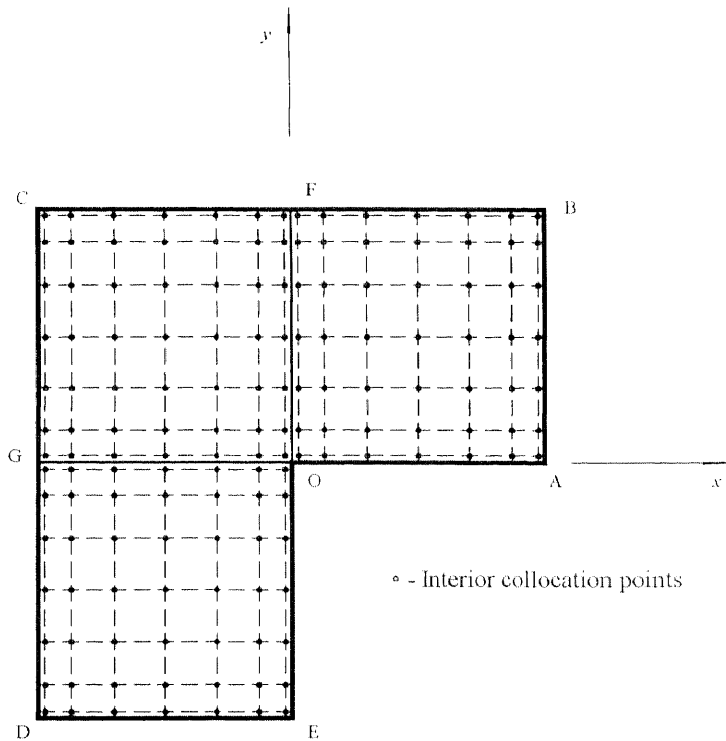


Figure 4.18 L-shaped domain for Laplace's equation is shown with three elements, and 9×9 mesh size for each element.

In this study, the *p*-version technique is adopted in solving the problem using the Legendre Collocation Method. Therefore the entire L-shaped region is broken up into three major elements: EOGD, OFCG and OABF (see Figure 4.18). Two major steps are required for solving the problem that contains a singularity. First, the approximate solution is obtained through the Legendre Collocation Method, and second the circular sector in the neighborhood of singularity is isolated (see Figure 3.1 or 3.2), then the series solution in this sector is formulated and obtained by determining its coefficients either by the least-squares or minimax approach.

Similar procedures to the problem of Motz are applied. Thus, at each interior collocation point of each element, Laplace's equation is satisfied by Equation (4.8). In addition to these equations, the solution and first normal derivative are required to be continuous across element boundaries. The use of a

global numbering scheme guarantees satisfaction of solution continuity (see Table 4.19); derivative continuity is ensured by applying Equation (2.52) in the x direction (OF line), and a similar procedure is applied in the y direction (line OG - see Section 2.8). The boundary conditions defined in Equation (4.24) for lines EO and OA, also Equations (4.34) and (4.35) for lines AB, BC, CD and DE are satisfied as described in Section 2.8. The corner points are treated according to the procedures outlined in Section 2.9. The resulting set of simultaneous linear equations is solved by LU decomposition and the backward substitution method. The desired accuracy is achieved by increasing the order of Legendre polynomial used to construct the approximate solution until two successive approximations are sufficiently close to each other.

Figure 4. 18 shows the domain divided into three major elements with 9×9 mesh size for each element. Thus, there are 225 points for the entire domain as indicated in Table 4.19, and the number of equations is also 225. In Table 4.20 the exact solution values are compared with the Legendre Collocation Method results at the collocation points. Table 4.21 shows the relative errors. It is noted that higher errors occurred in a neighborhood of the singularity, ranging from 4.96% to 9.25%. For the rest of the region, very accurate results are obtained. Thus, it confirms the need of special treatment in the neighborhood of the singularity. Furthermore, for the problem containing singularity it will not be appropriate to use the solution values at the collocation points in computing the derivatives since error near re-entrant corner will introduce higher error in the entire domain. Good convergence is noted in Table 4.22, and the three-dimensional view of the solution obtained through the Legendre Collocation Method with a 9×9 mesh for each element is shown in Figure 4.19.

Table 4.19 Numbering scheme for the domain shown in Figure 4.18

209	210	211	212	213	214	215	216	217	218	219	220	221	222	223	224	225
192	193	194	195	196	197	198	199	200	201	202	203	204	205	206	207	208
175	176	177	178	179	180	181	182	183	184	185	186	187	188	189	190	191
158	159	160	161	162	163	164	165	166	167	168	169	170	171	172	173	174
141	142	143	144	145	146	147	148	149	150	151	152	153	154	155	156	157
124	125	126	127	128	129	130	131	132	133	134	135	136	137	138	139	140
107	108	109	110	111	112	113	114	115	116	117	118	119	120	121	122	123
90	91	92	93	94	95	96	97	98	99	100	101	102	103	104	105	106
73	74	75	76	77	78	79	80	81	82	83	84	85	86	87	88	89
64	65	66	67	68	69	70	71	72								63
55	56	57	58	59	60	61	62	54								45
46	47	48	49	50	51	52	53	45								36
37	38	39	40	41	42	43	44	36								27
28	29	30	31	32	33	34	35	27								18
19	20	21	22	23	24	25	26	18								1
10	11	12	13	14	15	16	17	1								2
								2								3
								3								4
								4								5
								5								6
								6								7
								7								8
								8								9

Table 4.20 Comparison results of the solution ϕ between the Legendre Collocation Method and exact solution at the collocation points:

First value - Legendre Collocation Method

Second value - Exact solution

1.2535 1.2599	1.2501 1.2492	1.2066 1.2057	1.1366 1.1356	1.0534 1.0525	0.9736 0.9727	0.9115 0.9107	0.8753 0.8746	0.8674 0.8660	0.8585 0.8576	0.8253 0.8246	0.7766 0.7759	0.7254 0.7248	0.6821 0.6816	0.6513 0.6509	0.6344 0.6339	0.6304 0.6300
1.2501 1.2492	1.2394 1.2385	1.1954 1.1945	1.1247 1.1238	1.0407 1.0398	0.9599 0.9591	0.8972 0.8963	0.8607 0.8599	0.8520 0.8513	0.8435 0.8428	0.8103 0.8095	0.7813 0.7806	0.7101 0.7095	0.6669 0.6664	0.6365 0.6360	0.6197 0.6192	0.6158 0.6153
1.2066 1.2057	1.1954 1.1945	1.1498 1.1489	1.0761 1.0752	0.9681 0.9672	0.9034 0.9025	0.8375 0.8367	0.7995 0.7987	0.7905 0.7897	0.7817 0.7809	0.7473 0.7466	0.6974 0.6968	0.6463 0.6458	0.6041 0.6037	0.5749 0.5744	0.5589 0.5585	0.5552 0.5548
1.1366 1.1356	1.1247 1.1238	1.0761 1.0752	0.9970 0.9961	0.9015 0.9006	0.8066 0.8077	0.7364 0.7355	0.6951 0.6943	0.6854 0.6847	0.6760 0.6752	0.6396 0.6389	0.5883 0.5877	0.5381 0.5375	0.4985 0.4980	0.4719 0.4715	0.4578 0.4573	0.4545 0.4541
1.0534 1.0525	1.0407 1.0398	0.9881 0.9872	0.9015 0.9006	0.7947 0.7937	0.6881 0.6872	0.6045 0.6036	0.5573 0.5564	0.5465 0.5456	0.5360 0.5350	0.4963 0.4955	0.4440 0.4434	0.3973 0.3969	0.3634 0.3630	0.3418 0.3415	0.3306 0.3302	0.3280 0.3277
0.9736 0.9727	0.9599 0.9591	0.9034 0.9025	0.8066 0.8077	0.6881 0.6872	0.5620 0.5609	0.4582 0.4570	0.3998 0.3986	0.3867 0.3856	0.3742 0.3732	0.3305 0.3296	0.2810 0.2805	0.2441 0.2438	0.2202 0.2200	0.2059 0.2057	0.1987 0.1984	0.1970 0.1968
0.9115 0.9107	0.8972 0.8963	0.8375 0.8367	0.7364 0.7355	0.6045 0.6036	0.4582 0.4570	0.3237 0.3221	0.2407 0.2390	0.2230 0.2214	0.2073 0.2056	0.1618 0.1610	0.1278 0.1274	0.1052 0.1080	0.0968 0.0967	0.0902 0.0901	0.0869 0.0866	0.0862 0.0861
0.8753 0.8746	0.8607 0.8599	0.7995 0.7987	0.6951 0.6943	0.5573 0.5564	0.3998 0.3986	0.2407 0.2390	0.1144 0.1090	0.0819 0.0749	0.0572 0.0545	0.0334 0.0335	0.0256 0.0254	0.0213 0.0214	0.0192 0.0191	0.0177 0.0178	0.0172 0.0171	0.0168 0.0170
0.8674 0.8660	0.8520 0.8513	0.7905 0.7897	0.6854 0.6847	0.5465 0.5456	0.3867 0.3856	0.2230 0.2214	0.0819 0.0749	0.0000 0.0000								
0.8585 0.8576	0.8435 0.8428	0.7817 0.7809	0.6760 0.6752	0.5360 0.5350	0.3742 0.3732	0.2073 0.2056	0.0572 0.0545	0.0000 0.0000								
0.8253 0.8246	0.8103 0.8095	0.7473 0.7466	0.6396 0.6389	0.4963 0.4955	0.3305 0.3296	0.1618 0.1610	0.0334 0.0335	0.0000 0.0000								
0.7766 0.7759	0.7613 0.7606	0.6974 0.6968	0.5883 0.5877	0.4440 0.4434	0.2810 0.2805	0.1278 0.1274	0.0256 0.0254	0.0000 0.0000								
0.7254 0.7248	0.7101 0.7095	0.6463 0.6458	0.5381 0.5375	0.3973 0.3969	0.2441 0.2438	0.1082 0.1080	0.0213 0.0214	0.0000 0.0000								
0.6821 0.6816	0.6669 0.6664	0.6041 0.6037	0.4965 0.4960	0.3634 0.3630	0.2202 0.2200	0.0968 0.0967	0.0192 0.0191	0.0000 0.0000								
0.6513 0.6509	0.6365 0.6360	0.5749 0.5744	0.4719 0.4715	0.3418 0.3415	0.2059 0.2057	0.0902 0.0901	0.0177 0.0178	0.0000 0.0000								
0.6344 0.6339	0.6197 0.6192	0.5589 0.5585	0.4578 0.4573	0.3306 0.3302	0.1987 0.1984	0.0869 0.0868	0.0172 0.0171	0.0000 0.0000								
0.6304 0.6300	0.6158 0.6153	0.5552 0.5548	0.4545 0.4541	0.3280 0.3277	0.1970 0.1968	0.0862 0.0861	0.0168 0.0170	0.0000 0.0000								

Table 4.21 Percentage relative error of the solution ϕ at the collocation points

0.5134	0.0731	0.0757	0.0803	0.0859	0.0903	0.0922	0.0848	0.1635	0.1000	0.0871	0.0849	0.0776	0.0729	0.0711	0.0723	0.0714
0.0731	0.0737	0.0764	0.0811	0.0869	0.0913	0.0946	0.0941	0.0902	0.0870	0.0921	0.0861	0.0794	0.0743	0.0729	0.0737	0.0739
0.0757	0.0764	0.0794	0.0849	0.0919	0.0982	0.0993	0.1000	0.1040	0.1069	0.0973	0.0938	0.0866	0.0810	0.0794	0.0804	0.0811
0.0803	0.0811	0.0849	0.0921	0.1024	0.1124	0.1202	0.1206	0.1163	0.1130	0.1190	0.1104	0.0998	0.0921	0.0899	0.0910	0.0913
0.0859	0.0869	0.0919	0.1024	0.1199	0.1430	0.1573	0.1623	0.1687	0.1732	0.1563	0.1418	0.1199	0.1062	0.1018	0.1031	0.1041
0.0903	0.0913	0.0982	0.1124	0.1430	0.1949	0.2610	0.2940	0.2811	0.2671	0.2628	0.1949	0.1453	0.1178	0.1133	0.1114	0.1115
0.0922	0.0946	0.0993	0.1202	0.1573	0.2610	0.5107	0.6905	0.7195	0.8112	0.5107	0.2564	0.1619	0.1280	0.1160	0.1174	0.1410
0.0848	0.0941	0.1000	0.1206	0.1623	0.2940	0.6905	4.9559	9.2518	4.9559	0.0516	0.6878	0.1124	0.3920	0.2012	0.4469	0.6844
0.1635	0.0902	0.1040	0.1163	0.1687	0.2811	0.7195	9.2518	0.0000	0.0000	0.0000	0.0000	0.0000	0.0000	0.0000	0.0000	
0.1000	0.0670	0.1069	0.1130	0.1732	0.2671	0.8112	4.9559									
0.0871	0.0921	0.0973	0.1190	0.1563	0.2628	0.5107	0.0516									
0.0849	0.0861	0.0938	0.1104	0.1416	0.1949	0.2564	0.6878									
0.0776	0.0794	0.0866	0.0998	0.1199	0.1453	0.1619	0.1124									
0.0729	0.0743	0.0810	0.0921	0.1062	0.1178	0.1280	0.3920	0.0000	0.0000	0.0000	0.0000	0.0000	0.0000	0.0000	0.0000	
0.0711	0.0729	0.0794	0.0899	0.1018	0.1133	0.1160	0.2012									
0.0723	0.0737	0.0804	0.0910	0.1031	0.1114	0.1174	0.4469									
0.0714	0.0739	0.0811	0.0913	0.1041	0.1115	0.1410	0.6844	0.0000								

Table 4.22 Pointwise convergence of the solution ϕ at 0.5×0.5 grid points:

First value - The Legendre Collocation Method with 3×3 mesh size
 Second value - The Legendre Collocation Method with 5×5 mesh size
 Third value - The Legendre Collocation Method with 7×7 mesh size
 Fourth value - The Legendre Collocation Method with 9×9 mesh size
 Fifth value - Exact solution in Equation (4.24)

1.180544	1.150178	1.059083	0.799745	0.661301
1.234199	1.059635	0.879675	0.729065	0.633247
1.248412	1.054614	0.869581	0.726155	0.630980
1.253453	1.053434	0.867441	0.725404	0.630410
1.259921	1.052531	0.866025	0.724841	0.629961
1.150178	0.900076	0.649974	0.450038	0.350434
1.059635	0.801025	0.552486	0.400512	0.330570
1.054614	0.795880	0.547570	0.397940	0.328459
1.053434	0.794653	0.546482	0.397326	0.328031
1.052531	0.793701	0.545562	0.396850	0.327689
1.059083	0.649974	0.000000	0.000000	0.000000
0.879675	0.552486	0.000000	0.000000	0.000000
0.869581	0.547570	0.000000	0.000000	0.000000
0.867441	0.546482	0.000000	0.000000	0.000000
0.866025	0.545562	0.000000	0.000000	0.000000
0.799745	0.450038	0.000000	0.000000	0.000000
0.729065	0.400512	0.000000	0.000000	0.000000
0.726155	0.397940	0.000000	0.000000	0.000000
0.725404	0.397326	0.000000	0.000000	0.000000
0.724841	0.396850	0.000000	0.000000	0.000000
0.661301	0.350434	0.000000	0.000000	0.000000
0.633247	0.330570	0.000000	0.000000	0.000000
0.630980	0.328459	0.000000	0.000000	0.000000
0.630410	0.328031	0.000000	0.000000	0.000000
0.629961	0.327689	0.000000	0.000000	0.000000

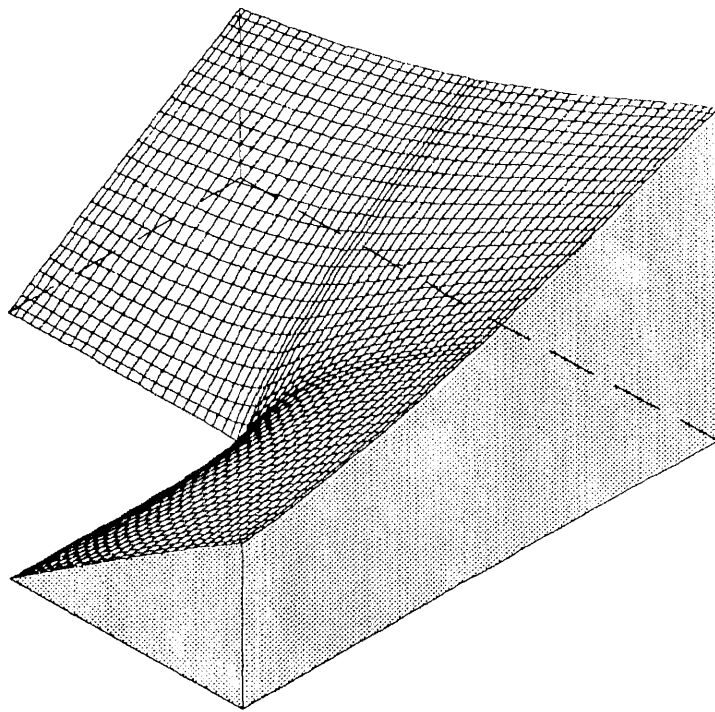


Figure 4.19 Three-dimensional view of the solution ϕ of Laplace's equation with the boundary conditions defined in Figure 4.16

It is important to show that the coefficients in the series solution determined by a using least-square or minimax approach will produce results that are in good agreement with the exact solution along the sector arc. Note that the solution along the sector arc is the boundary condition for the series solution formulated for the isolated sector near the singular point. The most accurate approximate solution along the arc will make the approximate solution closest to the exact solution. Table 4.23 shows good agreement with the series solution along the sector arc; the data in this table is plotted in Figure 4.20.

Table 4.23 Comparison the solution ϕ along the sector arc with a fixed radius $r = 0.5$ and at various angles θ (from 0 to 1.5π)

Point No.	Angle θ in radians	Exact solution	Interpolated LCM (9×9)	Least-squares Approx. (2 odd coeffs.)	Minimax Approx. (2 odd coeffs.)
1	0.000000	0.000000	0.000000	0.000000	0.000000
2	0.471239	0.194669	0.195661	0.194703	0.195363
3	0.942478	0.370282	0.370975	0.370327	0.371238
4	1.413717	0.509649	0.510404	0.509678	0.510346
5	1.884956	0.599128	0.600469	0.599130	0.599359
6	2.356194	0.629961	0.629967	0.629950	0.629967
7	2.827433	0.599128	0.600469	0.599130	0.599359
8	3.298672	0.509649	0.510404	0.509678	0.510346
9	3.769911	0.370282	0.370975	0.370327	0.371238
10	4.241150	0.194669	0.195661	0.194703	0.195363
11	4.712389	0.000000	0.000000	0.000000	0.000000

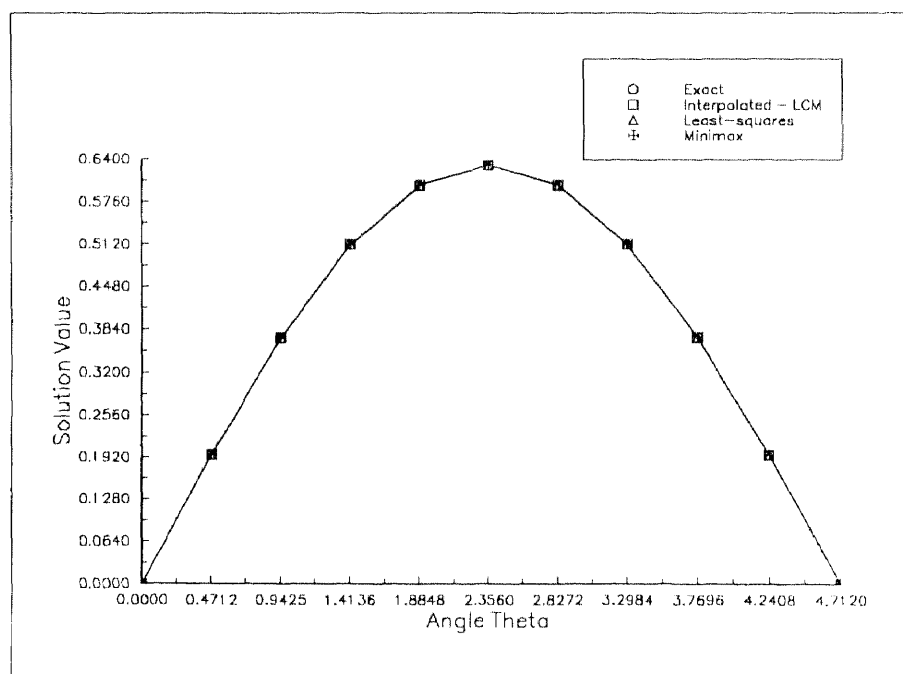


Figure 4.20 Plot of the solution ϕ along the sector arc as tabulated in Table 4.23

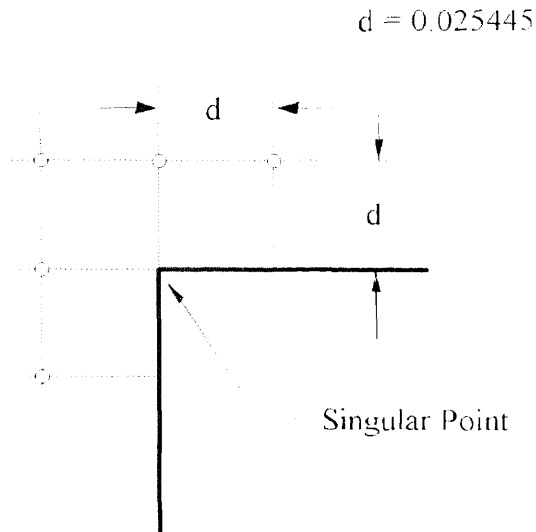


Figure 4.21 Grid points nearest to the singularity for each element with 9×9 mesh size

As shown in Figure 4.21 and Table 4.21, the errors in the neighborhood of singularity are from 4.96% to 9.25%, and the size of grid points is 0.025445×0.025445 . Table 4.24 shows not only the convergence of the series solution in the neighborhood of singularity, but also a solution with remarkable accuracy and negligible errors in a neighborhood that is ten times smaller than the neighborhood provided by the Legendre Collocation Method using 9×9 mesh size. Tables 4.25 and 4.26 show convergence of the derivatives and good agreement with the exact solution.

It is important to note here that the minimax approach also produces almost the same rate of convergence and accuracy. Thus, either approach is good for this type of problem. Tables 4.27, 4.28 and 4.29 show a comparison of results obtained by the least-squares and minimax series solution with the exact solution. Very good agreement is seen. Figure 4.22 shows the contour lines of the solution ϕ .

Table 4.24 Pointwise convergence of the Least-squares solution ϕ at 0.0025×0.0025 grid points near singularity

0.058482	0.053622	0.046856	0.044324	0.040199	0.036623	0.039645	0.031217	0.029241
0.058548	0.053682	0.048911	0.044374	0.040244	0.036565	0.036684	0.031253	0.029275
0.058559	0.053692	0.048920	0.044382	0.040251	0.036671	0.036690	0.031258	0.029280
0.058542	0.053676	0.048906	0.044369	0.040240	0.036660	0.033680	0.031249	0.029271
0.058480	0.053620	0.048854	0.044323	0.040197	0.036627	0.039644	0.031216	0.029240
0.053622	0.048276	0.042938	0.037806	0.033183	0.029358	0.026392	0.024138	0.022405
0.053682	0.048331	0.042987	0.037848	0.033221	0.029381	0.026422	0.024166	0.022431
0.053692	0.048339	0.042995	0.037855	0.033227	0.029397	0.026426	0.024170	0.022435
0.053676	0.048326	0.042983	0.037844	0.033217	0.029386	0.026418	0.024163	0.022428
0.053620	0.048274	0.042937	0.037804	0.033182	0.029357	0.026391	0.024137	0.022404
0.048856	0.042939	0.036682	0.030777	0.025324	0.021195	0.018421	0.016547	0.015211
0.048911	0.042987	0.036683	0.030812	0.025352	0.021219	0.018442	0.016566	0.015228
0.048920	0.042996	0.036690	0.030818	0.025357	0.021223	0.018445	0.016569	0.015231
0.048906	0.042963	0.036679	0.030609	0.025349	0.021217	0.018440	0.016564	0.015226
0.048854	0.042937	0.0366840	0.030776	0.025339	0.021194	0.018420	0.016547	0.015210
0.044324	0.037806	0.030777	0.023209	0.015953	0.011604	0.009582	0.008448	0.007701
0.044374	0.037848	0.030812	0.023235	0.015971	0.011618	0.009593	0.008457	0.007710
0.044382	0.037855	0.030818	0.023239	0.015974	0.011620	0.009595	0.008459	0.007712
0.044369	0.037844	0.030809	0.023232	0.015959	0.011616	0.009592	0.008456	0.007709
0.044323	0.037804	0.030776	0.023208	0.015952	0.011604	0.009582	0.008447	0.007701
0.040199	0.033163	0.025324	0.015953	0.000000	0.000000	0.000000	0.000000	0.000000
0.040244	0.035221	0.025352	0.015971	0.000000	0.000000	0.000000	0.000000	0.000000
0.040251	0.033227	0.025357	0.015974	0.000000	0.000000	0.000000	0.000000	0.000000
0.040240	0.033217	0.025349	0.015969	0.000000	0.000000	0.000000	0.000000	0.000000
0.040197	0.033182	0.025323	0.015952	0.000000	0.000000	0.000000	0.000000	0.000000
0.036623	0.020358	0.021195	0.011604	0.000000	0.000000	0.000000	0.000000	0.000000
0.036665	0.029391	0.021219	0.011618	0.000000	0.000000	0.000000	0.000000	0.000000
0.036671	0.029397	0.021223	0.011620	0.000000	0.000000	0.000000	0.000000	0.000000
0.036660	0.029386	0.021217	0.011616	0.000000	0.000000	0.000000	0.000000	0.000000
0.036622	0.029357	0.021194	0.011604	0.000000	0.000000	0.000000	0.000000	0.000000
0.033645	0.026362	0.018421	0.009562	0.000000	0.000000	0.000000	0.000000	0.000000
0.033684	0.026427	0.018442	0.009593	0.000000	0.000000	0.000000	0.000000	0.000000
0.033690	0.026426	0.018445	0.009595	0.000000	0.000000	0.000000	0.000000	0.000000
0.033680	0.026418	0.018440	0.009592	0.000000	0.000000	0.000000	0.000000	0.000000
0.033644	0.026391	0.018420	0.009582	0.000000	0.000000	0.000000	0.000000	0.000000
0.031217	0.024138	0.016547	0.008448	0.000000	0.000000	0.000000	0.000000	0.000000
0.031253	0.024166	0.016566	0.008457	0.000000	0.000000	0.000000	0.000000	0.000000
0.031258	0.024170	0.016569	0.008459	0.000000	0.000000	0.000000	0.000000	0.000000
0.031249	0.024163	0.016564	0.008456	0.000000	0.000000	0.000000	0.000000	0.000000
0.031216	0.024137	0.016547	0.008447	0.000000	0.000000	0.000000	0.000000	0.000000
0.029241	0.022405	0.015211	0.007701	0.000000	0.000000	0.000000	0.000000	0.000000
0.029275	0.022431	0.015228	0.007710	0.000000	0.000000	0.000000	0.000000	0.000000
0.029280	0.022435	0.015231	0.007712	0.000000	0.000000	0.000000	0.000000	0.000000
0.029271	0.022428	0.015226	0.007709	0.000000	0.000000	0.000000	0.000000	0.000000
0.029240	0.022404	0.015210	0.007701	0.000000	0.000000	0.000000	0.000000	0.000000

The numbers in the table have the following significance:
 First value - by using two odd-number coefficients
 Second value - by using three odd-number coefficients
 Third value - by using four odd-number coefficients
 Fourth value - by using five odd-number coefficients
 Fifth value - exact solution

Table 4.25 Pointwise convergence of $\frac{\partial\phi}{\partial x}$ of the Least-squares solution ϕ at 0.0025×0.0025 grid points near singularity

-1.949415	-1.932979	-1.870468	-1.742982	-1.547251	-1.310191	-1.075524	-0.873868	-0.713534
-1.951558	-1.935104	-1.872523	-1.744902	-1.548939	-1.311611	-1.076678	-0.874794	-0.714278
-1.951918	-1.935460	-1.872868	-1.745225	-1.549227	-1.311858	-1.076883	-0.874963	-0.714419
-1.951386	-1.934943	-1.872370	-1.744764	-1.548824	-1.311524	-1.076618	-0.874758	-0.714260
-1.949345	-1.932910	-1.870402	-1.742931	-1.547196	-1.310146	-1.075487	-0.873838	-0.713510
-2.125064	-2.145609	-2.111354	-1.973900	-1.702971	-1.353466	-1.030778	-0.785346	-0.611476
-2.127423	-2.147991	-2.113697	-1.976147	-1.704851	-1.354951	-1.031897	-0.786188	-0.612120
-2.127810	-2.148382	-2.114081	-1.976507	-1.705164	-1.355201	-1.032091	-0.786338	-0.612240
-2.127224	-2.147790	-2.113499	-1.975966	-1.704702	-1.354842	-1.031826	-0.786145	-0.612099
-2.124988	-2.145532	-2.111278	-1.973889	-1.702910	-1.353418	-1.030742	-0.785319	-0.611455
-2.321827	-2.409233	-2.456111	-2.356645	-1.949416	-1.355077	-0.898998	-0.623869	-0.458960
-2.324423	-2.411928	-2.458859	-2.359281	-1.951591	-1.356579	-0.899984	-0.624544	-0.458448
-2.324842	-2.412362	-2.459302	-2.359705	-1.951944	-1.356827	-0.900150	-0.624862	-0.459537
-2.324186	-2.411680	-2.458606	-2.359039	-1.951397	-1.356454	-0.899912	-0.624504	-0.459427
-2.321742	-2.409145	-2.458021	-2.356559	-1.949345	-1.355028	-0.898966	-0.623848	-0.458945
-2.519200	-2.702517	-2.925319	-3.094506	-2.456111	-1.132668	-0.578253	-0.358241	-0.249877
-2.522036	-2.705561	-2.928615	-3.097994	-2.458578	-1.133934	-0.578093	-0.358031	-0.250144
-2.522486	-2.706043	-2.929137	-3.098546	-2.459315	-1.134138	-0.578099	-0.358698	-0.250192
-2.521759	-2.705262	-2.928291	-3.097650	-2.458806	-1.133818	-0.578642	-0.358806	-0.250131
-2.519107	-2.702418	-2.925212	-3.094393	-2.456021	-1.132626	-0.578234	-0.358229	-0.249868
-2.679922	-2.949636	-3.376490	-4.254111	SINGULAR POINT	0.000000	0.000000	0.000000	0.000000
-2.682956	-2.952975	-3.380312	-4.258927		0.000000	0.000000	0.000000	0.000000
-2.683431	-2.953497	-3.380911	-4.259660		0.000000	0.000000	0.000000	0.000000
-2.682644	-2.952631	-3.379919	-4.258431		0.000000	0.000000	0.000000	0.000000
-2.679823	-2.949526	-3.376365	-4.253953		0.000000	0.000000	0.000000	0.000000
-2.769079	-3.060761	-3.503576	-4.227176	-4.912225				
-2.772230	-3.064241	-3.507556	-4.231977	-4.917801				
-2.772717	-3.064780	-3.508175	-4.232723	-4.918666				
-2.771891	-3.063869	-3.507134	-4.231489	-4.917213				
-2.768876	-3.060647	-3.503445	-4.227019	-4.912042				
-2.780791	-3.033106	-3.355113	-3.711726	-3.898836				
-2.783970	-3.036572	-3.358943	-3.715959	-3.903282				
-2.784456	-3.037102	-3.359530	-3.716810	-3.903965				
-2.783614	-3.036186	-3.358519	-3.715494	-3.902795				
-2.780687	-3.032993	-3.354987	-3.711587	-3.898690				
-2.736546	-2.930962	-3.142138	-3.327432	-3.405948				
-2.739692	-2.934327	-3.145743	-3.331247	-3.409851				
-2.740166	-2.934536	-3.146289	-3.331825	-3.410444				
-2.739324	-2.933937	-3.145328	-3.330810	-3.409405				
-2.736443	-2.930851	-3.142020	-3.327307	-3.405820				
-2.662966	-2.806855	-2.946000	-3.053192	-3.094510				
-2.666034	-2.810096	-2.949390	-3.056712	-3.098077				
-2.666492	-2.810570	-2.949907	-3.057229	-3.086011				
-2.665659	-2.809704	-2.948990	-3.056291	-3.097651				
-2.662655	-2.806746	-2.945868	-3.053076	-3.094393				

The numbers in the table have the following significance:
 First value - by using two odd-number coefficients
 Second value - by using three odd-number coefficients
 Third value - by using four odd-number coefficients
 Fourth value - by using five odd-number coefficients
 Fifth value - exact solution

Table 4.26 Pointwise convergence of $\frac{\partial\phi}{\partial y}$ of the Least-squares solution ϕ at 0.0025×0.0025 grid points near singularity

1.949415	2.125064	2.321827	2.519200	2.679922	2.76079	2.780791	2.736546	2.662956
1.951558	2.127423	2.324423	2.522036	2.682956	2.772230	2.783970	2.739662	2.666034
1.951918	2.127810	2.324842	2.522486	2.683431	2.772717	2.784456	2.740166	2.666492
1.951396	2.127224	2.324186	2.521759	2.682644	2.771891	2.763614	2.739324	2.665659
1.949345	2.124988	2.321742	2.519107	2.679823	2.768976	2.760687	2.736443	2.662855
1.932979	2.145809	2.409233	2.702517	2.949636	3.060761	3.033106	2.930962	2.806855
1.935104	2.147991	2.411928	2.705561	2.952975	3.064241	3.036572	2.934327	2.810096
1.935460	2.148382	2.412362	2.706043	2.953497	3.064780	3.037102	2.934636	2.810579
1.934943	2.147790	2.411680	2.705262	2.952631	3.063869	3.036166	2.933937	2.809704
1.932910	2.145532	2.409145	2.702418	2.949526	3.060647	3.032993	2.930851	2.806748
1.870468	2.111354	2.456111	2.925319	3.376490	3.503576	3.355113	3.142138	2.946000
1.872523	2.113697	2.458859	2.928615	3.380312	3.507558	3.358943	3.145743	2.949399
1.872868	2.114081	2.459302	2.929137	3.380911	3.508175	3.359530	3.146289	2.949907
1.872370	2.113499	2.458606	2.928291	3.379919	3.507134	3.358519	3.145328	2.948990
1.870402	2.111276	2.456021	2.925212	3.376365	3.503445	3.354987	3.142020	2.945888
1.742992	1.973960	2.356645	3.094506	4.254111	4.227176	3.711726	3.327432	3.053192
1.744902	1.976147	2.359261	3.097994	4.258927	4.231977	3.715959	3.331247	3.056712
1.745225	1.976507	2.359705	3.098546	4.259680	4.232723	3.716610	3.331825	3.057239
1.744764	1.975866	2.356030	3.097650	4.258431	4.231469	3.715494	3.330810	3.056291
1.742931	1.973889	2.356559	3.094393	4.253953	4.227019	3.711587	3.327307	3.053076
1.547251	1.702971	1.949416	2.456111	SINGULAR POINT	4.912225	3.896836	3.405948	3.094510
1.548939	1.704851	1.951591	2.458576		4.917801	3.903282	3.409851	3.098077
1.549227	1.705164	1.951944	2.459315		4.918668	3.903965	3.410444	3.098611
1.548824	1.704702	1.951397	2.458606		4.917213	3.902795	3.409405	3.097651
1.547196	1.702910	1.949345	2.456021		4.912042	3.898690	3.405820	3.094393
1.310191	1.353466	1.355077	1.132668	0.000000				
1.311611	1.354951	1.356579	1.133934	0.000000				
1.311858	1.355201	1.356827	1.134138	0.000000				
1.311524	1.354842	1.356454	1.133618	0.000000				
1.310146	1.353418	1.355028	1.132626	0.000000				
1.075524	1.030778	0.898998	0.578255	0.000000				
1.076678	1.031897	0.899984	0.578893	0.000000				
1.076883	1.032091	0.900150	0.578999	0.000000				
1.076618	1.031826	0.899912	0.578842	0.000000				
1.075487	1.030742	0.898966	0.578234	0.000000				
0.873868	0.785346	0.623869	0.358241	0.000000				
0.874794	0.786188	0.624544	0.358631	0.000000				
0.874963	0.786338	0.624662	0.358698	0.000000				
0.874758	0.786145	0.624504	0.358606	0.000000				
0.873838	0.785319	0.623848	0.358229	0.000000				
0.713534	0.611476	0.458960	0.249877	0.000000				
0.714278	0.612120	0.459448	0.250144	0.000000				
0.714419	0.612240	0.459537	0.250192	0.000000				
0.714260	0.612099	0.458427	0.250131	0.000000				
0.713510	0.611455	0.458945	0.249868	0.000000				

The number in the table have the following significance:
 First value - by using two odd-number coefficients
 Second value - by using three odd-number coefficients
 Third value - by using four odd-number coefficients
 Fourth value - by using five odd-number coefficients
 Fifth value - exact solution

Table 4.27 Comparison of the solution ϕ at 0.0025×0.0025 grid points near singularity:

First value - Exact solution

Second value - Least-squares series solution with two odd-number coefficients

Third value - Minimax series solution with two odd-number coefficients

0.058480	0.053620	0.048854	0.044323	0.040197	0.036622	0.033644	0.031216	0.029240
0.058482	0.053622	0.048856	0.044324	0.040199	0.036623	0.033645	0.031217	0.029241
0.058538	0.053673	0.048902	0.044366	0.040237	0.036658	0.033678	0.031247	0.029270
0.053620	0.048274	0.042937	0.037804	0.033182	0.029357	0.026391	0.024137	0.022404
0.053622	0.048276	0.042939	0.037806	0.033183	0.029358	0.026392	0.024138	0.022405
0.053673	0.048322	0.042980	0.037842	0.033215	0.029386	0.026417	0.024161	0.022427
0.048854	0.042937	0.036840	0.030776	0.025323	0.021194	0.018420	0.016547	0.015210
0.048856	0.042939	0.036842	0.030777	0.025324	0.021195	0.018421	0.016547	0.015211
0.048902	0.042980	0.036877	0.030807	0.025348	0.021216	0.018439	0.016563	0.015225
0.044323	0.037804	0.030776	0.023208	0.015952	0.011604	0.009582	0.008447	0.007701
0.044324	0.037806	0.030777	0.023209	0.015953	0.011604	0.009582	0.008448	0.007701
0.044366	0.037842	0.030807	0.023231	0.015968	0.011616	0.009591	0.008456	0.007709
0.040197	0.033182	0.025323	0.015952	0.000000	0.000000	0.000000	0.000000	0.000000
0.040199	0.033183	0.025324	0.015953	0.000000	0.000000	0.000000	0.000000	0.000000
0.040237	0.033215	0.025348	0.015968	0.000000	0.000000	0.000000	0.000000	0.000000
0.036622	0.029357	0.021194	0.011604	0.000000	0.000000	0.000000	0.000000	0.000000
0.036623	0.029358	0.021195	0.011604	0.000000	0.000000	0.000000	0.000000	0.000000
0.036658	0.029386	0.021216	0.011616	0.000000	0.000000	0.000000	0.000000	0.000000
0.033644	0.026391	0.018420	0.009582	0.000000	0.000000	0.000000	0.000000	0.000000
0.033645	0.026392	0.018421	0.009582	0.000000	0.000000	0.000000	0.000000	0.000000
0.033678	0.026417	0.018439	0.009591	0.000000	0.000000	0.000000	0.000000	0.000000
0.031216	0.024137	0.016547	0.008447	0.000000	0.000000	0.000000	0.000000	0.000000
0.031217	0.024138	0.016547	0.008448	0.000000	0.000000	0.000000	0.000000	0.000000
0.031247	0.024161	0.016563	0.008456	0.000000	0.000000	0.000000	0.000000	0.000000
0.029240	0.022404	0.015210	0.007701	0.000000	0.000000	0.000000	0.000000	0.000000
0.029241	0.022405	0.015211	0.007701	0.000000	0.000000	0.000000	0.000000	0.000000
0.029270	0.022427	0.015225	0.007709	0.000000	0.000000	0.000000	0.000000	0.000000

Table 4.28 Comparison of $\frac{\partial \phi}{\partial x}$ at 0.0025×0.0025 grid points near singularity:

First value - Exact solution

Second value - Least-squares series solution with two odd-number coefficients

Third value - Minimax series solution with two odd-number coefficients

-1.949345	-1.932910	-1.870402	-1.742931	-1.547196	-1.310146	-1.075487	-0.873838	-0.713510
-1.949415	-1.932979	-1.870468	-1.742992	-1.547251	-1.310191	-1.075524	-0.873868	-0.713534
-1.951231	-1.934780	-1.872210	-1.744612	-1.548683	-1.311397	-1.076505	-0.874657	-0.714169
-2.124988	-2.145532	-2.111278	-1.973889	-1.702910	-1.353418	-1.030742	-0.785319	-0.611455
-2.125064	-2.145609	-2.111354	-1.973960	-1.702971	-1.353466	-1.030778	-0.785346	-0.611476
-2.127061	-2.147625	-2.113337	-1.975812	-1.704564	-1.354725	-1.031728	-0.786062	-0.612025
-2.321742	-2.409145	-2.456021	-2.356559	-1.949345	-1.355028	-0.898966	-0.623848	-0.458945
-2.321827	-2.409233	-2.456111	-2.356645	-1.949416	-1.355077	-0.898998	-0.623869	-0.458960
-2.324023	-2.411512	-2.458435	-2.358874	-1.951256	-1.356349	-0.899834	-0.624442	-0.459376
-2.519107	-2.702418	-2.925212	-3.094393	-2.456021	-1.132626	-0.578234	-0.358229	-0.249868
-2.519200	-2.702517	-2.925319	-3.094506	-2.456111	-1.132668	-0.578255	-0.358241	-0.249877
-2.521596	-2.705089	-2.928104	-3.097453	-2.458447	-1.133739	-0.578796	-0.358572	-0.250104
-2.679823	-2.949526	-3.376365	-4.253953	SINGULAR POINT	0.000000	0.000000	0.000000	0.000000
-2.679922	-2.949636	-3.376490	-4.254111		0.000000	0.000000	0.000000	0.000000
-2.682484	-2.952455	-3.379718	-4.258177		0.000000	0.000000	0.000000	0.000000
-2.768976	-3.060647	-3.503445	-4.227019		-4.912042			
-2.769079	-3.060761	-3.503576	-4.227176		-4.912225			
-2.771738	-3.063698	-3.506937	-4.231229		-4.916932			
-2.780687	-3.032993	-3.354987	-3.711587		-3.898690			
-2.780791	-3.033106	-3.355113	-3.711726		-3.898836			
-2.783472	-3.036029	-3.358343	-3.715297		-3.902586			
-2.736443	-2.930851	-3.142020	-3.327307		-3.405820			
-2.736546	-2.930962	-3.142138	-3.327432		-3.405948			
-2.739197	-2.933799	-3.145177	-3.330648		-3.409239			
-2.662855	-2.806748	-2.945888	-3.053076		-3.094393			
-2.662956	-2.806855	-2.946000	-3.053192		-3.094510			
-2.665549	-2.809585	-2.948863	-3.056157		-3.097515			

Table 4.29 Comparison of $\frac{\partial \hat{\phi}}{\partial y}$ at 0.0025×0.0025 grid points near singularity:

First value - Exact solution

Second value - Least-squares series solution with two odd-number coefficients

Third value - Minimax series solution with two odd-number coefficients

1.949345	2.124988	2.321742	2.519107	2.679823	2.768976	2.780687	2.736443	2.662855
1.949415	2.125064	2.321827	2.519200	2.679922	2.769079	2.780791	2.736546	2.662956
1.951231	2.127061	2.324023	2.521596	2.682484	2.771738	2.783472	2.739197	2.665549
1.932910	2.145532	2.409145	2.702418	2.949526	3.060647	3.032993	2.930851	2.806748
1.932979	2.145609	2.409233	2.702517	2.949636	3.060761	3.033106	2.930962	2.806855
1.934780	2.147625	2.411512	2.705089	2.952455	3.063698	3.036029	2.933799	2.809585
1.870402	2.111278	2.456021	2.925212	3.376365	3.503445	3.354987	3.142020	2.945888
1.870468	2.111354	2.456111	2.925319	3.376490	3.503576	3.355113	3.142138	2.946000
1.872210	2.113337	2.458435	2.928104	3.379718	3.506937	3.358343	3.145177	2.948863
1.742931	1.973889	2.356559	3.094393	4.253953	4.227019	3.711587	3.327307	3.053076
1.742992	1.973960	2.356645	3.094506	4.254111	4.227176	3.711726	3.327432	3.053192
1.744612	1.975812	2.358874	3.097453	4.258177	4.231229	3.715297	3.330648	3.056157
1.547196	1.702910	1.949345	2.456021	SINGULAR POINT	4.912042	3.898690	3.405820	3.094393
1.547251	1.702971	1.949416	2.456111		4.912225	3.898836	3.405948	3.094510
1.548683	1.704564	1.951231	2.458447		4.916932	3.902586	3.409239	3.097515
1.310146	1.353418	1.355028	1.132626	0.000000				
1.310191	1.353466	1.355077	1.132668	0.000000				
1.311397	1.354725	1.356349	1.133739	0.000000				
1.075487	1.030742	0.898966	0.578234	0.000000				
1.075524	1.030778	0.898998	0.578255	0.000000				
1.076505	1.031728	0.899834	0.578796	0.000000				
0.873838	0.785319	0.623848	0.358229	0.000000				
0.873868	0.785346	0.623869	0.358241	0.000000				
0.874657	0.786062	0.624442	0.358572	0.000000				
0.713510	0.611455	0.458945	0.249868	0.000000				
0.713534	0.611476	0.458960	0.249877	0.000000				
0.714169	0.612025	0.459376	0.250104	0.000000				

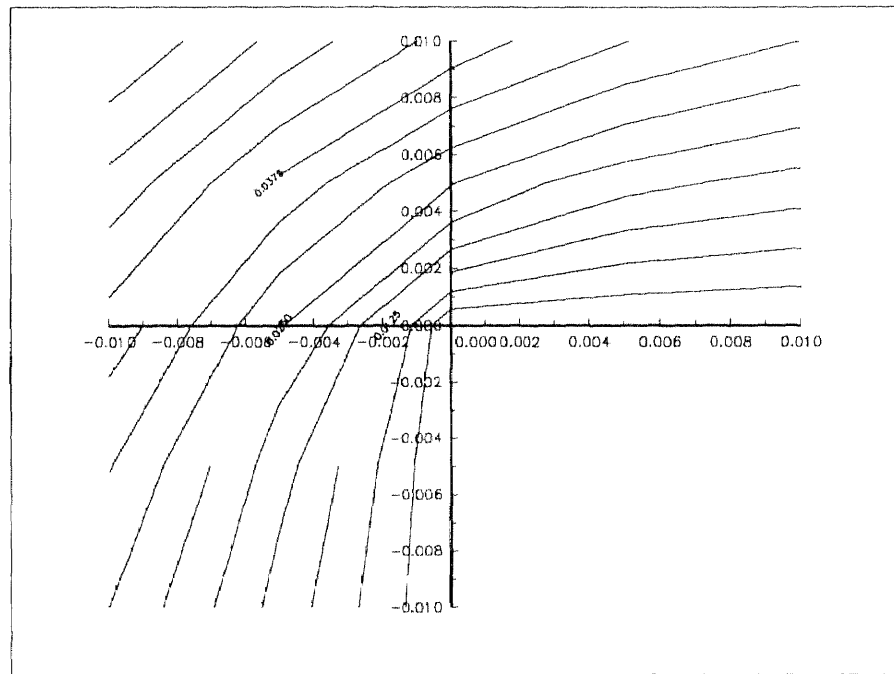


Figure 4.22 Contour plot of solution ϕ in the neighborhood of singularity

CHAPTER 5

CONCLUDING REMARKS

In this study, a fully automated two-dimensional p -version of the Legendre Collocation Method is formulated. The trial solution is constructed in terms of the value of the solution at the collocation points, and these values become known once the problem has been solved. The solution at any other points can be easily obtained by means of interpolation. The trial solution satisfies the governing differential equation and the boundary conditions at the collocation points. This *mixed collocation* is a completely general method. The use of Lagrangian interpolation functions in constructing the approximate solution and the zeros of a Legendre polynomial as the interior collocation points makes it possible to fully automate the computer code so that the accuracy of the solution is achieved solely by increasing the order of the Legendre polynomial. Hence the number of roots determines the number of collocation points and the accuracy of the approximate solution. The choice of the zeros of a Legendre polynomial for collocation points serves not only to produce more accurate results, but also "ready-to-use" function values for the widely used Gauss-Legendre integration. The most significant virtue of the Legendre Collocation Method is its ease in application via the digital computer. The matrix elements of the defining equation yield directly the solution and its derivatives. There is no numerical integration as in the Galerkin method.

In the h -version of the orthogonal collocation method on finite elements, the accuracy is achieved by refining the mesh while using lower order polynomials. In the p -version accuracy is increased by increasing the polynomial degree. Thus, we know that for a given number of unknowns, the p -version

technique yields higher accuracy. This was found in our numerical experiments where both techniques were implemented. Also, due to the repeated change in the size of elements in order to increase accuracy, from the point of view of programming, the *h*-version would require much more human effort to be implemented than the *p*-version.

For problems containing a boundary singularity, it is not feasible to compute the derivatives using the solution obtained by the Legendre Collocation Method. The relatively high errors in the solution function in a neighborhood of the singularity cause much higher errors in the derivatives. This difficulty has been overcome by a combination of the Legendre Collocation Method and the use of an eigenfunction solution near the singularity. With regard to computational effort, the Legendre Collocation Method requires the solution of a set of N linear algebraic equations. These equations are almost directly available in the Legendre Collocation Method, whereas most standard methods require integrations. Therefore the combined method developed in this study not only gives a very accurate approximation, but also an effective means of handling problems containing a boundary singularity. The coefficients of the eigenfunctions solution in the neighborhood of the singularity are determined by either the least-squares or minimax approach; we noted the rapid convergence of the solution obtained by both approximations. In fact, both techniques produce almost the same accuracy. The minimax approach requires less mathematical derivations, but requires the solution of a set of simultaneous equations.

As demonstrated in the examples, the present formulations and numerical procedures are accurate, efficient and dependable for practical problems governed by partial differential equations and subjected to various boundary conditions. Engineering accuracy is achieved with relatively little effort, both by hand and by the computer. This makes it possible to carry out the numerical calculations in this

study on a personal computer with a conventional memory for storage. For all calculations in the example problems, a very short computation time on a 386-33MHz PC was observed. With such successful developments, this method provides an attractive alternative for the study of many problems governed by partial differential equations.

APPENDIX A

SOLUTION OF DIRICHLET PROBLEM FOR LAPLACE'S EQUATION BY SEPARATION OF VARIABLES

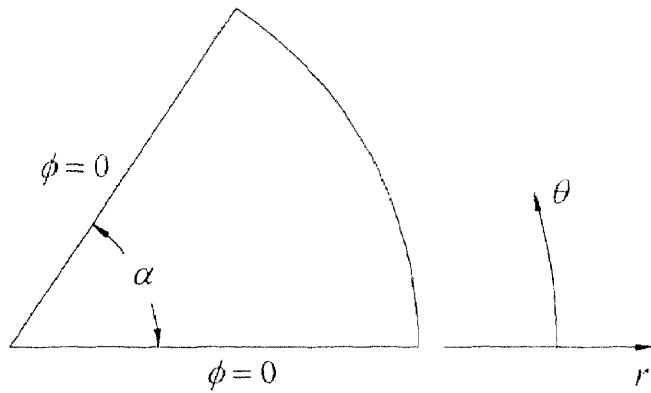


Figure A.1 Boundary conditions for Laplace's equation

Consider the following problem for the domain depicted in Figure A.1

$$\phi_{rr} + \frac{1}{r} \phi_r + \frac{1}{r^2} \phi_{\theta\theta} = 0 \quad (\text{A.1})$$

and subject to the following boundary conditions

$$\phi = 0 \text{ along } \theta = 0 \quad (\text{A.2})$$

$$\phi = 0 \text{ along } \theta = \alpha \quad (\text{A.3})$$

Separation of variables can be applied to the differential equation (A.1) by assuming a trial solution in the form

$$\phi = R(r) T(\theta) \quad (\text{A.4})$$

Successive differentiation of Equation (A.4) gives

$$\phi_r = R'(r) T(\theta) \quad (\text{A.5})$$

$$\phi_{rr} = R''(r) T(\theta) \quad (\text{A.6})$$

and

$$\phi_{\theta\theta} = R(r) T''(\theta) \quad (\text{A.7})$$

Substituting Equations (A.5), (A.6) and (A.7) into Equation (A.1) yields

$$R''(r)T(\theta) + \frac{1}{r}R'(r)T(\theta) + \frac{1}{r^2}R(r)T''(\theta) = 0$$

or

$$r^2 \frac{R''(r)}{R(r)} + r \frac{R'(r)}{R(r)} = -\frac{T''(\theta)}{T(\theta)} = \lambda$$

where λ is the separation constant.

Hence, we obtain for T and R the two differential equations

$$T''(\theta) + \lambda T(\theta) = 0 \quad (\text{A.8})$$

and

$$r^2 R''(r) + r R'(r) - \lambda R(r) = 0 \quad (\text{A.9})$$

The boundary conditions in Equations (A.2) and (A.3) imply that

$$T(\theta) = 0 \quad \text{along } \theta = 0 \quad (\text{A.10})$$

$$T(\theta) = 0 \quad \text{along } \theta = \alpha \quad (\text{A.11})$$

Three cases are possible for the value of λ in Equation (A.8):

1. For $\lambda < 0$, and by taking a trial solution in the form

$$T = \hat{c} e^{k\theta} \quad (\text{A.12})$$

we obtain the characteristic equation

$$k^2 - \lambda = 0$$

$$\text{or} \quad k_{1,2} = \pm\sqrt{-\lambda}.$$

Hence, the general solution has the form

$$T(\theta) = \hat{c}_1 e^{\sqrt{-\lambda}\theta} + \hat{c}_2 e^{-\sqrt{-\lambda}\theta}$$

while the boundary conditions as given in Equations (A.10) and (A.11) are

$$\begin{aligned}T(0) &= \hat{c}_1 + \hat{c}_2 = 0 \\T(\alpha) &= \hat{c}_1 e^{\sqrt{\lambda} \alpha} + \hat{c}_2 e^{-\sqrt{\lambda} \alpha} = 0\end{aligned}$$

Since the value of $\sqrt{\lambda} \alpha$ in the above equation is real and positive, we have

$$\hat{c}_1 = 0, \quad \hat{c}_2 = 0.$$

Therefore Equation (A.8) possesses no nontrivial solution for $\lambda < 0$.

2. For $\lambda = 0$, similarly, no nontrivial solution exists, since the general solution is

$$T(\theta) = \tilde{c}_1 \theta + \tilde{c}_2$$

while the boundary conditions are

$$\begin{aligned}T(0) &= \tilde{c}_2 = 0 \\T(\alpha) &= \tilde{c}_1 \alpha = 0\end{aligned}$$

Again, we have $\tilde{c}_1 = \tilde{c}_2 = 0$, thus

$$T(\theta) \equiv 0.$$

3. For $\lambda > 0$, using Equation (A.12) as a trial solution, one has the following characteristic equation

$$\begin{aligned}k^2 + \lambda &= 0 \\ \text{or} \quad k_{1,2} &= \pm i\sqrt{\lambda}.\end{aligned}$$

and the general solution can be written as

$$T(\theta) = \check{c}_1 e^{i\sqrt{\lambda} \theta} + \check{c}_2 e^{-i\sqrt{\lambda} \theta}$$

The above solution contains imaginary exponents, and therefore can be represented in the form

$$T(\theta) = \check{c}_1 \cos \sqrt{\lambda} \theta + \check{c}_2 \sin \sqrt{\lambda} \theta \tag{A.13}$$

where \check{c}_1 and \check{c}_2 are arbitrary constants.

By inspecting Equation (A.13) and the boundary conditions in Equations (A.10) and (A.11), it is clear that a nontrivial solution exists for $\lambda > 0$.

The eigenvalues with their corresponding eigenfunctions will be determined later. We will proceed to find the solution for Equation (A.9).

The second differential equation (A.9) can be solved by taking a trial solution in the form

$$R(r) = r^\mu \quad (\text{A.14})$$

Substituting Equation (A.14) into Equation (A.9), we obtain

$$\mu(\mu-1)r^\mu + \mu r^\mu - \lambda r^\mu = 0$$

As mentioned above, $\lambda \leq 0$ is excluded. Simplifying, we obtain

$$\mu^2 - \lambda = 0$$

or $\mu_{1,2} = \pm\sqrt{\lambda}$, for $\lambda > 0$.

Consequently, Equation (A.14) becomes

$$R(r) = B r^{\sqrt{\lambda}} + C r^{-\sqrt{\lambda}} \quad (\text{A.15})$$

where B and C are arbitrary constants. As indicated in Figure A.1, the solution has to be finite at the origin; in this case equal to zero when $r = 0$. This is possible only for $C = 0$. Thus, Equation (A.15) becomes

$$R(r) = B r^{\sqrt{\lambda}}, \quad \lambda > 0$$

Now, the general solution to a Dirichlet problem for Laplace's equation for the domain shown in Figure A.1 is given by

$$\phi(r, \theta) = r^{\sqrt{\lambda}} (c_1 \cos \sqrt{\lambda} \theta + c_2 \sin \sqrt{\lambda} \theta) \quad (\text{A.16})$$

and it is still required for $\phi(r, \theta)$ to satisfy the boundary conditions (A.2) and (A.3) such that

$$\begin{aligned} \phi(r, 0) &= c_1 = 0 \\ \phi(r, \alpha) &= c_2 r^{\sqrt{\lambda}} \sin \sqrt{\lambda} \alpha = 0 \end{aligned}$$

If $\phi(r, \theta)$ does not vanish identically, then $c_2 \neq 0$ so that

$$\sin \sqrt{\lambda} \alpha = 0$$

and consequently,

$$\sqrt{\lambda} = \frac{n\pi}{\alpha} \quad \text{for } n = 1, 2, \dots, \infty$$

Therefore a nontrivial solution is possible only for the values

$$\lambda_n = \left(\frac{n\pi}{\alpha} \right)^2.$$

These eigenvalues λ_n correspond to the eigenfunctions

$$c_n \sin \frac{n\pi}{\alpha} \theta$$

Hence for those eigenvalues of λ_n , there exist only the nontrivial solutions

$$\phi(r, \theta) = c_n r^{\frac{n\pi}{\alpha}} \sin \frac{n\pi}{\alpha} \theta \quad \text{for } n = 1, 2, \dots, \infty$$

The sum of these solutions,

$$\phi(r, \theta) = \sum_{n=1}^{\infty} c_n r^{\frac{n\pi}{\alpha}} \sin \frac{n\pi}{\alpha} \theta \tag{A.17}$$

satisfies Equation (A.1) and the boundary conditions (A.2) and (A.3). It follows, if $\alpha > \pi$, that the derivative of ϕ may become infinite in magnitude as $r \rightarrow 0$, and it is not surprising, when such singularities arise, that it is difficult to compute ϕ accurately in this region.

The solution in Equation (A.17) can also be written as

$$\phi(r, \theta) = \sum_{n=1}^{\infty} R_n(r) \sin \frac{n\pi}{\alpha} \theta \tag{A.18}$$

The solution in this form is suitable for solving Poisson's equation. The right side of the differential equation is expanded in terms of the same eigenfunctions, and by substituting $\phi(r, \theta)$ in Equation (A.18) into Poisson's equation, one obtains a non-homogeneous differential equation for function of r only. The solution $R_n(r)$ is then comprised of complementary and particular solutions. The particular solution obtained in this way not only satisfies the differential equation, but also

the boundary conditions along two straight lines forming the angular sector. The discussion of this method can be found in Chapter 3.

APPENDIX B

SOLUTION OF MIXED-BOUNDARY CONDITIONS FOR LAPLACE'S EQUATION BY SEPARATION OF VARIABLES

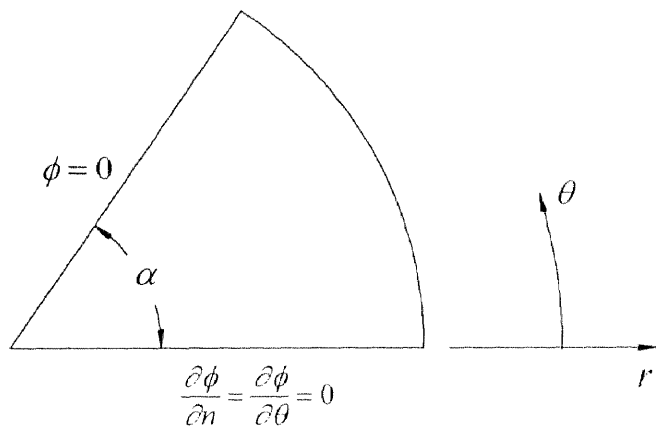


Figure B.1 Mixed-boundary conditions for Laplace's equation

The governing equation for the circular sector shown in Figure B.1 in polar coordinates is

$$\phi_{rr} + \frac{1}{r}\phi_r + \frac{1}{r^2}\phi_{\theta\theta} = 0 \quad (\text{B.1})$$

The boundary conditions along both straight lines forming the sector are given by

$$\frac{\partial\phi}{\partial\theta} = 0 \quad \text{along } \theta = 0 \quad (\text{B.2})$$

$$\phi = 0 \quad \text{along } \theta = \alpha \quad (\text{B.3})$$

Note that the boundary condition along the arc will not be considered in this formulation.

Similar to the development in Appendix A, the use of the separation of variables method assumes a trial solution in the form

$$\phi = R(r)T(\theta) \quad (\text{B.4})$$

Substitution of Equation (B.6) into Equation (B.1) gives two differential equations in R and T :

$$T''(\theta) + \lambda T(\theta) = 0 \quad (\text{B.5})$$

and

$$r^2 R''(r) + rR'(r) - \lambda R(r) = 0 \quad (\text{B.6})$$

where λ is the separation constant. For the same reasons described in Appendix A., $\lambda \leq 0$ is excluded since it produces no nontrivial solution. Thus, the solution to Laplace's equation (B.1) is found to be

$$\phi(r, \theta) = r^{\sqrt{\lambda}} (c_1 \cos \sqrt{\lambda} \theta + c_2 \sin \sqrt{\lambda} \theta), \quad \lambda > 0 \quad (\text{B.7})$$

and

$$\frac{\partial \phi}{\partial \theta} = r^{\sqrt{\lambda}} (-c_1 \sqrt{\lambda} \sin \sqrt{\lambda} \theta + c_2 \sqrt{\lambda} \cos \sqrt{\lambda} \theta) \quad (\text{B.8})$$

Along $\theta = 0$, the normal derivative

$$\frac{\partial \phi}{\partial \theta} = 0,$$

and this makes $c_2 = 0$. The boundary condition in Equation (B.3) gives

$$\cos \sqrt{\lambda} \alpha = 0$$

and consequently,

$$\sqrt{\lambda} = \frac{(2n-1)}{\alpha} \frac{\pi}{2} \quad \text{for } n = 1, 2, \dots, \infty$$

Hence, we have the eigenfunctions and eigenvalues

$$c_n \cos \left(\frac{(2n-1)}{\alpha} \frac{\pi}{2} \theta \right), \quad \lambda_n = \left(\frac{(2n-1)}{\alpha} \frac{\pi}{2} \right)^2$$

and as a result, Equation (B.7) can be written as

$$\phi(r, \theta) = \sum_{n=1}^{\infty} c_n r^{\frac{(2n-1)\pi}{2\alpha}} \cos \frac{(2n-1)\pi}{2\alpha} \theta \quad (\text{B.9})$$

It satisfies Laplace's equation (B.1) and the boundary conditions (B.2) and (B.3).

In the case of non-homogeneous boundary conditions, for example

$$\frac{\partial \phi}{\partial \theta} = A \quad \text{along } \theta = 0 \quad (\text{B.10})$$

$$\phi = B \quad \text{along } \theta = \alpha \quad (\text{B.11})$$

where A and B are arbitrary constants. We proceed as follows. It is clear that Equation (B.9) is obtained for $\lambda > 0$ and satisfies the homogeneous boundary conditions given in Equations (B.2) and (B.3). In order to satisfy the boundary conditions, it is necessary to find another solution that can be combined with Equation (B.9) to form the general solution satisfying the Laplace differential equation and the non-homogeneous boundary conditions. As shown in Appendix A., when $\lambda = 0$, the general solution of the Equation (B.5) is

$$T(\theta) = \tilde{c}_1 \theta + \tilde{c}_2 \quad (\text{B.12})$$

and its derivative with respect to θ is defined by

$$T'(\theta) = \tilde{c}_1.$$

The boundary conditions stated in Equations (B.10) and (B.11) give

$$T'(0) = \tilde{c}_1 = A$$

and

$$T(\alpha) = A\alpha + \tilde{c}_2 = B$$

$$\text{or } \tilde{c}_2 = B - A\alpha.$$

Hence, the solution in Equation (B.12) becomes

$$T(\theta) = B + A(\theta - \alpha) \quad (\text{B.13})$$

Note that the boundary conditions in Equations (B.10) and (B.11) are independent of r ; therefore it is not necessary to find the solution in Equation (B.6) which is only function of r .

Linearly combining Equations (B.9) and (B.13) gives the solution in the form

$$\phi(r, \theta) = B + A(\theta - \alpha) + \sum_{n=1}^{\infty} c_n r^{\frac{(2n-1)\pi}{2\alpha}} \cos \frac{(2n-1)\pi}{2\alpha} \theta \quad (\text{B.14})$$

which satisfies the differential equation (B.1) and the boundary conditions (B.10) and (B.11). Note that the first two functions satisfy the non-homogeneous boundary conditions, while the third satisfies the homogeneous boundary conditions.

Examining Equation (B.14) reveals that, if $\alpha > \frac{\pi}{2}$, the derivative of ϕ with respect to r tends to ∞ as $r \rightarrow 0$. Thus, the problem contains a singularity, and special attention has to be given for this type of problems.

APPENDIX C

WEIGHTS OF GAUSS-LEGENDRE QUADRATURE

It is well-known that the integration of $f(\xi)$ in the interval $-1 \leq \xi \leq +1$ can be approximated by

$$\int_{-1}^{+1} f(\xi) d\xi \approx \sum_{i=1}^N w_i f(\xi_i) \quad (\text{C.1})$$

where ξ_i are the zeros of Legendre polynomial $P_N(\xi)$, and w_i is the weight associated with ξ_i .

The function $f(\xi)$ can be defined by

$$f(\xi) = \sum_{i=1}^N \ell_i(\xi) f(\xi_i)$$

where

$$\ell_i(\xi) = \frac{P_N(\xi)}{(\xi - \xi_i) P'_N(\xi_i)}$$

is a Lagrangian interpolation polynomial with $P_N(\xi)$ a Legendre polynomial of N^{th} -degree. Equation (C.1) can now be written as

$$\int_{-1}^{+1} \sum_{i=1}^N \ell_i(\xi) f(\xi_i) d\xi \approx \sum_{i=1}^N w_i f(\xi_i) \quad (\text{C.2})$$

From above, the weight w_i can be defined as

$$\begin{aligned} w_i &= \int_{-1}^{+1} \ell_i(\xi) d\xi \\ &= \int_{-1}^{+1} \frac{P_N(\xi)}{(\xi - \xi_i) P'_N(\xi_i)} d\xi \end{aligned} \quad (\text{C.3})$$

Since $P'_N(\xi_i)$ is a constant, it can be taken outside the integral; then Equation (C.3) becomes

$$w_i = \frac{1}{P'_N(\xi_i)} \int_{-1}^{+1} \frac{P_N(\xi)}{(\xi - \xi_i)} d\xi \quad (\text{C.4})$$

In order to calculate Equation (C.4), the recursion formula [25]

$$(i+1)P_{i+1}(\xi) = (2i+1)\xi P_i(\xi) - iP_{i-1}(\xi)$$

will be multiplied by $P_i(\eta)$ such that [9]

$$(2i+1)\xi P_i(\xi)P_i(\eta) = (i+1)P_{i+1}(\xi)P_i(\eta) - iP_{i-1}(\xi)P_i(\eta) \quad (\text{C.5})$$

Interchanging ξ with η in Equation (C.5), one obtains

$$(2i+1)\eta P_i(\eta)P_i(\xi) = (i+1)P_{i+1}(\eta)P_i(\xi) - iP_{i-1}(\eta)P_i(\xi) \quad (\text{C.6})$$

and next, subtracting Equation (C.6) from Equation (C.5) yields

$$(2i+1)(\eta - \xi)P_i(\xi)P_i(\eta) = (i+1)[P_{i+1}(\eta)P_i(\xi) - P_{i+1}(\xi)P_i(\eta)] - i[P_i(\eta)P_{i-1}(\xi) - P_{i-1}(\eta)P_i(\xi)] \quad (\text{C.7})$$

Performing summation from $i = 1$ to N for Equation (C.7):

$$(\eta - \xi) \sum_{i=1}^N (2i+1)P_i(\xi)P_i(\eta) = \sum_{i=1}^N \{(i+1)[P_{i+1}(\eta)P_i(\xi) - P_{i+1}(\xi)P_i(\eta)] - i[P_i(\eta)P_{i-1}(\xi) - P_{i-1}(\eta)P_i(\xi)]\} \quad (\text{C.8})$$

It is easily seen that the right-hand side of Equation (C.8) is simply:

$$(N+1)[P_{N+1}(\eta)P_N(\xi) - P_N(\eta)P_{N+1}(\xi)] - [P_0(\xi)P_1(\eta) - P_0(\eta)P_1(\xi)]$$

due to cancellation of

$$(i+1)[P_{i+1}(\eta)P_i(\xi) - P_{i+1}(\xi)P_i(\eta)]$$

by

$$j[P_{j-1}(\xi)P_j(\eta) - P_{j-1}(\eta)P_j(\xi)] \quad \text{for } j = i+1.$$

Noting that $P_0(\xi) = P_0(\eta) = 1$, $P_1(\xi) = \xi$ and $P_1(\eta) = \eta$, then Equation (C.8) becomes

$$(\eta - \xi) \sum_{i=1}^N (2i+1) P_i(\xi) P_i(\eta) = (N+1) [P_{N+1}(\eta) P_N(\xi) - P_N(\eta) P_{N+1}(\xi)] - (\eta - \xi)$$

Moving the term $(\eta - \xi)$ from right-hand to left-hand side, and setting $i = 0$ as the starting integer for summation, one obtains

$$(\eta - \xi) \sum_{i=0}^N (2i+1) P_i(\xi) P_i(\eta) = (N+1) [P_{N+1}(\eta) P_N(\xi) - P_N(\eta) P_{N+1}(\xi)] \quad (\text{C.9})$$

Let ξ_i be a zero of $P_N(\xi)$. Replacing η with ξ_i in Equation (C.9), and noting that $P_N(\xi_i) = 0$, one has

$$(\xi_i - \xi) \sum_{i=0}^N (2i+1) P_i(\xi) P_i(\xi_i) = (N+1) P_{N+1}(\xi_i) P_N(\xi) \quad (\text{C.9})$$

or

$$\frac{(N+1) P_{N+1}(\xi_i) P_N(\xi)}{(\xi - \xi_i)} = - \sum_{i=0}^N (2i+1) P_i(\xi) P_i(\xi_i) \quad (\text{C.10})$$

Now, integrate Equation (C.10) from -1 to +1,

$$(N+1) P_{N+1}(\xi_i) \int_{-1}^{+1} \frac{P_N(\xi)}{(\xi - \xi_i)} d\xi = - \int_{-1}^{+1} \sum_{i=0}^N (2i+1) P_i(\xi) P_i(\xi_i) d\xi \quad (\text{C.11})$$

$P_i(\xi_i)$ are constants that can be taken outside the integral. Due to the following orthogonality condition

$$\int_{-1}^{+1} P_0(\xi) P_i(\xi) d\xi = 0 \quad \text{for } i \neq 0$$

the right-hand side of Equation (C.11) is

$$\begin{aligned} \int_{-1}^{+1} \sum_{i=0}^N (2i+1) P_i(\xi) d\xi &= \int_{-1}^{+1} [P_0(\xi) P_0(\xi_i) + P_1(\xi) P_1(\xi_i) + \dots + P_N(\xi) P_N(\xi_i)] d\xi \\ &= 2 \end{aligned}$$

Equation (C.11) can now be written as

$$\int_{-1}^{+1} \frac{P_N(\xi)}{(\xi - \xi_i)} d\xi = -\frac{2}{(N+1)P_{N+1}(\xi_i)} \quad (\text{C.12})$$

Substitute $\xi = \xi_i$ into the following recursion formula,

$$\begin{aligned} (N+1)P_{N+1}(\xi_i) &= (2N+1)\xi_i P_N(\xi_i) - NP_{N-1}(\xi_i) \\ &= -NP_{N-1}(\xi_i) \end{aligned} \quad (\text{C.13})$$

and again the final result of Equation (C.13) is substituted into Equation (C.12).

Then

$$\int_{-1}^{+1} \frac{P_N(\xi)}{(\xi - \xi_i)} d\xi = \frac{2}{NP_{N-1}(\xi_i)} \quad (\text{C.14})$$

The recursion formula for the derivative of a Legendre polynomial can be defined as [25]

$$(1 - \xi^2)P'_N(\xi) + N\xi P_N(\xi) = NP_{N-1}(\xi)$$

Letting $\xi = \xi_i$, a zero of $P_N(\xi)$, the above equation becomes

$$(1 - \xi_i^2)P'_N(\xi_i) = NP_{N-1}(\xi_i)$$

Using the above result, again Equation (C.14) becomes

$$\int_{-1}^{+1} \frac{P_N(\xi)}{(\xi - \xi_i)} d\xi = \frac{2}{(1 - \xi_i^2)[P'_N(\xi_i)]^2} \quad (\text{C.15})$$

and finally, the weights of Gauss-Legendre quadrature formerly expressed in Equation (C.4) can be computed by

$$w_i = \frac{2}{(1 - \xi_i^2)[P'_N(\xi_i)]^2} \quad (\text{C.16})$$

Note that again, Equation (C.16) is simple and very suitable for automated computing. $P'_N(\xi_i)$ is defined by

$$P'_N(\xi_i) = \frac{d}{dx} [P_N(\xi)] = \prod_{\substack{j=1 \\ j \neq i}}^N (\xi_i - \xi_j) \quad \text{for } \xi = \xi_i \quad (\text{C.17})$$

APPENDIX D

THE POSITION OF THE COLLOCATION POINTS

The position of the odd number of the collocation points used in this study is listed in the table below. Note that the interior points are the zeros of $(N - 2)^{\text{th}}$ degree Legendre polynomial.

Number of Points N	Interval	
	$-1 \leq \xi \leq +1$	$0 \leq \xi \leq +1$
5 points	-1.000000	0.000000
	-0.774597	0.112702
	0.000000	0.500000
	0.774597	0.887298
	1.000000	1.000000
7 points	-1.000000	0.000000
	-0.906180	0.046910
	-0.538469	0.230765
	0.000000	0.500000
	0.538469	0.769235
	0.906180	0.953090
	1.000000	1.000000
9 points	-1.000000	0.000000
	-0.949180	0.025446
	-0.741531	0.129234
	-0.405845	0.297077
	0.000000	0.500000
	0.405845	0.702923
	0.741531	0.870766
	0.949108	0.974554
	1.000000	1.000000
11 points	-1.000000	0.000000
	-0.968160	0.015919
	-0.836031	0.081984
	-0.613371	0.193314
	-0.324253	0.337873
	0.000000	0.500000
	0.324253	0.662127
	0.613371	0.806686
	0.836031	0.918016
	0.968160	0.984080
	1.000000	1.000000

REFERENCES

1. Villadsen, J., and M.L. Michelsen. "Solution of Differential Equation Models by Polynomial Approximation." Prentice-Hall, Inc., Englewood Cliffs, N.J., (1978).
2. Finlayson, B.A. "The Method of Weighted Residuals and Variational Principles." Academic Press, New York, (1972).
3. Prenter, P.M. "Splines and Variational Methods." John Wiley & Sons, New York, (1975).
4. Chang, P.W., and B.A. Finlayson. "Orthogonal Collocation on Finite Elements for Elliptic Equations." *Advances in Computer Methods for Partial Differential Equations - II*, (1977).
5. Frazer, R.A., W.P. Jones and S.W. Skan. "Approximations to Functions and to the Solutions of Differential Equations." *Gt. Brit. Air Ministry Aero. Res. Comm. Tech. Rept.*, 1, (1937): 517-549.
6. Lanczos, C. "Trigonometric Interpolation of Empirical and Analytical Functions." *Journal of Mathematical Physics*, 17, (1938): 123-199.
7. Lanczos, C. "Applied Analysis." Prentice Hall, Inc., Englewood Cliffs, N.J.. (1957).
8. Clenshaw, C.W., and H.J. Norton. "The Solution of Non-Linear Ordinary Differential Equations in Chebyshev Series." *Comp. Journal*, 6, (1963): 88-92.
9. Norton, H.J. "The Iterative Solution of Nonlinear Ordinary Differential Equations in Chebyshev Series." *Comp. Journal*, 7, (1964): 76-85.
10. Wright, K. "Chebyshev Collocation Methods for Ordinary Differential Equations." *Comp. Journal*, 6, (1964): 358-365.
11. Horvay, G., and F.N. Spiess. "Orthogonal Edge of Polynomials in the Solution of Boundary Value Problems." *Quarterly Applied Mathematics*, 12, (1954): 57-69.

12. Villadsen, J., and W.E. Stewart. "Solution of Boundary Value Problems by Orthogonal Collocation." *Chemical Engineering Science*, Vo. 22, (1967): 1483-1501.
13. Rank, E., and I. Babuska. "An Expert System for the Optimal Mesh Design in the hp-Version of the Finite Element Method." *International Journal for Numerical Methods in Engineering*, Vol. 24, (1987): 2087-2106.
14. Babuska, I., and M. Suri. "The p- and h-p Versions of the Finite Element Method, an overview." *Computer Methods in Applied Mechanics and Engineering*, 80, (1990): 5-26.
15. Szabo, B.A. "The p and h-p Versions of the Finite Element Method in Solid Mechanics." *Computer Methods in Applied Mechanics and Engineering*, 80, (1990): 185-195.
16. Costabel, M., V.J. Ervin and E.P. Stephan. "Experimental Asymptotic Convergence of the Collocation Method for Boundary Integral Equations on Polygons Governing Laplace's Equation." *Computational Mechanics*, 6, (1990): 271-278.
17. Rank, E., "Adaptive h-, p- and hp-Versions for Boundary Integral Element Methods." *International Journal for Numerical Methods in Engineering*, Vol. 28, (1989): 1335-1349.
18. Babuska, I., B.Q. Guo and E.P. Stephan. "The h-p Version of the Boundary Element Method with Geometric Mesh on Polygonal Domains." *Computer Methods in Applied Mechanics and Engineering*, 80, (1990): 319-325.
19. Villadsen, J., and J.P. Sørensen. "Solution of Parabolic Partial Differential Equations by a Double Collocation Method." *Chemical Engineering Science*, Vol. 24, (1969): 1337-1349.
20. Villadsen, J. "Selected Approximation Methods for Chemical Engineering Problems." *Instituttet for Kemiteknik*, Danmarks tekniske Højskole, (1970).
21. Brebbia, C.A., and J. Dominguez. "Boundary Elements An Introductory Course." *Computational Mechanics Publications*, Southampton UK and Boston USA, (1989).
22. Zienkiewicz, O.C. "The Finite Element Method." 3rd Edition, McGraw Hill Book Company, London, (1977).

23. Bathe, K.J., and E.L. Wilson. "Numerical Methods in Finite Element Analysis." Prentice-Hall, Inc., Englewood Cliffs, N.J., (1976).
24. Burden, R.L., J.D. Faires and A.C. Reynolds. "Numerical Analysis." 2nd Edition, Prindle, Weber & Schmidt, Boston, (1981).
25. Spiegel, M.R. "Mathematical Handbook of Formulas and Tables." Schaum's Outline Series in Mathematics, McGraw-Hill Book Co., New York. (1968).
26. Abramowitz, M., and I.A. Stegun. "Handbook of Mathematical Functions." Dover Publications, Inc., New York, (1965).
27. Michelsen, M.L., and J. Villadsen. "A Convenient Computation Procedure for Collocation Constants." *The Chemical Engineering Journal*, 4, (1972): 64-68.
28. Finlayson, B.A. "Packed Bed Reactor Analysis by Orthogonal Collocation." *Chemical Engineering Science*, Vol. 26, (1971): 1081-1091.
29. Ferguson, N.B., and B.A. Finlayson. "Transient Chemical Reaction Analysis by Orthogonal Collocation." *The Chemical Engineering Journal*, 1, (1970): 327-336.
30. Prenter, P.M., and R.D. Russell. "Orthogonal Collocation for Elliptic Partial Differential Equations." *SIAM Journal of Numerical Analysis*, Vol. 13, (1976): 923-939.
31. Frind, E.O., and G.F. Pinder. "A Collocation Finite Element Method for Potential Problems in Irregular Domains." *International Journal of Numerical Methods in Engineering*, Vol. 14, (1979): 681-701.
32. Timoshenko, S., and J.N. Goodier. "Theory of Elasticity." 2nd Edition, McGraw-Hill Book Co., New York, N.Y., (1951).
33. Lefebvre, D. "Solving Problems with Singularities using Boundary Elements." Computational Mechanics Publications, Southampton UK and Boston USA, (1989).
34. Blum, H. "Numerical Treatment of Corner and Crack Singularities." *Summary of lectures held at CISM summer school "FEM and BEM techniques from mathematical and engineering point of view"*, Udine, (September 1986).

35. Fox, L., and I.B. Parker. "Chebychev Polynomials in Numerical Analysis." Oxford University Press, London, (1968).
36. Whiteman, J.R., and N. Papamichael. "Treatment of Harmonic Mixed Boundary Problems by Conformal Transformation Methods." *Journal of Applied Mathematics and Physics*, Vol. 23, (1972).
37. Symm, G.T. "Treatment of Singularities in the Solution of Laplace's Equation by an Integral Equation Method." *National Physical Laboratory Report NAC 31*, (January 1973).
38. Jaswon, M.A., and G.T. Symm. "Integral Equation Methods in Potential Theory and Elastostatics." Academic Press, New York, (1977).
39. Motz, H. "The Treatment of Singularities of Partial Differential Equations by Relaxation Methods." *Quarterly of Applied Mathematics*, Vol. IV, No.3, (Oct. 1946): 371-377.
40. Weinberger, H.F. "Partial Differential Equations with Complex Variables and Transform Method." Blaisdell Publishing Company, (1965).
41. Kopal, Z. "Numerical Analysis." John Wiley & Sons, Inc., New York, (1955).
42. Irons, B., and N.G. Shrive. "Numerical Methods in Engineering and Applied Science." Ellis Horwood Limited, Chichester, England, (1987).
43. Atkinson, K.E. "Elementary Numerical Analysis." John Wiley & Sons, New York, (1985).
44. Isaacson, E., and H.B. Keller. "Analysis of Numerical Methods." John Wiley & Sons, Inc., New York, (1966).
45. Sokolnikoff, I.S. "Mathematical Theory of Elasticity." 2nd Edition, McGraw-Hill Book Co., New York, N.Y., (1956).
46. Kelman, R.B. "Harmonic Mixed Boundary Value Problems in Composite Rectangular Domains." *Quarterly Journal Mechanics and Applied Mathematic*, Vol. XXIII, (1970).
47. Jolley, L.B.W. "Summary of Series." 2nd Edition, Dover Publications, Inc., New York, (1961).

48. Tottenham, H. "A Direct Numerical Method for the Solution of Field Problems." *International Journal for Numerical Methods in Engineering*, Vol. 2, (1970): 117-131.
49. Scheid, F. "Theory and Problems of Numerical Analysis." Schaum's Outline Series, McGraw-Hill Book Co., New York. (1968).
50. Todd, J. "Survey of Numerical Analysis." McGraw-Hill Book Co., New York. (1962).
51. Gipson, G.S. "Boundary Elements Fundamentals." *Computational Mechanics Publications*, Southampton UK and Boston USA, (1987).
52. Tikhonov, A.N., and A.A. Samarskii. "Equations of Mathematical Physics." Dover Publications, Inc., New York, (1990).
53. Carslaw, H.S. "Introduction to the Theory of Fourier's Series & Integrals." Dover Publications, Inc., New York, (1950).
54. Costabel, M., and E.P. Stephan. "On the Convergence of Collocation Methods for Boundary Integral Equations on Polygons." *Mathematics of Computation*, Vol. 49, No. 180, (Oct. 1987): 461-478.
55. Fox, L. "Chebyshev Methods for Ordinary Differential Equations." *Computer Journal*, 4, (1962): 318-331.
56. Clenshaw, C.W. "The Numerical Solution of Linear Differential Equations in Chebyshev Series." *Proceeding Cambridge Phil. Soc.*, 53, (1957): 134-149.
57. Press, W.H., B.P. Flannery, S.A. Teukolsky and W.T. Vettering. "Numerical Recipes, The Art of Scientific Computing." Cambridge University Press, Cambridge, (1987).
58. Deville, M.O. "Chebychev Collocation Solutions of Flow Problems." *Computer Methods in Applied Mechanics and Engineering*, 80, (1990): 27-37.
59. Houstis, E.N., and J.R. Rice. "Software for Linear Elliptic Problems on General Two-Dimensional Domains." *Advances in Computer Methods for Partial Differential Equations - II*, (1977): 7-12.

60. Papamicheal, N., and G.T. Symm. "Numerical Techniques for Two-Dimensional Laplacian Problems." *Computer Methods Appl. Mechanical Engineering*, 6, (1975): 175-194.
61. Boor, C. De, and B. Swartz. "Collocation at Gaussian Points." *SIAM Journal of Numerical Analysis*, Vol. 10, No. 4, (September 1973): 582-606.
62. Ahlberg, J.H., and T. Ito. "A Collocation Method for Two-Point Boundary Value Problems." *Mathematical of Computation*, Vol. 29, No. 131, (July 1975): 761-776.
63. Houstis, E.N., E.A. Vavalis and J.R. Rice. "Convergence of $O(h^4)$ Cubic Spline Collocation Methods for Elliptic Partial Differential Equations." *SIAM Journal of Numerical Analysis*, Vol. 25, No. 1, (February 1988): 54-74.
64. DeVille, M., and E. Mund. "Chebyshev Pseudospectral Solution of Second-Order Elliptic Equations with Finite Element Preconditioning." *Journal of Computational Physics*, 60, (1985): 517-533.
65. Ronquist, E.M., and A.T. Patera. "A Legendre Spectral Element Method for the Stephan Problem." *International Journal for Numerical Methods in Engineering*, Vo. 24, (1987): 2273-2299.
66. Liu, B., and A.N. Beris. "The Stability of Numerical Approximations to Nonlinear Hyperbolic Equations." *Computer Methods in Applied Mechanics and Engineering*, 76, (1989): 179-204.
67. Weiser, A., S.C. Eisenstat and M.H. Schultz. "On Solving Elliptic Equations to Moderate Accuracy." *SIAM Journal of Numerical Analysis*, 17, (1980): 908-929.
68. Funaro, D. "A Preconditioning Matrix for the Chebyshev Differencing Operator." *SIAM Journal of Numerical Analysis*, Vol. 24, No. 5, (October 1987): 1024-1031.
69. Carey, G.F. "Derivative Calculation from Finite Element Solutions." *Computer Methods in Applied Mechanics and Engineering*, 35, (1982): 1-14.

70. Bakker, M. "One-Dimensional Galerkin Methods and Superconvergence at Interior Nodal Points." *SIAM Journal of Numerical Analysis*, Vol. 21, No. 1, (February 1984): 101-110.
71. Whittaker, Sir E., and G. Robinson. "The Calculus of Observations - A Treatise on Numerical Mathematics." Blackie & Son Limited, London & Glasgow, (1944).
72. Morse, P.M., and H. Freshbach. "Methods of Theoretical Physics." McGraw Hill Book Company, Inc., Vol. I & II, New York, (1953).
73. Timoshenko, S., and S. Woinowsky-Krieger. "Theory of Plates and Shells." McGraw Hill Book Company, Inc., New York, (1959).
74. Ugural, A.C. "Stresses in Plates and Shells." McGraw Hill Book Company, Inc., New York, (1981).
75. Forsythe, G.E., M.A. Malcolm and C.B. Moler. "Computer Methods for Mathematical Computations." Prentice-Hall, Englewood Cliffs, New Jersey, (1977).
76. Golub, G.H., and C.F. Van Loan. "Matrix Computations." Johns Hopkins University Press, Baltimore, (1983).